2005

Development of high performance hybrid syntactic foams: structure and material property characterization

Rahul R. Maharsia
Louisiana State University and Agricultural and Mechanical College

DEVELOPMENT OF HIGH PERFORMANCE HYBRID SYNTACTIC FOAMS: STRUCTURE AND MATERIAL PROPERTY CHARACTERIZATION

A Dissertation

Submitted to the Graduate Faculty of the
Louisiana State University and
Agricultural and Mechanical College
in partial fulfillment of the
requirements for the degree of
Doctor of Philosophy

in

The Interdepartmental Program in Engineering Science

by
Rahul R. Maharsia
B.Eng., University of Mumbai, Mumbai, India, 1999
M. Sci., Louisiana Tech University, Ruston, U.S.A., 2001
August, 2005

ACKNOWLEDGMENTS

I would like to acknowledge the support and guidance provided by my major professor, Dr. H. Dwayne Jerro during the course of this study. I would like to thank the support and guidance provided by the members of my graduate committee, Dr. Eyassu Woldesenbet, Dr. George Voyiadjis, Dr. Charles McAllister and Dr. George Stanley who is acting as the Dean's representative. Discussions and suggestions by Dr. Guoqiang Li, Dr. Paul Russo and Dr. Lin-Bing Wang are truly appreciated.

I would like to thank the DOW Chemical Company and 3M Corporation for providing epoxy resin and glass microballoons respectively, and related technical information for the experimental study.

I wish to acknowledge the constant help and guidance provided by my family in pursuing my Ph.D. degree. This work would not have been possible without the extensive help and guidance provided by Dr. Nikhil Gupta from defining the outline of the study, to the actual experimentation and characterization process. Extensive help by Priya David during the fabrication process and manuscript documentation is gratefully acknowledged. Help of Dr. Jiechao Jiang in TEM and XPS is gratefully acknowledged.

This research has been funded by National Science Foundation and Louisiana Board of Regents grant number NSF/LEQSF (2000-01)-NCA-JFAP-10.

TABLE OF CONTENTS

LIST OF TABLES

LIST OF FIGURES

ABSTRACT

Syntactic foams are light weight particulate composites that use hollow particles (microballoons) as reinforcement in a polymer resin matrix. High strength microballoons provide closed cell porosity which helps in reducing weight of the material. Due to their wide range of possible applications such as in aerospace and marine structures, it is desirable to modify the physical and mechanical properties of syntactic foams as per the requirements of an application. Various filler materials can be used to modify the foam microstructure to attain these desired properties.

Compression tests have revealed that high density syntactic foams demonstrate poor damage tolerance and low fracture strain, when compared with low density syntactic foams, which exhibit higher damage tolerance and fracture strains. The present study deals with increasing the fracture strain and damage tolerance properties of high density syntactic foams. An approach of modifying the matrix resin with the incorporation of filler particles as a third phase is adopted, resulting in hybrid syntactic foam. Two types of high performance hybrid foam composites are developed using waste tire rubber particles and low cost nanoclay particle respectively. Such highly damage tolerant hybrid foams will be useful as sandwich core material in automobile, aerospace, and marine structures.

An analytical study is performed in order to observe the behavior of microballoons in syntactic foams upon loading. All hybrid foams are characterized for compressive strength and flexural strength properties. Rubber hybrid foams are further characterized for hygrothermal properties.

Mechanical properties of hybrid foams are compared with those of plain syntactic foams. Changes in properties are correlated with the change in structural composition due to incorporation of rubber and nanoclay particles respectively. High magnification Scanning Electron Microscopy (SEM) is used to study microstructure of all the specimens. Change in properties of rubber type hybrid foams due to change in the size of rubber particles is studied. The dispersion and intercalation of nanoclay particles in nanoclay hybrid foams is studied using Transmission Electron Microscopy and X-ray photoelectron spectroscopy.

Deformation behavior of hybrid foams and pure syntactic foams are compared and correlated to the presence of different types of particles in them.

1 INTRODUCTION

1.1 Composite Materials

1.1.1 Definition

Research and development of new, high performance materials is the key to success in developing a better world around us. Composite materials are leading the way into the development of such high performance materials.

By definition, composite materials constitute a mixture of two or more materials which possess significantly different physical properties as compared to each other [1]. The composite itself has significantly different and enhanced properties as compared to the constituent materials. Metal alloys and plastics using additives such as color pigments are composites by definition. However, they are not generally referred to as composites, because, generally metal alloys constitute materials which do not have significantly different properties from each other, and additives as such do not provide any significant change in the physical properties of plastics. The mechanical and physical properties of Polymers can be significantly enhanced by adding various types of fiber or particle reinforcements. Hence fiber reinforced polymers can be termed as composite materials.

1.1.2 Classification

The constituents of a composite include a matrix phase and a reinforcing phase. The matrix material is a single phase and generally consists of polymeric (e.g. epoxy) or metallic (e.g. aluminum) material. Polymer matrix composites are more widely used due to several advantages associated with them such as high strength to weight ratio, resistance to chemicals, resistance to corrosion, low thermal and electrical conductivity, and low coefficient of moisture absorption. Further discussion in this study deals with polymer matrix based composites only. The reinforcement may be either a single phase or multiple phases combined together. A multi-phase reinforcement is achieved when various types of particles are used together or with a fibrous material. Depending upon the type of reinforcement, composites are classified into fiber reinforced and particulate composites [2].

Fiber reinforced polymer (FRP) composites consist of one or more discontinuous reinforcing phase in a continuous matrix phase. The type of reinforcement and matrix material used depends on the type of application and the properties desired. Examples of fiber reinforced polymer composites include, vinyl ester resin matrix reinforced with glass fibers, epoxy matrix reinforced with carbon fibers etc.

Particulate polymer composites are made up of a continuous matrix phase reinforced with one or more types of particulate reinforcements. Several types of metallic, ceramic and polymeric particles are used as fillers in polymer matrix materials to fabricate particulate composites [2]. Appropriate choice of fillers can produce composites with superior strength, damage tolerance, wear resistance and chemical resistance. Examples of particulate composites include polymer resin matrix containing aluminum, steel or glass particles.

1.1.3 Advantages

Some of the advantages associated with composites, which make them an attractive choice among materials are listed below:

- Higher design flexibility, enables them to attain desired mechanical and physical properties by varying the composition of constituent materials.

- Properties such as high strength, high thermal resistance, low coefficient of moisture absorption, and excellent resistance to chemicals and corrosion.
- Wide range of possible applications, ranging from military aircraft, naval submarines, and aerospace structures to automobile components and sports equipment.
- High strength to weight ratio, which results in reduction of costs due to decrease in weight of structures used in the applications mentioned above.

1.1.4 Disadvantages

Some of the disadvantages associated with composites include:

- Mass production of composites is difficult.
- Higher costs of fabrication and repair.
- Analysis and modeling of composites is difficult as compared to metals, which limits the reliability with which they can be used in new applications.

1.2 Syntactic Foam Particulate Composites

Hollow particle filled polymer composites known as syntactic foams are an important class of materials used in various applications. The syntactic foam matrix is reinforced with hollow spherical particles which have a controlled systematic arrangement in the matrix, hence the name Syntactic. Hollow particles, called microballoons, provide closed cell porosity within syntactic foams which results in a lower density material when compared with solid particle composites and FRP composites. The density of syntactic foams generally varies from 200 - 700 kg/m^3. Regular foams have open cell porosity and have a density less than 100 kg/m^3 [3]. Despite the added weight due to hollow particles, syntactic foams have better mechanical and physical properties, and lower moisture absorption characteristics as compared to open cell foams [3].

Glass particles are particularly attractive for use as fillers in composites due to their high strength properties, as well as their low cost and ease of fabrication. Hollow glass particles have very low densities as compared to corresponding hollow metallic and ceramic particles [4]. A diverse set of properties that include high specific compressive strength, low moisture absorption, higher thermal and chemical stability make syntactic foams suitable for structural applications compared to open cell structured foams and other low density materials [4].

1.3 Applications

Syntactic foams were basically developed as buoyancy aid materials, particularly for use in deep sea applications where enormous hydrostatic pressures are involved. Recently they have found use in other marine and aerospace applications [5]. They have very low radar detectability, which is a desirable property in aircrafts and submarines. They can be easily molded into various shapes desired as per different applications. Generally they are used as core material for sandwich structures that can be used in automobile, space shuttle and submarine applications [6, 7, 8, 9].

1.4 Structure of Syntactic Foams

Syntactic foams consist of a matrix resin phase and a reinforcing microballoon phase. The following Figure 1 is a micrograph showing the microstructure of a glass-microballoon syntactic foam. Glass microballoons can be clearly seen as round particles embedded in an epoxy polymer matrix. The debris indicates some microballoon damage due to the shearing while cutting the samples.

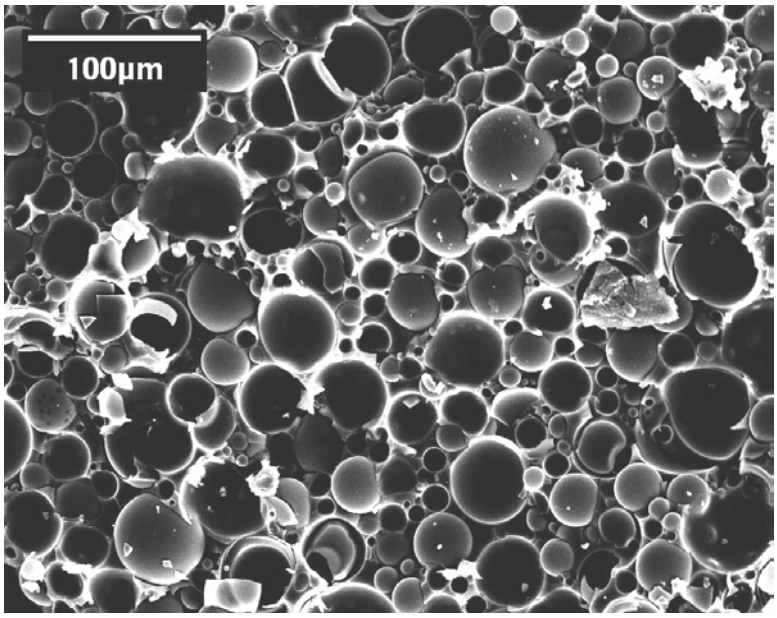

Figure 1 Microstructure of a Glass Microballoon Syntactic Foam.

2 LITERATURE SURVEY

Large number of studies can be found published on solid and hollow glass particle filled composites [10, 11, 12]. Several processing techniques have been investigated by researchers for the fabrication of syntactic foams [12, 13]. Techniques derived from these studies have been used in the present study to achieve minimal air entrapment and appropriate wetting of microballoons, so that void content is reduced and a strong resin-microballoon interface is obtained.

Studies on compressive [14-15], impact [16, 17, 18], hygrothermal [7, 18, 20], fire performance [21] properties, and microstructural fracture features of syntactic foams under various fracture conditions [22-25], have been published previously in the literature. Bunn et al [14] have reported the compressive properties of syntactic foams made from phenolic microballoons with different volume fractions. As the microballoon volume fraction was increased, a decrease in compressive strength was observed. Compressive properties of these foams were found to be relatively poor when compared with foams made from glass microballoons. With a microballoon volume fraction of 0.553, a compressive strength of 28 MPa and a compressive modulus of nearly 1400 MPa, was obtained, which indicates a good load absorption capacity but low compressive strength. Gupta et al [15] have reported a compressive strength of nearly 22.4 MPa for foams made from 0.68 volume fraction glass microballoons. This is a reasonably high compressive strength when compared to foams made from phenolic microballoons considering the high percentage of glass microballoons used (68%), and the lower aspect ratio of test specimens. Impact studies [16, 17], have shown an improvement in impact properties of syntactic foams with an increase in glass microballoon volume fraction. However, this is accompanied with a reduction in fracture toughness and flexural strength of the composite [17].

Syntactic foams composed of epoxy resin matrix and low density (220 kg/m^3) glass microballoons show damage tolerant properties due to the low strength of microballoons. Low strength of microballoons causes them to fracture under the applied load and keep the damage localized. A large amount of load energy is absorbed in the crushing of microballoons upon application of load. However, high density microballoon foams (460 kg/m^3) are relatively brittle, and have a lower energy absorption capacity. High density foams tend to fail catastrophically soon after the yield stress, which is undesirable for applications requiring high damage tolerance [25].

Properties of matrix material also affect the fracture strain of syntactic foams as observed clearly in previous studies performed on flexural strength properties of syntactic foams. Gupta et al studied the flexural properties of syntactic foam core sandwich structures after three point bending, four point bending, and short beam shear testing of the specimen [9]. It was observed that glass microballoon properties do not influence the flexural properties of syntactic foams when tested in three or four-point bending configurations. This was due to the fact that fracture occurs on the tensile side of a specimen primarily due to fracture of the resin matrix. Therefore, it can be envisioned that an increase in resin tensile strength may increase the flexural strength of syntactic foams. Flexural strength of syntactic foams is observed to be influenced primarily by the properties of the resin matrix, and an increase in elasticity of the matrix may increase the fracture strain of a specimen, which may delay the initiation of failure.

Thus, the damage tolerance of syntactic foams can be increased further if the epoxy matrix material can be toughened to reduce the brittleness. For damage tolerant applications it is

desired to reduce the modulus of syntactic foams, to reduce premature crack formation in specimens, and increase the fracture strain without a considerable change in the strength. It is observed previously in the published hygrothermal studies that the plasticization of matrix can lead to increase in the fracture strain of high density foams [7, 20]. These studies have looked into analyzing the effect of water absorption on mechanical properties of syntactic foams. Gupta et al [20] have reported about 50% decrease in compressive modulus and a small decrease in the strength of syntactic foams after hygrothermal testing of syntactic foams at room temperature till saturation. However, plasticization of matrix by hygrothermal means is not an acceptable or feasible solution for most applications. Hence, an approach of using rubber particles and nanoclay particles for matrix toughening is adopted in the present study.

Rubber particles are known to have modified the matrix of syntactic foams for achieving better impact and fracture toughening properties [26]. Some earlier published studies have examined the fatigue properties of similar hybrid foams containing rubber particles and glass microballoons [26]. It was found that fracture toughness of the composite increased and brittleness reduced due to the presence of rubber particles in the composite.

Published studies have shown that the use of nanoclay particles increases the tensile strength, modulus, resistance to thermal failure, and impact resistance of polymers [27]. This improvement in performance has been attributed to the unique phase morphology and better interfacial properties in the nanocomposite [28-30]. In conventional composites, phase mixing occurs on a macroscopic scale, whereas nanocomposite materials are formed when phase mixing occurs on a nanometer length scale [27]. A large number of interfaces are created in a nanocomposite upon dispersion of nanoparticles, resulting in an increase in strength of the composite matrix [31].

Hence, in the present work, high damage tolerance hybrid syntactic foams are developed by adding rubber and nanoclay particles in the foam matrix. Rubber particles are filled in syntactic foams in a small volume fraction of 2%, to fabricate rubber hybrid foams of high toughness and damage tolerance under compressive and flexural loading conditions. Even though the rubber particle volume fraction in the composite is 2%, the ratio of rubber to polymer matrix volume fraction is nearly 5.7%, which is sufficient for changing the properties of the matrix. The rubber particles used in the present study are obtained from waste tires and are known as crumb rubber. Millions of waste tires generated each year add to the environmental hazard and use up valuable landfill space. Therefore, innovative use of the waste tire material to fabricate high performance composites is a novel approach in contributing towards environmental safety and developing new types of material. Nanoclay particles are added in 2 and 5% volume fraction in the foam matrix to develop highly damage tolerant nanoclay hybrid foams. Nanoclay particle to matrix resin ratio is nearly 5.7% and 10% which is significant enough to change properties of the syntactic foams. Also, small volume fraction of nanoclay (2% and 5%) will not lead to significant increase in density of these composites.

3 RESEARCH OBJECTIVE

The objective of the present study is to develop and characterize two types of hybrid syntactic foams. Rubber and nanoclay particles are used to modify the structure of glass microballoon syntactic foams in order to achieve higher damage tolerance properties. Two approaches are used in this study to characterize the loading and failure behavior of syntactic foams. First, an analytical study is conducted in order to study the effect of various parameters on the stresses acting around a microballoon in syntactic foam upon loading. This is followed by an experimental study, in which the various hybrid foams are characterized for various mechanical and hygrothermal properties as discussed below.

3.1 Analytical Study

In order to better understand the fracture and deformation mechanism in syntactic foams, it is imperative to study the micromechanical effects of applied stress in the vicinity of a microballoon. Syntactic foams are multi-particle systems, and they involve a large number of parameters which govern their failure mechanism. Therefore, it is very difficult to use a single model to ascertain the behavior of syntactic foams. Hence, as an initial step, a simple two dimensional model using the Stress Intensity Factor approach can be developed to study the loading behavior of microballoons in the foam matrix. Such a study will help in determining the stress distribution behavior around a microballoon, and may form a basis for developing future complex models to analyze the behavior of a multi-particle system involving different types of particles in it. Such analysis will also demonstrate the need for developing hybrid composites using rubber and nanoclay filler particles that reduce stress concentration and relieve stresses within the foam matrix.

3.2 Experimental Study

3.2.1 Rubber Hybrid Syntactic Foams

Rubber hybrid foam samples are tested for compressive and flexural strength properties. Hygrothermal testing is done to determine the moisture absorption behavior and subsequent damage to the foam structure using compression testing.

Two different rubber particle sizes are selected for the present study. When the same volume fraction of particles is used the smaller size particles generate higher interfacial area between particles and the matrix resin. Hence, this approach will allow evaluating the effect of interfacial bonding between rubber particles and matrix resin. Four types of microballoons are used to fabricate hybrid foams. Results of earlier studies are compared here with the properties of hybrid foams to gain understanding of the role of rubber particles in hybrid foams.

3.2.2 Nanoclay Hybrid Syntactic Foams

Nanoclay foam samples are tested for compressive and flexural strength properties in order to determine the effect of incorporation of nanoclay particles in syntactic foams.

Phase mixing will occur at the nano scale which creates a large number of interfaces within the nanocomposite upon dispersion of nano particles. Nanoparticle dispersion in the nanocomposite will be studied. Strength of the nanocomposite will be compared with that of syntactic foam without nanoparticles in order to understand the role of nanoparticles in altering syntactic foam properties.

4 RESULTS AND DISCUSSION

4.1 Analytical Study

A simple two dimensional model using the Stress Intensity Factor approach is developed in order to study the loading behavior of microballoons in a foam matrix. Experimental values from tensile testing of syntactic foams are considered for modeling the behavior of microballoons [40]. First the stress concentration around microballoons is studied to observe increase in stresses on the surface of a microballoon upon loading. This is followed by studying the effect of change in stress intensity factor around a crack or a flaw in a material. Such a flaw may be circular, elliptical or random shaped, and there are several models available to ascertain the stress intensity factor for different types of flaws [33].

In this study, a closed form solution for stress intensity factor on a circular crack in a material is considered [38]. A microballoon has been considered equivalent to a two dimensional circular flaw or crack in the system. Change in stress intensity factor is studied by varying parameters such as distance away from the surface of a microballoon, concentration of microballoons in the foam matrix, and the relative position of adjacent microballoons. Such an approach helps in studying microballoon interaction and the effect of orientation of adjacent microballoons on stress distribution between them upon loading.

4.1.1 Stress Concentration on a Microballoon

Stress concentration factor 'K' gives a measure of the amplification of stress on the surface of a crack or a flaw in a material. In ductile materials the value of K is below its theoretical value because of the plastic deformation and uniform stress distribution around a flaw, which results in lowering of the stress concentration factor. However, syntactic foams are brittle materials, and stress concentration is an important parameter in determining the initiation and propagation of cracks leading to failure of the material.

Figure 2 below shows a microballoon embedded within a foam matrix, which is assumed equivalent to a circular flaw in a material.

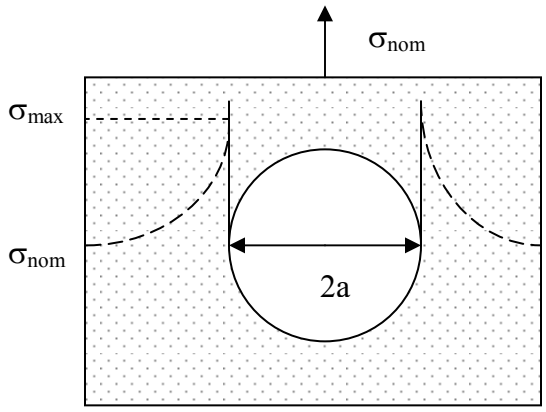

Figure 2. Schematic representation of stress distribution around a microballoon

It is known that the applied tensile stress σ_{nom} is amplified at the surface of the flaw and it diminishes to a value equivalent to the nominal stress as we move away from the flaw.
Maximum stress on the surface of the flaw is given by Equation 1 below.

$$\sigma_{\max} = \sigma_{nom}\left[1 + 2*\left(\frac{a}{\rho_t}\right)^{1/2}\right] \quad (1)$$

where,

a is half length of the flaw,

ρ_t is the radius of curvature of the flaw, and,

σ_{nom} is the applied/nominal stress.

The right side of Equation 1 gives a stress concentration factor 'K' if we divide it by σ_{nom}. Thus we get,

$$K = \frac{\sigma_{\max}}{\sigma_{nom}} = \left[1 + 2*\left(\frac{a}{\rho_t}\right)^{1/2}\right] \quad (2)$$

Since the flaw considered is a microballoon in our analysis, the radius of curvature and half length of the flaw, are both equal to the microballoon radius. Therefore the Equation 1 gives

$$\sigma_{\max} = 3*\sigma_{nom} \quad (3)$$

Or, K = 3.

Thus it can be seen that the applied stress is amplified three times on the surface of a microballoon as compared to nominal stress in the surrounding matrix. Figure 3 shows the variation of 'K' with respect to the '2a/W' ratio.

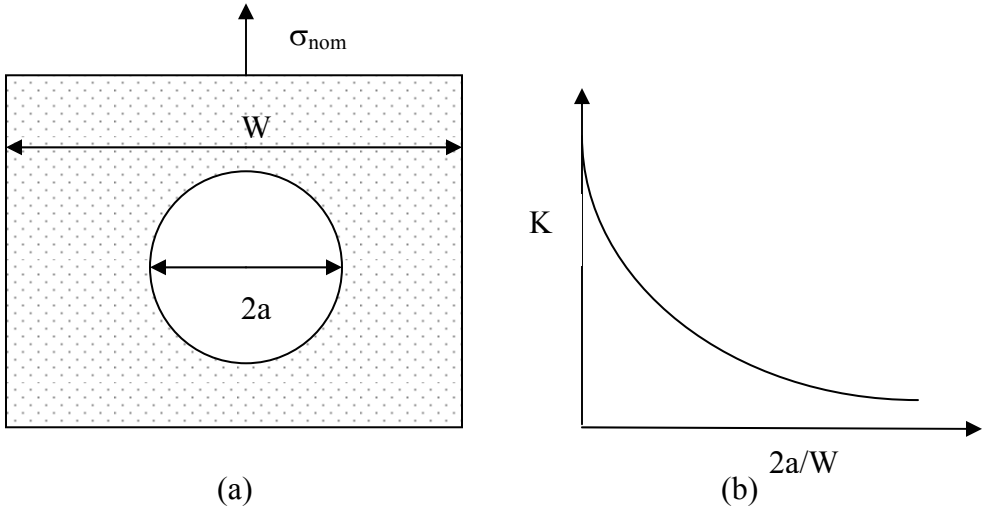

Figure 3. Variation of Stress concentration with respect to a change in 2a/W ratio

4.1.2 Stress Intensity Factor

In order to study and characterize the stress distribution around a microballoon, the stress intensity factor is now analyzed. A two dimensional Mode I configuration of crack formation is assumed under tensile loading. Figure 4 shows the debonding and crack formation around a microballoon. It also shows the stresses on an element in the vicinity of a microballoon due to the applied load.

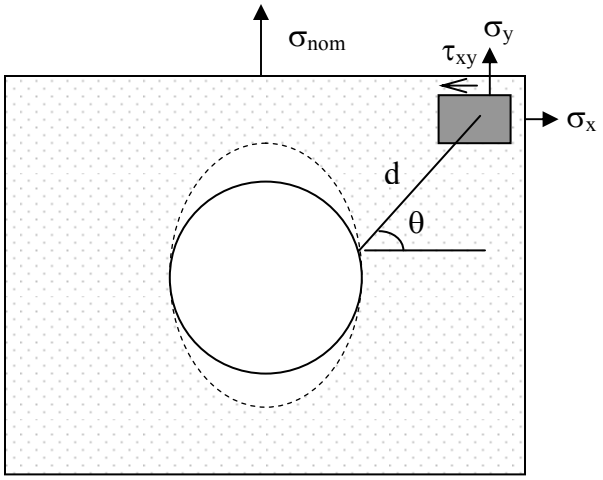

Figure 4. Crack formation and stresses on an element in the vicinity of a microballoon

Stresses acting on the element seen in Figure 4 are as follows:

$$\sigma_x = \frac{K_I}{\sqrt{2\pi d}}\left[\cos\frac{\theta}{2} * \left(1 - \sin\frac{\theta}{2} * \sin\frac{3\theta}{2}\right)\right] \tag{4}$$

$$\sigma_y = \frac{K_I}{\sqrt{2\pi d}}\left[\cos\frac{\theta}{2} * \left(1 + \sin\frac{\theta}{2} * \sin\frac{3\theta}{2}\right)\right] \tag{5}$$

$$\tau_{xy} = \frac{K_I}{\sqrt{2\pi d}}\left[\sin\frac{\theta}{2} * \cos\frac{\theta}{2} * \cos\frac{3\theta}{2}\right] \tag{6}$$

where,

'K_I' in the above equation is the stress intensity factor, which gives stress distribution around a microballoon,

'd' is the distance between microballoon surface and the point element considered,

'θ' is the angle made by the line joining the point element and microballoon surface.

Since only x-y plane has been considered, $\sigma_z = 0$ and a plane stress condition exists. Equation 7 gives the value of stress intensity factor.

$$K_I = Y * \sigma * \sqrt{\pi a} \tag{7}$$

$$Y = \left[\frac{W}{\pi a}\tan\left(\frac{\pi a}{W}\right)\right]^{1/2} \tag{8}$$

where,

'Y' is a parameter depending on the microballoon and specimen sizes (a, W) and geometries, and the manner of load application, and has units of $Mpa(m)^{1/2}$,

'σ' is applied load,

'a' microballoon radius.

At a critical value of the stress intensity factor K_t, known as the fracture toughness, fracture will occur in the material.

$$K_t = Y * \sigma_c * \sqrt{\pi a} \tag{9}$$

where 'σ_c' is the critical stress for crack propagation.

It is known that as the width 'W' for the specimen with respect to a microballoon considered decreases with respect to the microballoon radius, parameter 'Y' increases, which results in an increase in the value of stress intensity factor.

Therefore, if a specimen with same dimensions is considered, but now with two adjacent microballoons in it, then the width 'W' considered for each microballoon decreases. Consequently, as seen in Figure 5a below, the value of Y increases and the value of stress intensity factor K_I also increases. Figure 5b shows the actual variation Y parameter with a change in a/W ratio.

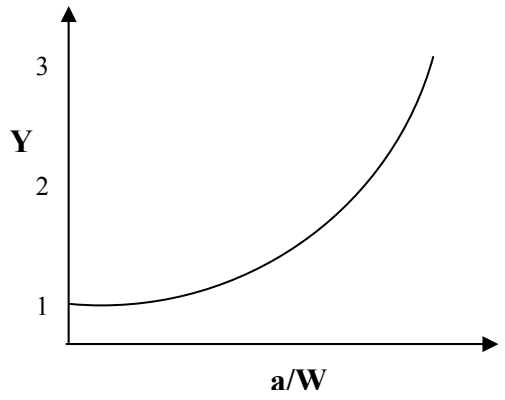

Figure 5. Variation of Stress concentration with respect to a change in a/W ratio

An increase in K_I translates to an increase in the stresses in the area around a microballoon. This increase in 'Y' (decrease in 'W' of specimen with respect to a microballoon) also means that the concentration of microballoons increases in the foam matrix. Maximum Principle stress on the microballoon surface can be calculated using Equation 11 below, and analyzed for variation in parameters including angular orientation of two microballoons, distance between two microballoons, and density of microballoons.

$$\sigma_p = \frac{\sigma_x + \sigma_y}{2} \sqrt{\left(\frac{\sigma_x - \sigma_y}{2} \right)^2 + \tau_{xy}^{\ 2}} \tag{11}$$

In order to model the behavior in terms of stress intensity factor and its associated parameters, experimental values from actual tensile testing of syntactic foam are now considered [32]. Foams with two types of microballoons having true particle density of 220 Kg/m^3 and 460 Kg/m^3 respectively are considered. First two digits of the true particle density are taken in order to designate these foams as SF22 and SF46 respectively. Four different microballoon volume fractions are considered for each type of foam as seen in Table 1 below.

Table 1. Microballoon volume fraction and measured density used in foams used for analytical study

No.	Microballoon Density (kg/m^3)	Microballoon Volume Fraction (%)	Sample Name	Measured Density (kg/m^3)
1	220	30	SF220-30	878
2		40	SF220-40	784
3		50	SF220-50	690
4		60	SF220-60	596
5	460	30	SF460-30	932
6		40	SF460-40	846
7		50	SF460-50	732
8		60	SF460-60	651
9	None	None	Resin	1160

In order to further analyze the variation in stresses around microballoon, the value of 'Y' parameter must be known. 'Y' depends on distance between adjacent microballoons, which can be found by using the formula for packing factor in a material containing spherical particles as shown in Equation 11 below.

$$Packing\ Factor = \frac{Volume\ Of\ Microballoons\ In\ Unit\ Cell}{Volume\ Of\ Unit\ Cell} \tag{11}$$

Face centered cubic structure (FCC) can be considered for a syntactic foam microstructure [39]. There are 4 microballoons in the unit cell of an FCC structure and volume of each microballoon is known from its average outer diameter of 40 □m. Therefore volume of a unit cell can be determined from the volume of microballoons in a unit cell, and the packing factor, which is the microballoon volume fraction in the foam. Length of the unit cell is this obtained from its volume and this gives the average distance between two adjacent microballoons in foams with a particular microballoon volume fraction. Table 2 below gives the average values of the length of a unit cell, the distance between adjacent microballoons and ultimately the 'Y' parameter.

Table 2. Values of 'Y' parameter and distance between adjacent microballoons in foams with various microballoon volume fractions.

Microballoon Volume Fraction	Volume of a Unit cell	Length of a Unit cell	Average distance between microballoons 'd'	W	Y
60%	$2.232*10^{-13}$	$6.067*10^{-5}$	$2.067*10^{-5}$	$6.067*10^{-5}$	1.275
50%	$2.679*10^{-13}$	$6.447*10^{-5}$	$2.447*10^{-5}$	$6.447*10^{-5}$	1.229
40%	$3.349*10^{-13}$	$6.945*10^{-5}$	$2.945*10^{-5}$	$6.945*10^{-5}$	1.185
30%	$4.465*10^{-13}$	$7.644*10^{-5}$	$3.644*10^{-5}$	$7.644*10^{-5}$	1.143

Based on these calculations a direct and important relationship between the microballoon concentration and 'Y' parameter is obtained as given in Equation 12 below.

$$Y = \left[\frac{0.814}{C^{1/3}} \tan\left(\frac{C^{1/3}}{0.814} \right) \right]^{1/2} \quad (12)$$

where, 'C' is the microballoon concentration in a foam. The value inside tangent function is in radians not in degrees. It should be noted that this relationship is independent of the average outer diameter of microballoons in a foam, and therefore can be used in syntactic foams with any value of average outer diameter. Figure 6 shows an increase in value of 'Y' parameter with an increase in concentration of microballoons, which is similar to the theoretical increase as seen in Figure 5.

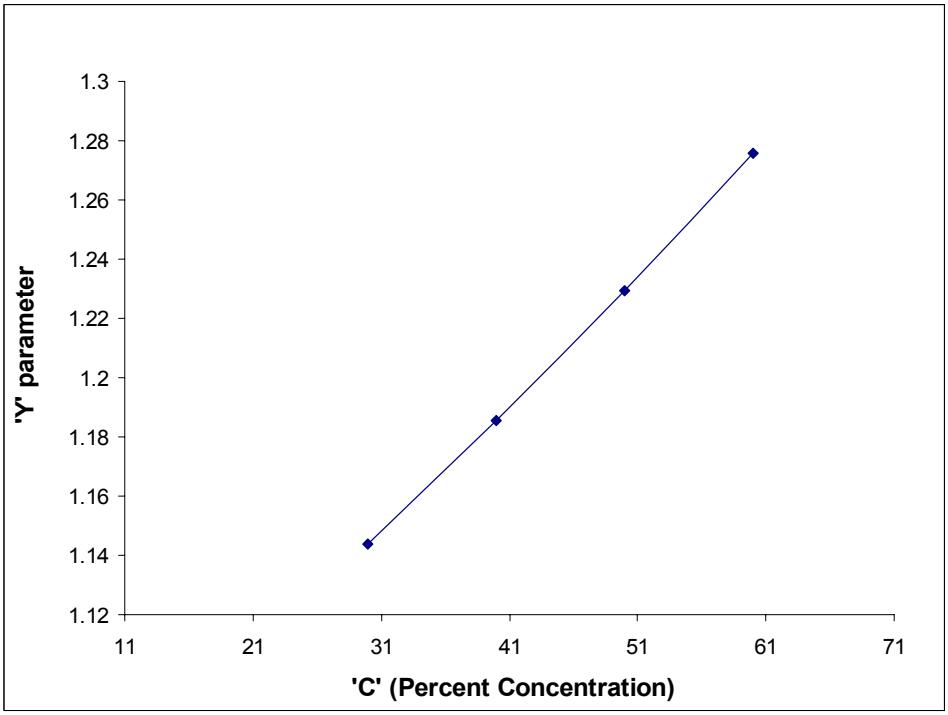

Figure 6. Variation in 'Y' parameter with change in microballoon concentration

Substituting this Equation in the relation for K_I we get a relationship between stress intensity factor and microballoon concentration in a syntactic foam.

$$K_I = \left[\frac{0.814}{C^{1/3}} \tan\left(\frac{C^{1/3}}{0.814} \right) \right]^{1/2} \sigma * \sqrt{\pi a} \quad (13)$$

This value of K_I is used to calculate the principle stresses around microballoons in all types of foams considered above. Figure 7 shows an increase in the value of principle stress σ_p (calculated from Equation 11 above) on a microballoon surface with an increase in Y. It can be seen that as microballoon concentration increases in the foam matrix, the stress σ_p around microballoons increases. Therefore a considerable amount of load is transferred to the microballoons, and crack formation and propagation will occur either due to microballoon fracture or due to debonding between microballoon surface and matrix. The change in stresses around microballoons with a change in their wall thicknesses is also seen in Figure 7. It is seen that high density and thick walled microballoon foams (SF46) involve lower stresses and a lower stress intensity factor around a microballoon, whereas low density microballoon foams (SF22) involve higher stresses and higher stress intensity factor around a microballoon.

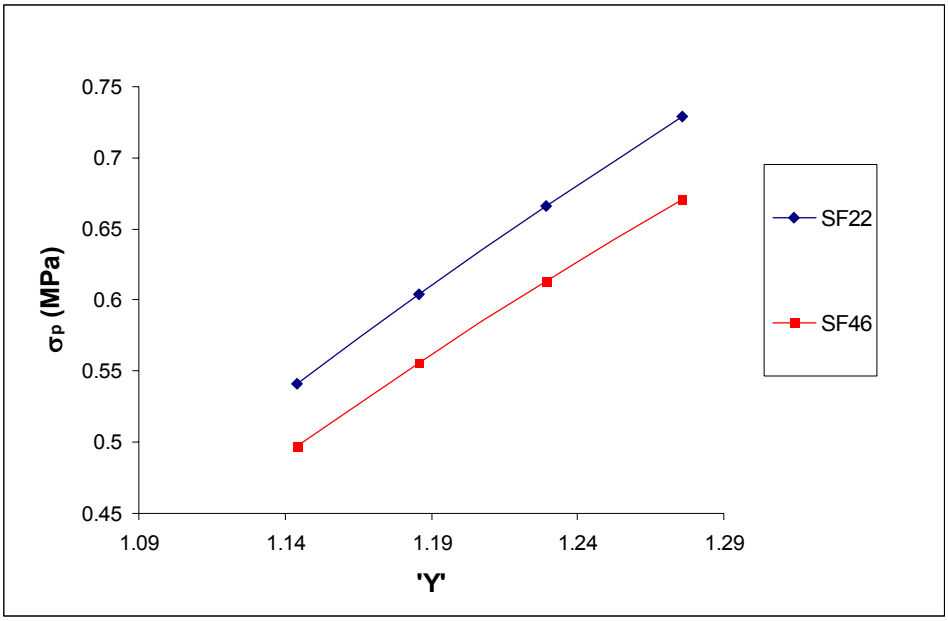

Figure 7. Change in stresses around a microballoon with change in 'Y' (or with change in concentration)

The primary cause of failure in low density foams (SF22) under tensile loading is due to fracture of microballoons and crack propagation through the resin matrix. High density microballoon foams (SF46) require higher loads for fracture and crack propagation. However they fail at lower loads due to debonding between interface of microballoon and resin matrix.

Figure 8 below shows stress (σ_p) distribution profile between two low density SF22 type adjacent microballoons. The distance between microballoons is represented by 'd' in the graph. It is seen that the stress σ_p is highest on the microballoon surface and diminishes away from it. Due to stress interaction between two microballoons, the overall stress is higher than stresses on an individual microballoon. The graph also shows change in stress profile because of the change in 'Y' (or concentration of microballoons). It can be seen that the stress increases around a microballoon, as the overall concentration of microballoons increases ('d' decreases) in the foam matrix. Therefore, increase in 'Y' translates to an increase in the brittleness of the material and results in early failure of the material. Figure 9 shows the stress variation on the surface of microballoon 1, when microballoon 2 is placed at different angular orientations. It is seen that stress gradually increases with angle θ to a maximum value at around 60° on the surface of the microballoon. Beyond this point, stress decreases back again to a lower value at 90°. Thus maximum stress intensity around a microballoon results because of microballoons oriented at an angle of 60° with respect to it.

It is concluded that stress concentration and stress intensity around microballoons is considerably high, which makes the material brittle. Since we are using very high volume fraction of microballoons, brittleness in the material tends to increase, and it is imperative to reduce this brittleness in order to increase damage tolerance of the material. Modification of the foam matrix using rubber and nanoclay particles would relieve stresses around microballoons and makes the foam matrix relatively ductile.

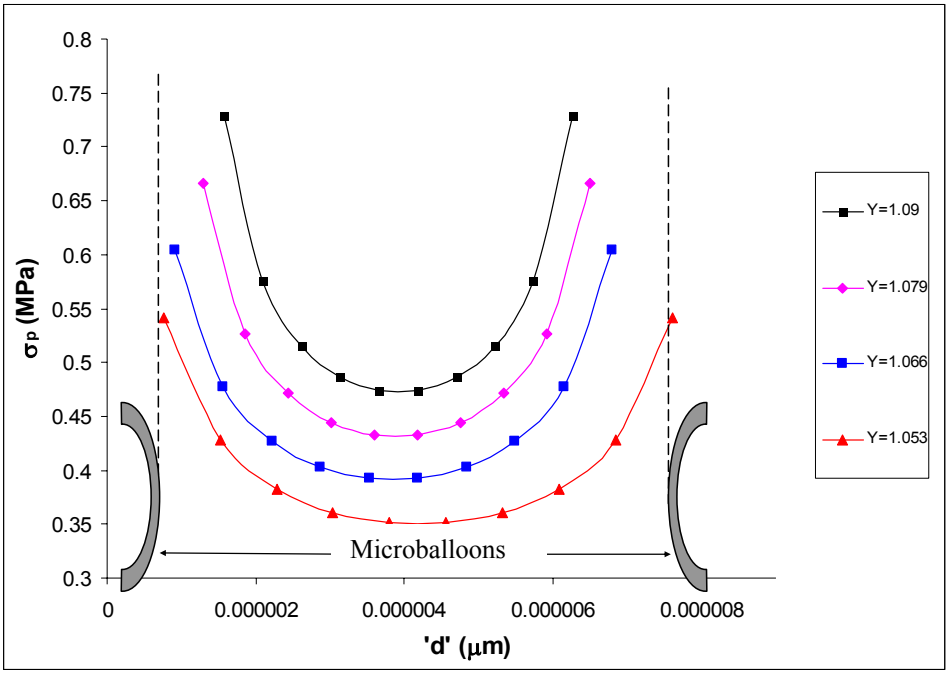

Figure 8. Stress distribution profile between two adjacent microballoons

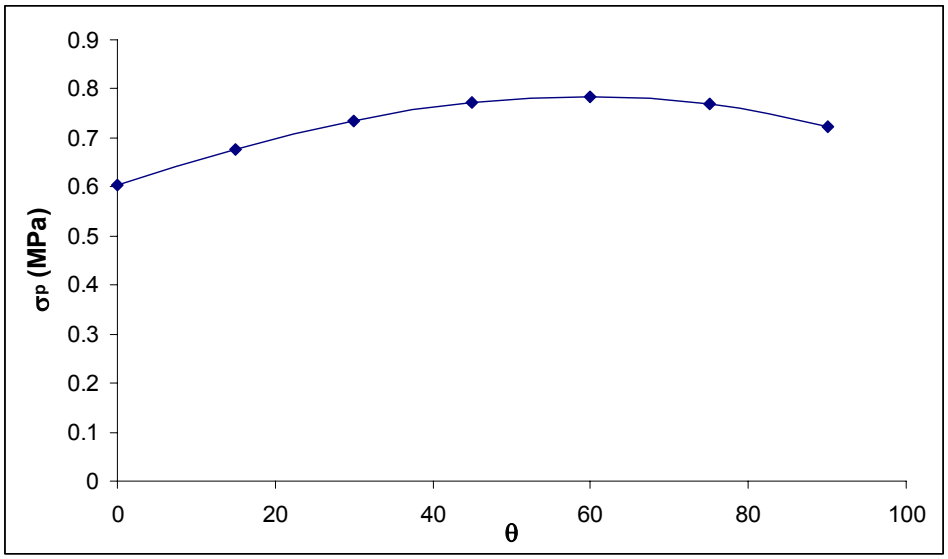

Figure 9. Stress profile on the surface of a microballoon due to interaction with another microballoon positioned at varying angular orientations

4.2 Experimental Study: Materials and Methods

4.2.1 Rubber Hybrid Syntactic Foam

4.2.1.1 Raw Materials

4.2.1.1.1 Wall Thickness Effects and Selection of Microballoons

Density and strength of microballoons of the same outer diameter is dependent on their wall thickness. The wall thickness of microballoons is defined in terms of a parameter called Radius Ratio, η, [40, 42] which is presented in Equation 14.

$$\eta = \frac{r_i}{r_o} \tag{14}$$

where r_i and r_o are the inner and the outer radii of microballoons. Increase in the value of η represents decrease in the microballoon wall thickness and corresponds to a decrease in microballoon density and strength. When the matrix and particle volume fractions are kept constant in hybrid foams, any change in mechanical properties of syntactic foams can be related to the change in microballoon η alone. The glass microballoons are brittle and give rise to small fragments upon fracture. These fragments occupy more volume than the volume of the material composing the microballoon due to spatial mismatch between them. It is known that if microballoons have η lower than the critical value, 0.71, the wall thickness of the micro balloons is too high and the resulting debris after fracture will occupy more volume than the microballoon before fracture [26]. Hence it is imperative to use microballoons of η greater than the critical value; so that the resulting debris occupies lesser volume after fracture and the stress concentration is reduced. This helps in further relieving the stress and in absorbing more energy by the foam specimen [40]. In the present study four types of microballoons of nearly the same average outer diameter, 40 μm, but different η values, all greater than the critical value of 0.71, are selected for the fabrication of hybrid foams.

4.2.1.1.2 Glass Microballoons

Glass microballoons are manufactured and supplied by 3M under the trade name Scotchlite. Physical properties of selected microballoons, supplied by the manufacturer, are presented in Table 3 below.

Table 3. Properties of microballoons.

Microballoon Type	Microballoon Size Distribution (μm)			Average True Particle Density (kg/m^3)	Average Wall Thickness (μm)	Pressure for Min. 80% Fractional Survival (MPa)	Radius Ratio η
	10^{th} percentile	50^{th} percentile	90^{th} percentile				
S22	20	35	60	220	1.26	2.76	0.9703
S32	20	40	75	320	1.86	13.79	0.9561
S38	15	40	75	380	2.23	27.58	0.9474
K46	15	40	70	460	2.74	41.37	0.9356

All the selected microballoon types have nearly the same mean outer diameter of 40 μm. The mean inner diameter has been calculated by taking a difference in the average true particle density of solid and hollow particles made of same material. Subsequently, the average wall thickness of microballoons is calculated. The difference in wall thickness of different types of microballoons causes the difference in their density. The calculated η for all types of microballoons is also given in Table 3. The microballoon type in Table 3 is the manufacturer's code for the identification of selected microballoons.

4.2.1.1.3 Rubber Particles

Four types of microballoons and two types of rubber particles are used in the fabrication of eight types of foam samples in the present study. The rubber particles selected for the study are (-)80 and (-)170 mesh size. These rubber particles are commercially supplied by Rouse Polymerics under the trade name GF-80 and GF-170 and have a mean particle size of 75 and 40

μm, respectively, and are referred to as R75 and R40 in this study. The specific gravity of rubber particles is in the range of 1.12-1.15 as supplied by the manufacturer. These particles are produced from the waste tires by mechanical grinding process. Rubber particles of R75 and R40 type are shown in scanning electron micrographs (SEM) in Figure 10 and Figure 11, respectively. Figure 12 shows a high magnification micrograph of R40 particles.

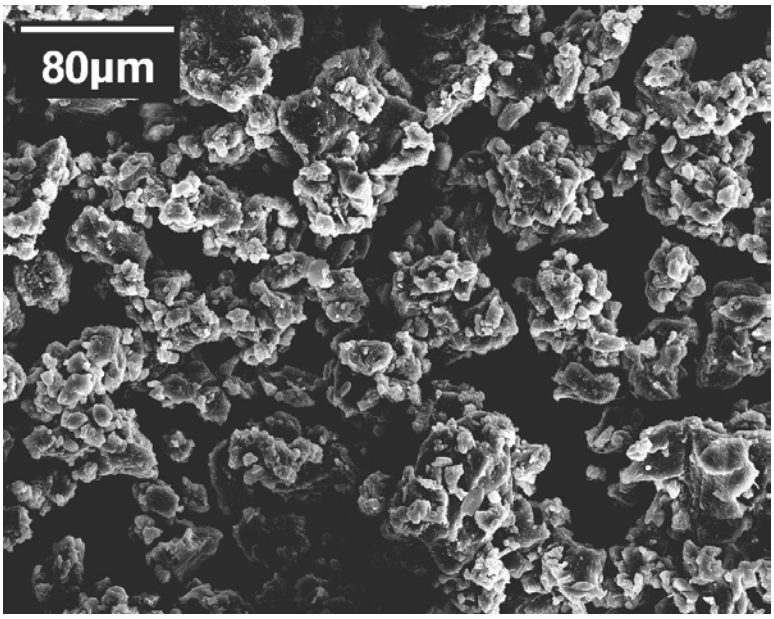

Figure 10. Scanning electron micrograph of R40 rubber particles.

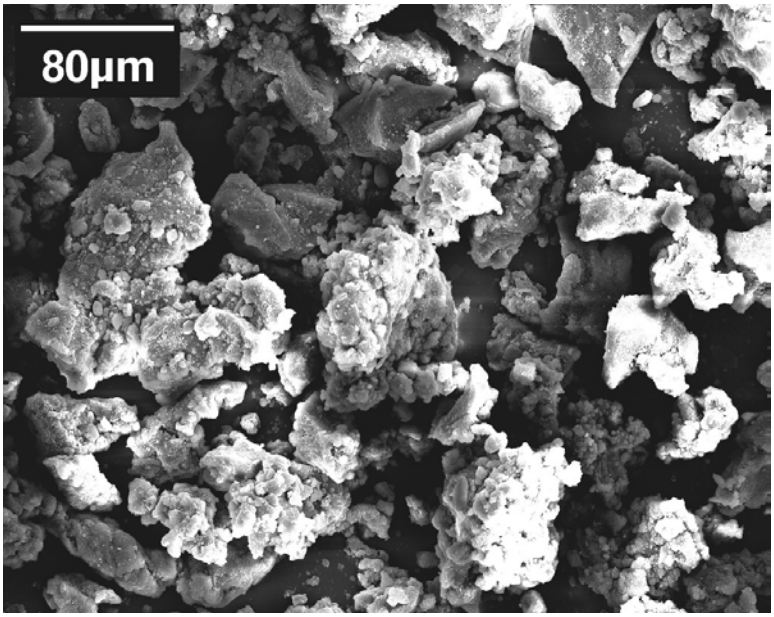

Figure 11. Scanning electron micrograph of R75 rubber particles.

Figure 12 shows a micrograph of a rubber particle used in the present study. The rubber particles are produced from heavy shearing of waste tires and possess a highly irregular surface

as seen from the SEM micrograph above. Due to this, a very large interface is obtained between the rubber particles and matrix material.

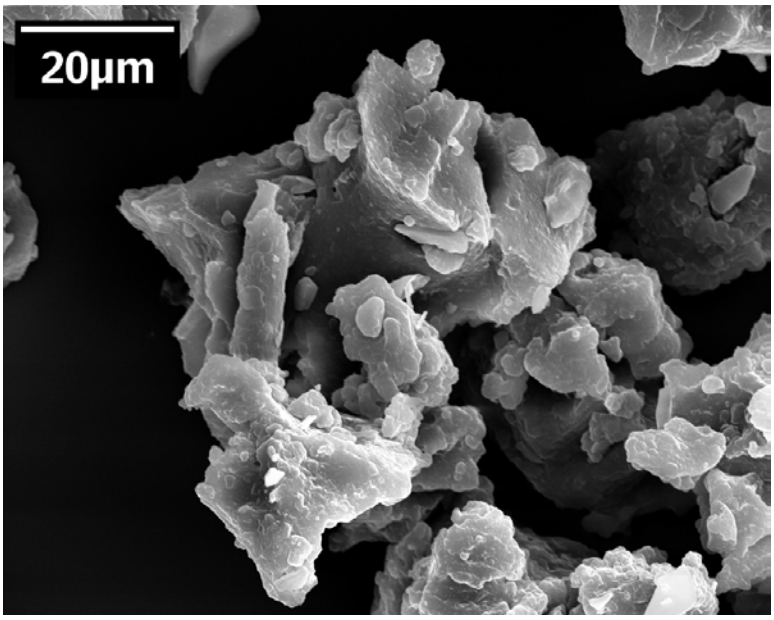

Figure 12 High magnification SEM micrograph of a rubber particle used in the study.

4.2.1.1.4 Resin System

Epoxy resin D.E.R. 332, manufactured by DOW Chemical Company is used as matrix material. This resin blends easily with other epoxy components to obtain an optimum block hardness for samples. It appears colorless to yellow liquid, and has a specific gravity of 1.16 at 25°. It's epoxide equivalent is between 171-175.

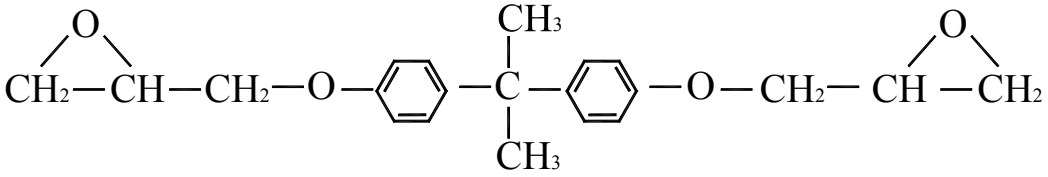

Figure 13. Chemical formula of the D.E.R. 332 epoxy resin

Amine based hardener D.E.H. 24 is used with the selected epoxy resin. This epoxy curing agent, aliphatic polyamine hardener, triethylenetetraamine (TETA, $C_6H_{18}N_4$) that offers a short pot life and cures in minutes with liquid epoxy resins. Its amine hydrogen equivalent weight is approximately 24. It has a viscosity of 19.5-22.5 mPa.s and a density of 0.98g/ml at 25°C.A diluent C_{12}-C_{14} is mixed with the epoxy resin in 5% by weight quantity to reduce its viscosity. Reduction in viscosity makes it easier to mix higher volume fraction of particles in the matrix resin. Its equivalent epoxide weight (EEW) is nearly 285. It is commercially available as ERISYS-8, and when added in 5% by weight quantity it brings down the viscosity of the resin to nearly half its value, and increases the epoxy tensile strength and modulus.

4.2.1.2 Fabrication

For comparison with syntactic foams fabricated in earlier experiments [40], similar volume fractions of the constituent materials have been used in the present experiment. Volume fractions of the matrix resin, rubber particles and the microballoons have been kept constant at 0.35, 0.02 and 0.63 respectively. The volume fraction of microballoons has been reduced from 0.65 in earlier experiments [40] to 0.63 in order to allow the addition of 0.02 volume fraction of rubber particles.

Mechanical mixing followed by casting in stainless steel molds is used as the fabrication process of rubber syntactic foams. A silicone based Dow Corning 111 Sealant and Lubricant is used as release agent in the molds. It has a specific gravity of 1, works in a temperature range of -40 to 200°C, and has bleed characteristics of 0.5% in 24 hours at high temperatures. Cast foam slabs are cured at room temperature for at least 36 hrs and then post cured for 3 hrs at 100±3°C.

4.2.1.3 Specimen Nomenclature

The specimen nomenclature for hybrid foams is a six digit alphanumeric code. The first letter R represents rubber particles. Next two digits represent size of rubber particles. The fourth letter M represents microballoons and last two digits are related to the true particle density of the glass microballoons, e.g. 22 is used in the nomenclature for microballoon density of 220 kg/m^3.

A sample code for hybrid foam is R75M22, which contains rubber particles of 75 μm size and microballoons of 220 kg/m^3 density. The syntactic foam samples containing only glass microballoons in epoxy matrix have a four digit alphanumeric code such as SF22. Table 5 shows the nomenclature and measured density of syntactic foams without rubber particles. Here first two letters represent Syntactic Foam and next two digits are related to the true particle density of microballoons as explained for hybrid foams.

4.2.1.4 Mechanical Testing

4.2.1.4.1 Compression Test

ASTM C365-94 standard [32] is adopted for the compression testing of the hybrid foams. This standard recommends a specimen size of 25 × 25 × 12.5 mm^3 for length, width and height of the specimen.

The specimens are tested under a constant compression rate of 1.3 mm/min. Load-displacement data is obtained in the tests and converted to stress-strain information to calculate compressive strength and modulus of hybrid foams. A computer controlled MTS 810 mechanical test system is used to carry out the compression tests.

4.2.1.4.1.1 Density Measurement

The density of hybrid foams is measured by measuring weight and volume of at least five specimens of 25 × 25 × 12.5 mm^3 size of each type of composite. Measured densities of various hybrid foams are given in

Table 4.

Table 4. Nomenclature and Density of fabricated hybrid foams.

Type of Rubber Particles	Size of Rubber Particles (□m)	Microballoon Type	Corresponding Hybrid Syntactic Foam Type	Measured Density (kg/m^3)
R40	40	S22	R40M22	504
		S32	R40M32	563
		S38	R40M38	606
		K46	R40M46	601
R75	75	S22	R75M22	504
		S32	R75M32	516
		S38	R75M38	605
		K46	R75M46	617

Table 5 Nomenclature and Density of fabricated syntactic foam slabs.

Microballoon Type	Corresponding Syntactic Foam Type	Syntactic Foam Density (kg/m^3)
S22	SF22	493
S32	SF32	545
S38	SF38	575
K46	SF46	650

4.2.1.4.1.2 Results and Discussion

Compressive strength and modulus values calculated from the stress-strain graphs of hybrid foams tested in this study are presented in Figure 14 and Figure 15, respectively. Strength and modulus values of syntactic foams containing corresponding types of microballoons are also presented in these figures for comparison.

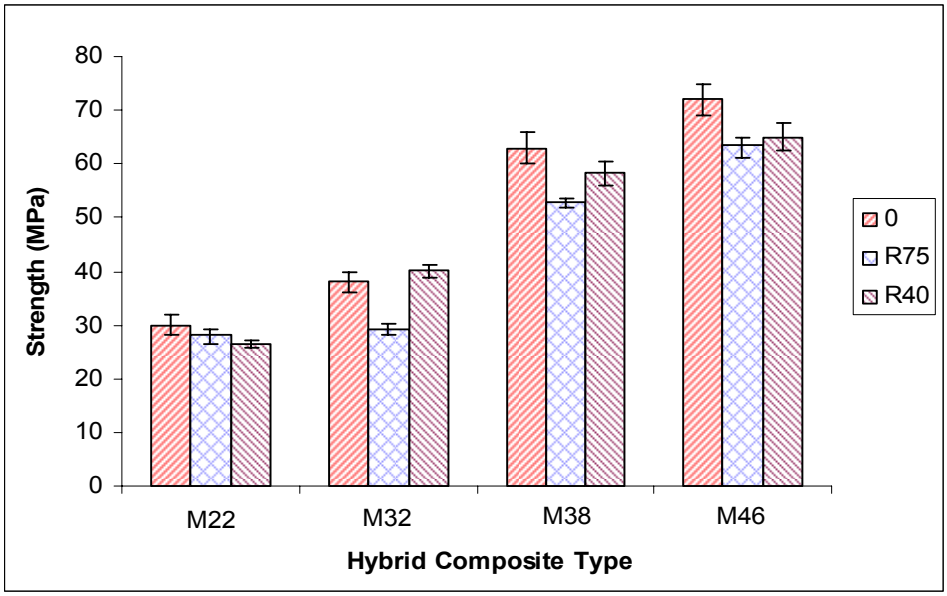

Figure 14. Compressive strength of various hybrid foams containing R75 and R40 rubber particles compared to the corresponding syntactic foams without rubber particles.

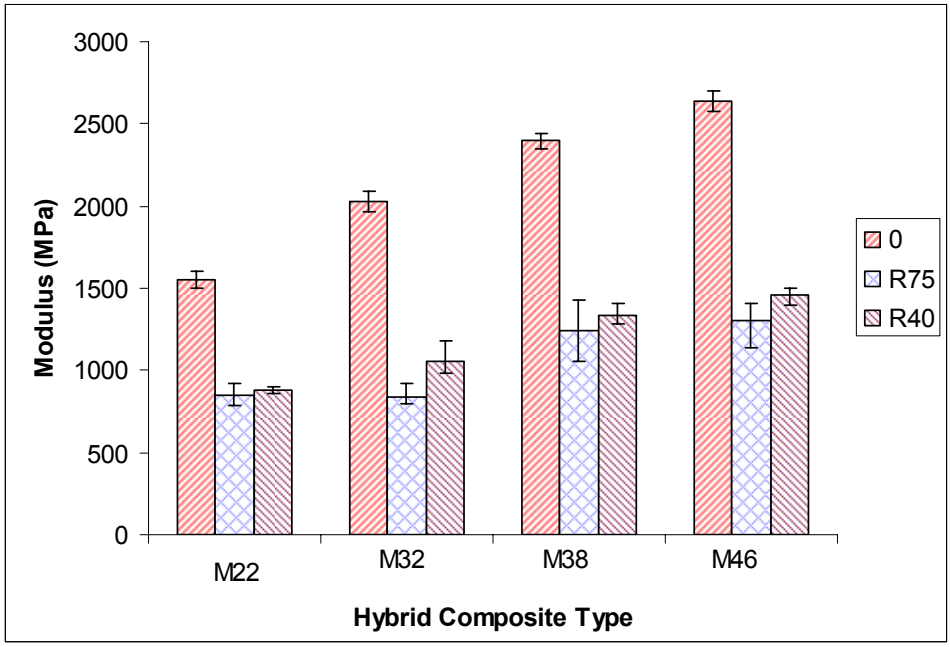

Figure 15. Modulus of various hybrid foams containing R75 and R40 rubber particles compared to the corresponding syntactic foams without rubber particles.

The effect of microballoon η is found to be similar in hybrid foams and syntactic foams. Decrease in η, which corresponds to increase in microballoon wall thickness and strength, leads to increase in the strength of the hybrid foams. It is observed as a general trend that hybrid foams containing smaller size rubber particles have higher strength and modulus. The same volume fraction of smaller size particles have higher surface area compared to the larger size particles.

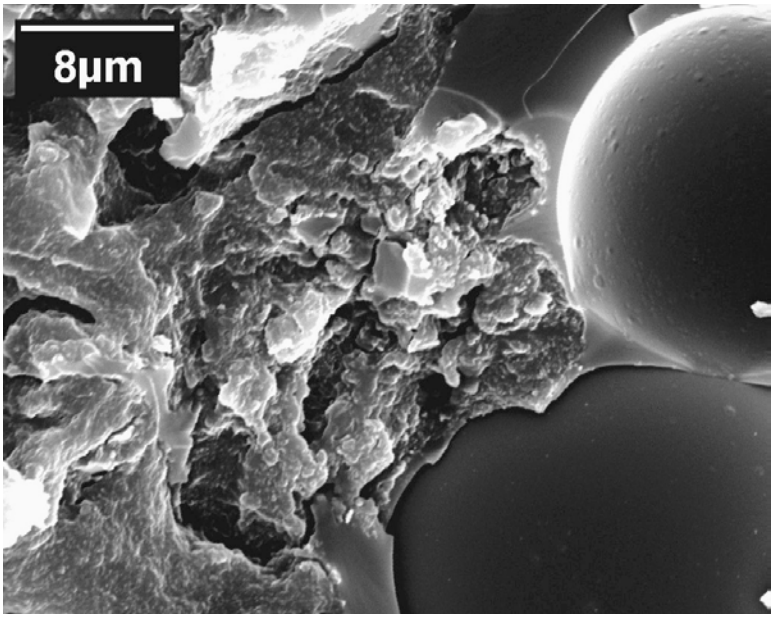

Figure 16. A rubber particle in matrix material. There is no definite interface between the particle and matrix resin.

Hence, the difference in the mechanical properties can be related to the difference in the interfacial area between the particles and the matrix resin in the hybrid foams. Several SEM micrographs were taken in order to analyze the interface between rubber particles and matrix resin. Figure 16 and Figure 17 show a rubber particle embedded in epoxy matrix.

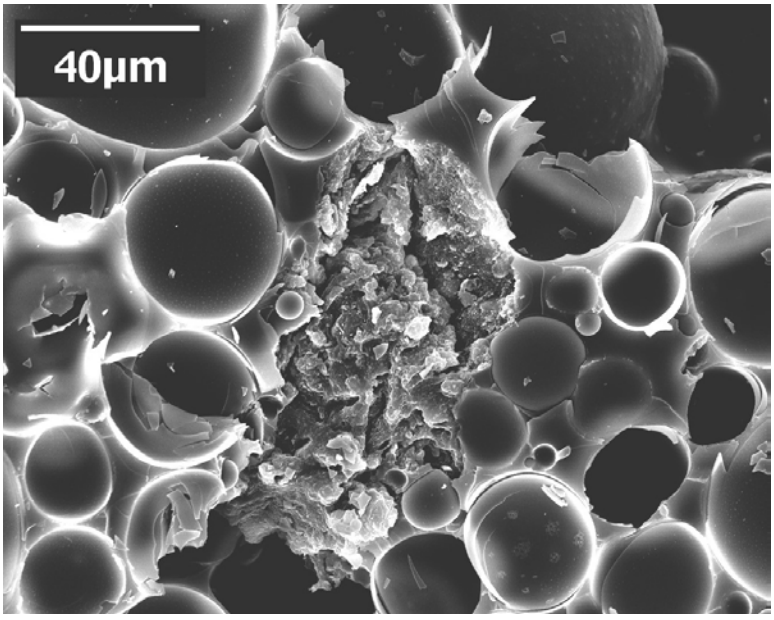

Figure 17. Another micrograph of a rubber particle in matrix material.

There is no visible interface between rubber particles and matrix materials in the Figure 16 above, which means that the interfacial bonding between rubber and matrix resin is good. Hence, the higher strength of hybrid foams containing the same volume fraction of smaller size rubber particles is justified. Low modulus of rubber particles is expected to decrease the modulus of hybrid foams. The volume fraction of rubber particles in the hybrid foams is only 0.02 but it still has a pronounced effect on the modulus of hybrid foams because the fraction of matrix material in hybrid foams is 0.35, which makes rubber to matrix resin ratio considerably high, nearly 0.057. It is observed that the modulus has decreased by about 50% due to the incorporation of rubber particles. It is also noted from Figure 14 and Figure 15 that there is only about 10% reduction in the compressive strength of most hybrid foams compared to the corresponding syntactic foams.

Comparison of representative stress-strain behavior of hybrid foams containing R75 and R40 type of rubber particles with various kinds of microballoons is shown in Figure 18 and Figure 19, respectively.

The maximum strain shown in the figures are not the final fracture points of the specimen. The testing was stopped if the specimen did not fracture until 40% strain. Stress-strain curves for representative specimens of corresponding four types of syntactic foams (without rubber particles) are presented in Figure 20 for comparison with those of hybrid foams. One of the major concerns in the stress-strain curves of syntactic foams is that foams containing microballoons of higher density deform only about 8-10% before failure. The specimens are found to fracture at this strain due to pronounced cracking and the tests were stopped.

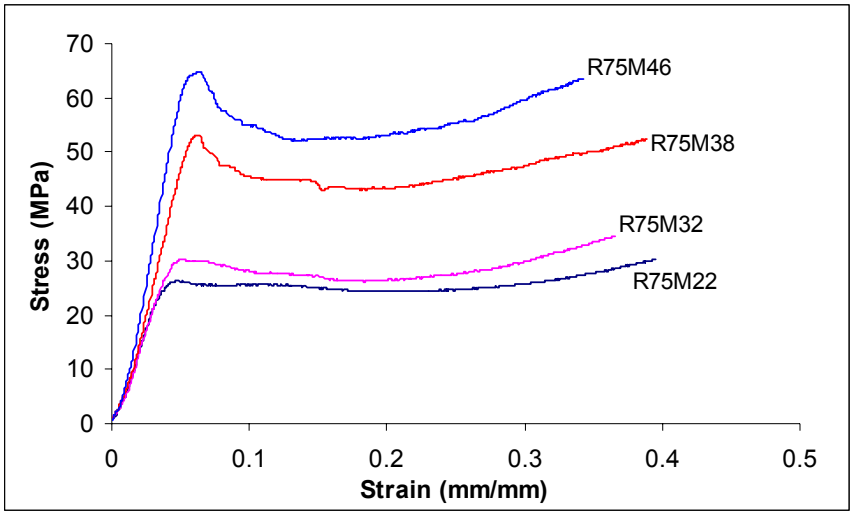

Figure 18. Representative stress-strain curves for hybrid foams containing R75 type rubber particles and various types of microballoons.

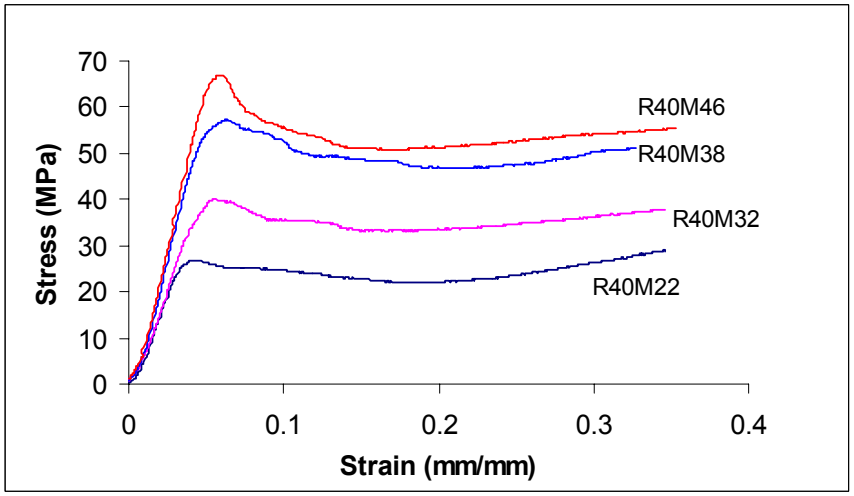

Figure 19. Representative stress-strain curves for hybrid foams containing R40 type rubber particles and various types of microballoons.

In syntactic foams it was observed that strain at peak stress was around 3.5%, irrespective of the microballoon η. However, it is observed in the stress-strain curves for all types of hybrid foams that the peak stress value occurs at around 6% strain. The most significant mechanical property enhancement in the hybrid foams is the considerable reduction in brittleness of higher density foams such as SF38 and SF46 due to the incorporation of rubber particles. A common feature in Figure 18, Figure 19 and Figure 20 is the appearance of stress plateau in curves for all kinds of foams. Such trend is observed by other researchers also [14, 15, 26]. The region in the stress strain curves where stress remains constant during compression is called stress plateau region. This is the region where a dynamic equilibrium exists between exposure of hollow space enclosed within microballoons and space consumption during compression. This process is called densification, which prevents the stress for increasing during the process of compression

and the appearance of the plateau region. At the end of the plateau region increase in stress is observed as a sign of completion of densification of the material.

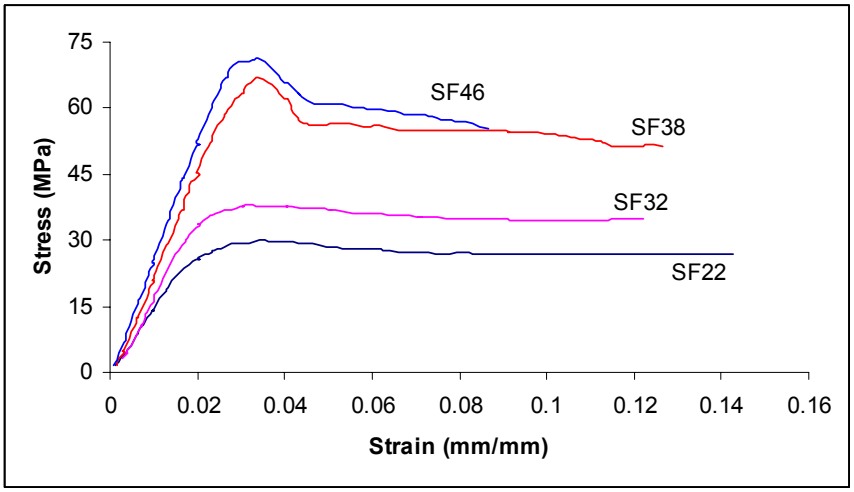

Figure 20. Stress-strain curves for various syntactic foams for comparison with those of hybrid foams.

The length of the plateau region, which is the region of energy absorption during compression, is considerably higher for hybrid foams, Figure 18 and Figure 19, compared to syntactic foams, Figure 20. It can be observed in Figure 20 that the plateau regions for high density syntactic foams SF38 and SF46 terminate and a decreasing trend in stress is observed around 12 and 6% strain respectively. Low density foams SF22 and SF32 could be compressed to 15-20% strain before failure. The primary reason for breakdown in the plateau region for SF38 and SF46 foams, containing lower η microballoons, was the initiation of cracks in the specimens under the lateral component of the applied compressive stress, called secondary tensile stress, due to Poisson's Ratio effect [26]. The incorporation of rubber particles leads to reduction in brittleness of matrix resin in hybrid foams and delays initiation of cracks. The crack propagation rate may also be delayed in hybrid foam specimens due to the ductility of rubber particles and the possibility of bridging of micro-cracks by ductile rubber particles. As a result, all kinds of specimens could be compressed to about 40% strain and achieved a stage where densification was complete and stress started increasing after plateau region. Specimens were able to absorb higher amount of energy demonstrating better compressive toughness. Figure 21 compares compression fracture features of a specimen of R75M22 hybrid foam with the features of SF22 syntactic foam.

Similarity is observed in the fracture features of both specimens. Signs of considerable amount of plastic deformation observed in hybrid foam near the edges represent flow of material towards edges of the specimen due to its low modulus. Deformation features of R75M46 type hybrid foam specimen are compared with features of SF46 syntactic foam in Figure 22.

Cracking due to secondary tensile stresses leads to failure of SF46 type specimen at lower strain of only about 10%. Two of these cracks are shown by arrow marks in Figure 22. A hybrid foam specimen containing K46 microballoons is also shown in the same figure. This specimen also shows similar fracture features but at about 40% strain compared to about 10% compression of the syntactic foam specimen. Microscopic fracture features of R40M22 and R40M46 are

shown in Figure 23 and Figure 24, respectively. Broken microballoons can be observed all over the fracture surface in these micrographs, which is a common feature of compressive fracture.

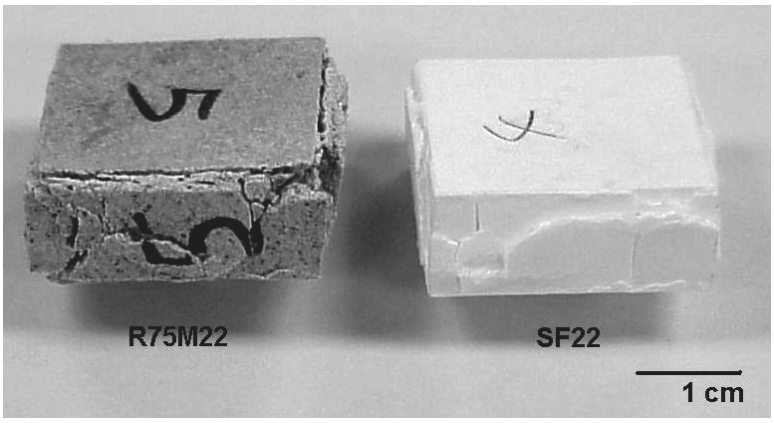

Figure 21. Comparison of deformation features of hybrid foam and syntactic foam containing S22 type of low density microballoons.

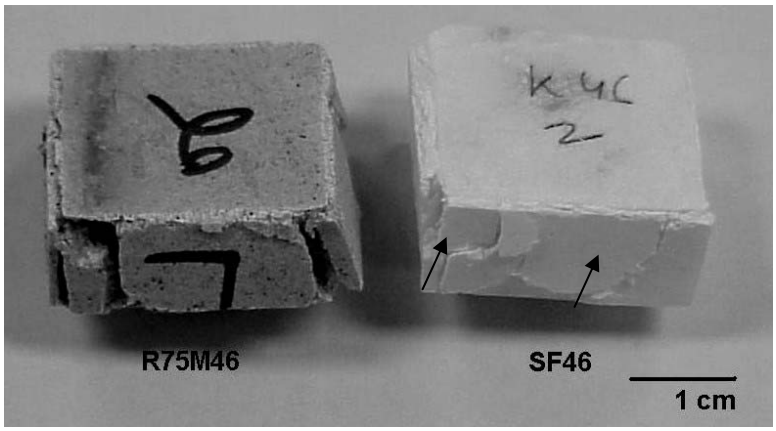

Figure 22. Comparison of deformation features of hybrid foam and syntactic foam containing K46 type of high density microballoons. Cracking under secondary tensile stresses is shown by arrow marks in syntactic foam samples.

4.2.1.4.1.3 Conclusion

It is observed in the study that inclusion of rubber particles in syntactic foams has considerably enhanced the fracture strain of all types of syntactic foams with a small decrease in their compressive strengths. For low density foams the fracture strain has increased by about two times with only about 10% decrease in compressive strength. Experimental results show that the enhancement in ductility is achieved in hybrid foams without any significant loss in strength. Compressive modulus is found to decrease by about 50%, whereas decrease of about 10% is observed in the compressive strength due to the incorporation of rubber particles. The fracture strain of high strength hybrid foams, especially the foams containing high density/low η microballoons, is improved significantly due to the presence of rubber particles. Considerable enhancement in compressive toughness due to the incorporation of rubber particles can be observed in terms of significantly extended stress plateau region in stress-strain curves of hybrid foams of all kinds.

The study also demonstrates potential of using environmentally hazardous waste tire rubber particles in the fabrication of high performance composite materials. Waste tires have become an environmental hazard over the years and occupy huge landfill areas. This study effectively demonstrates one possible method of recycling waste tires and also contributes towards developing environmentally friendly composites.

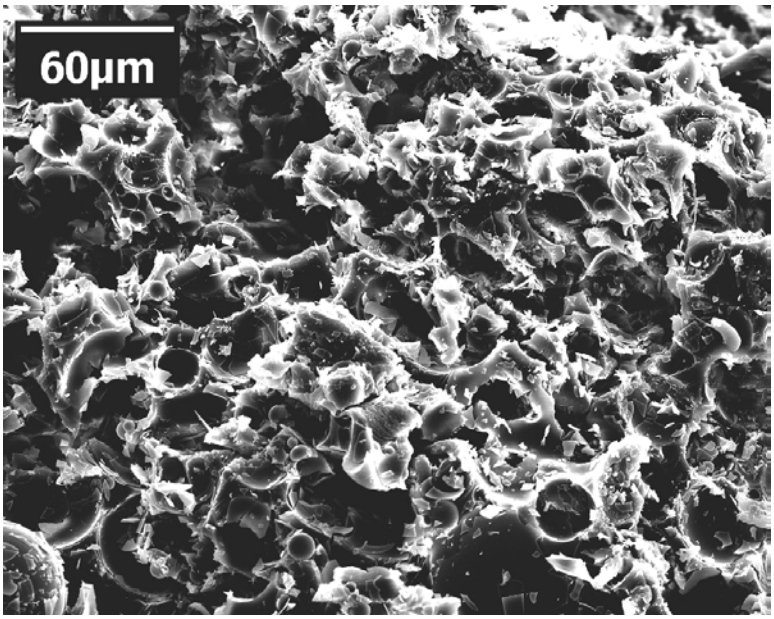

Figure 23. Fracture surface of a R40M22 low density hybrid foam showing extensive damage to microballoons.

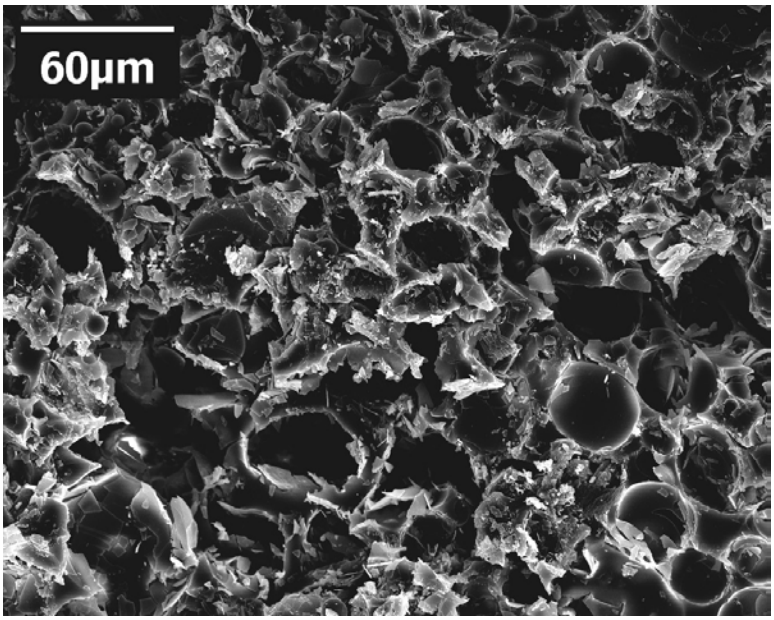

Figure 24. Fracture surface of R40M46 specimen showing fracture of microballoons.

4.2.1.4.2 Flexural Strength: Three Point Bending Test

ASTM D790 standard [44] is adopted for the flexural testing of all foams. This standard recommends a span length to thickness ratio of 16:1 for the 3-point bend tests. The test configuration and the conventions used to define specimen dimensions are shown in Figure 25.

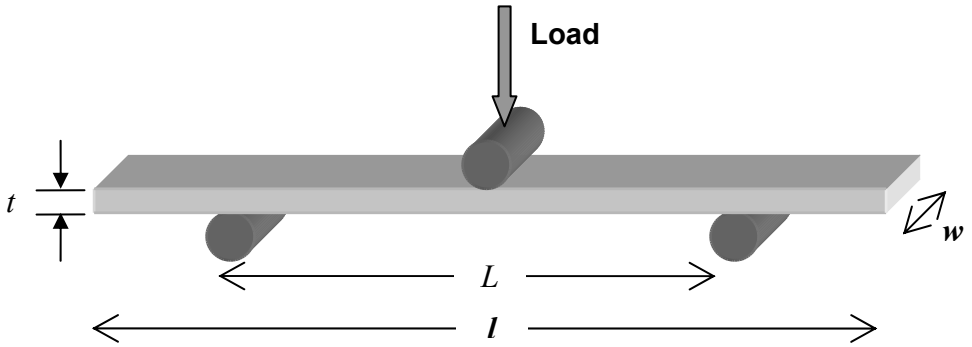

Figure 25 Specimen dimensions and 3-point bending test configuration

All foam specimens have a specimen length (l) and width (w) of 110 and 15 mm respectively. The average span length (L) is 64 mm and average sample thickness (t) is 4 mm. At least five specimens of each type of foam are tested in the three point bend configuration as shown in Figure 25.

A computer controlled MTS QTEST/150 mechanical test system is used to carry out the flexural tests. Load-displacement data obtained in the tests is used to calculate bending stress and deflection. Tangent modulus is calculated for all specimens using Equation 15 below.

$$E_B = \frac{L^3 m}{4bd^3} \quad (15)$$

Where m is the stiffness or the slope of the load displacement curve in the linear elastic region, L is the span length, b is the width and d is the depth of the specimen. The flexural strength is calculated using Equation 16.

$$\kappa = \frac{P}{\delta} \quad (16)$$

Where κ, P and δ represent flexural stiffness, load and deflection, respectively.

4.2.1.4.2.1 Density Measurement

The density of foams is measured by measuring weight and volume of at least five specimens of 64 × 12 × 4 mm^3 size. Measured densities and calculated void volume fraction of pure syntactic foams and rubber hybrid foams are given in Table 6 and Table 7 respectively. The void volume fractions are calculated by using measured and theoretical densities in Equation 17.

$$Void\ Content = \frac{\rho_t - \rho_m}{\rho_t} \quad (17)$$

Where, ρ_t is theoretical density and ρ_m is measured density of syntactic foams. The theoretical densities of all types of syntactic foams are calculated using Rule of Mixtures.

Table 6 Nomenclature and Density of fabricated syntactic foam slabs.

Microballoon Type	Corresponding Syntactic Foam Type	Syntactic Foam Density (kg/m^3)	Void Volume %
S22	SF22	493	7.78
S32	SF32	545	16.04
S38	SF38	575	13.53
K46	SF46	650	16.76

Table 7 Composition and density of rubber hybrid syntactic foams

Type of Rubber Particles	Size of Rubber Particles (□m)	Microballoon Type	Corresponding Hybrid Syntactic Foam Type	Measured Density (kg/m^3)	Void Volume %
R40	40	S22	R40M22	499.50	7.50
		S32	R40M32	519.50	14.83
		S38	R40M38	599.65	7.75
		K46	R40M46	618.27	11.68
R75	75	S22	R75M22	513.49	4.91
		S32	R75M32	566.60	7.11
		S38	R75M38	602.31	7.34
		K46	R75M46	607.12	13.27

4.2.1.4.2.2 Results and Discussion

The comparison of flexural properties of syntactic foams needs to be carried out with respect to two parameters. The first one is microballoon η, for the same foam composition, and the second one is the syntactic foam composition, for the same microballoon η.

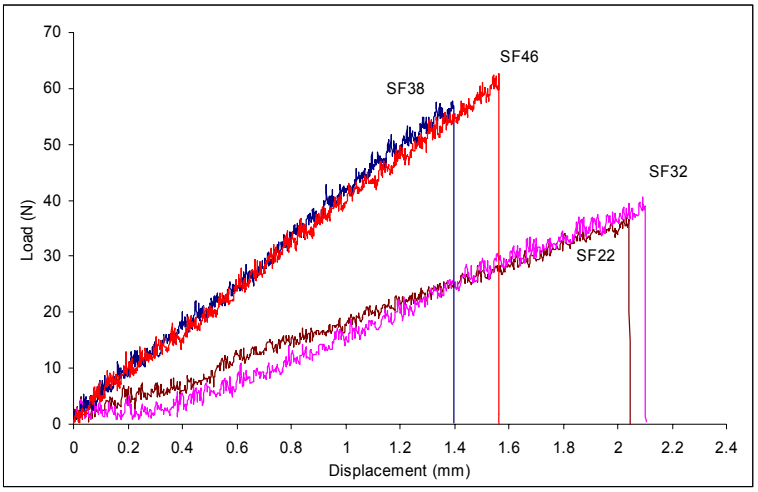

Figure 26. Representative load displacement curve for plain syntactic foams.

Figure 26 to Figure 28 show representative load displacement curves obtained from flexural testing of foams with various types of syntactic foams. These figures show that all types

of syntactic foams fail in the brittle fracture mode at the end of the elastic region. The load-displacement data is used to calculate the flexural modulus, stiffness and strength. All these properties are discussed below.

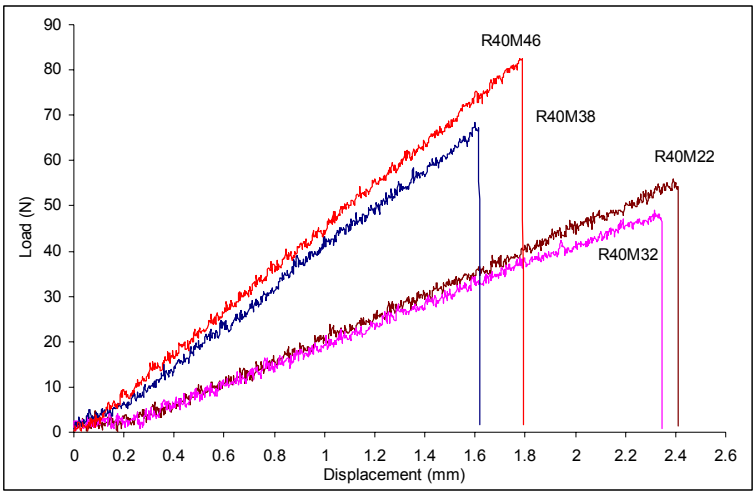

Figure 27. Representative load displacement curve for hybrid foams containing R40 type rubber particles.

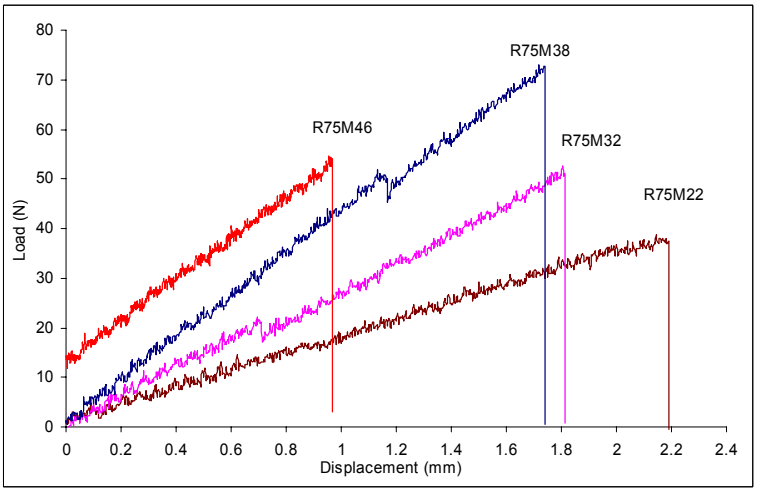

Figure 28. Representative load displacement curve for hybrid foams containing R75 type rubber particles.

Figure 29 shows a comparison of fracture strain values for various syntactic foams. Nearly 18% increase in fracture strain is observed with addition of both R75 and R40 type rubber particles. Figure 30 shows the comparison of flexural toughness as area under curve for various syntactic foams. As a general trend it is seen that the area under curve has increased upon the addition of R75 and R40 type rubber particles. Figure 31 and Figure 32 show comparisons of flexural stiffness and flexural modulus, respectively, for various types of foam samples. It can be noticed that the modulus and stiffness increase with decrease in microballoon η from SF22 to SF38 type foams and then decreases slightly for SF46 type foams. Similar trends are observed for all kinds of hybrid foams also.

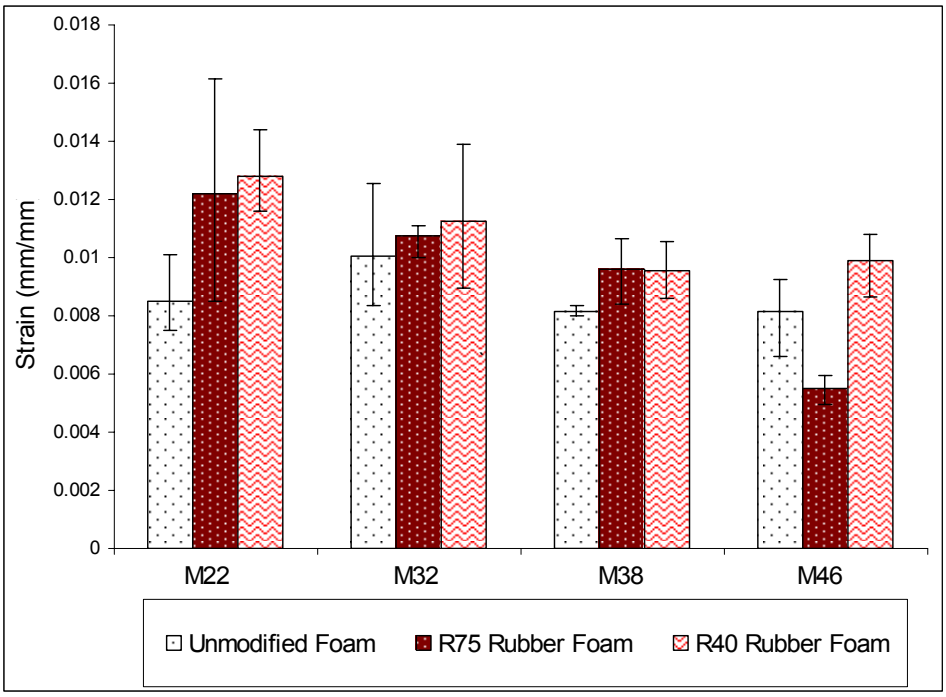

Figure 29. Comparison of strain values for plain syntactic foams and hybrid foams with R75 and R40 type rubber particles.

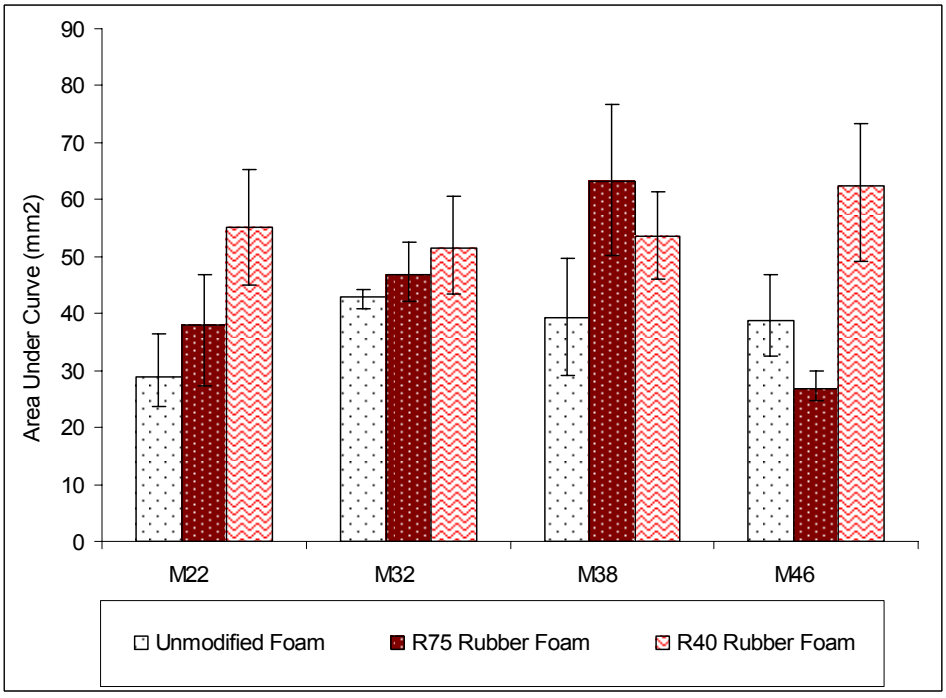

Figure 30. Comparison of flexural toughness as area under curve for plain syntactic foams and hybrid foams with R75 and R40 type rubber particles.

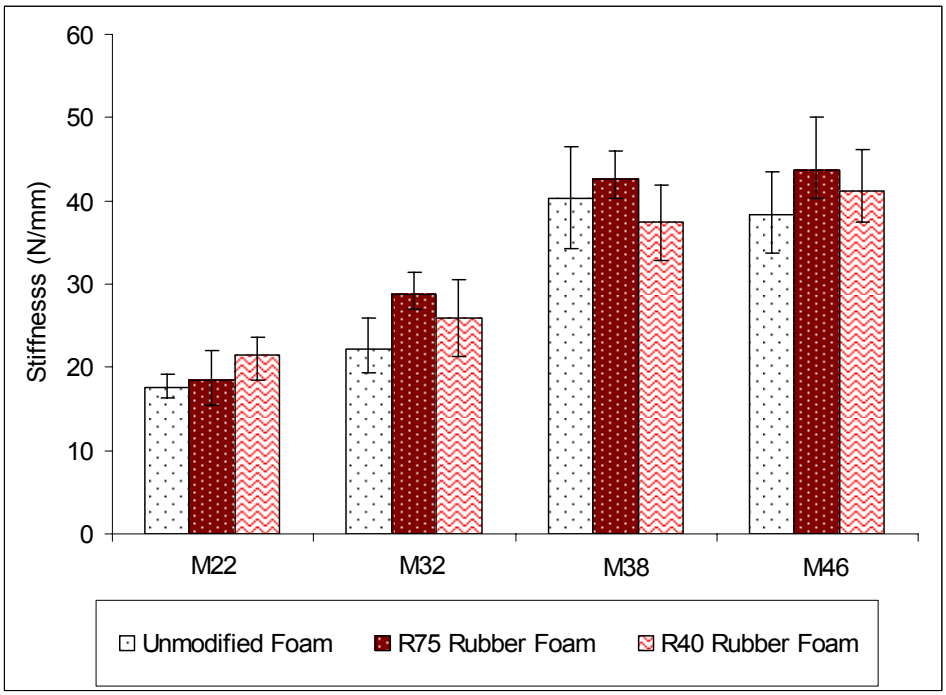

Figure 31. Stiffness comparison for various syntactic foam samples

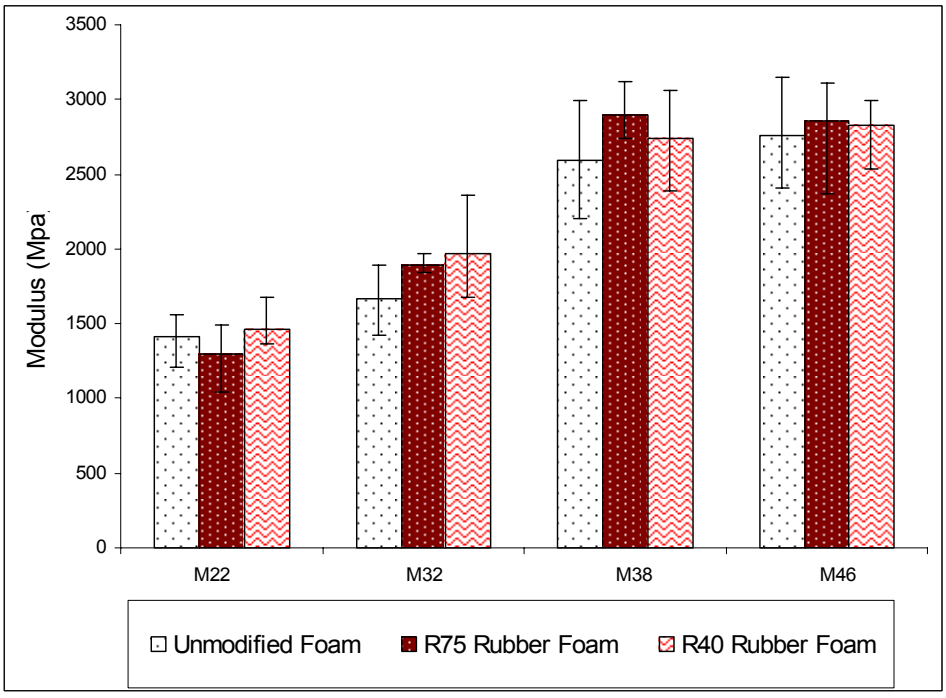

Figure 32. Comparison of tangent modulus for various types of foam samples.

The pronounced effect of η on the flexural modulus and stiffness can be related to the increasing microballoon strength with decreasing η. The stress conditions in the specimen and possible failure modes are shown schematically in Figure 33.

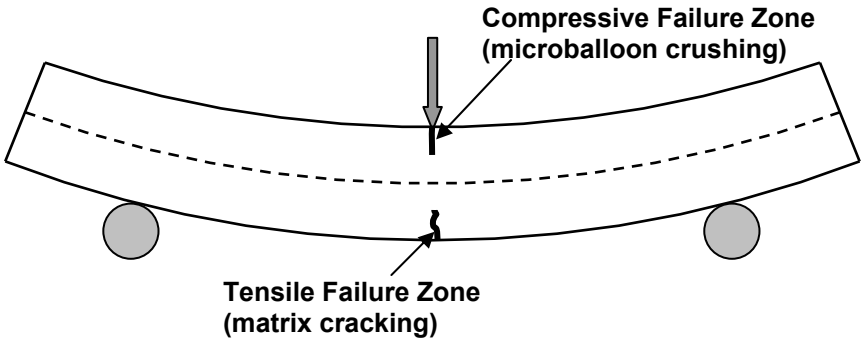

Figure 33. Stress conditions and failure modes in syntactic foams in three-point bend tests.

Figure 34 and Figure 36 shows the crack pattern seen in plain, rubber hybrid and nanoclay hybrid syntactic foams made from microballoons of various densities. Similar crack propagation and failure pattern is seen in all type of foam specimens.

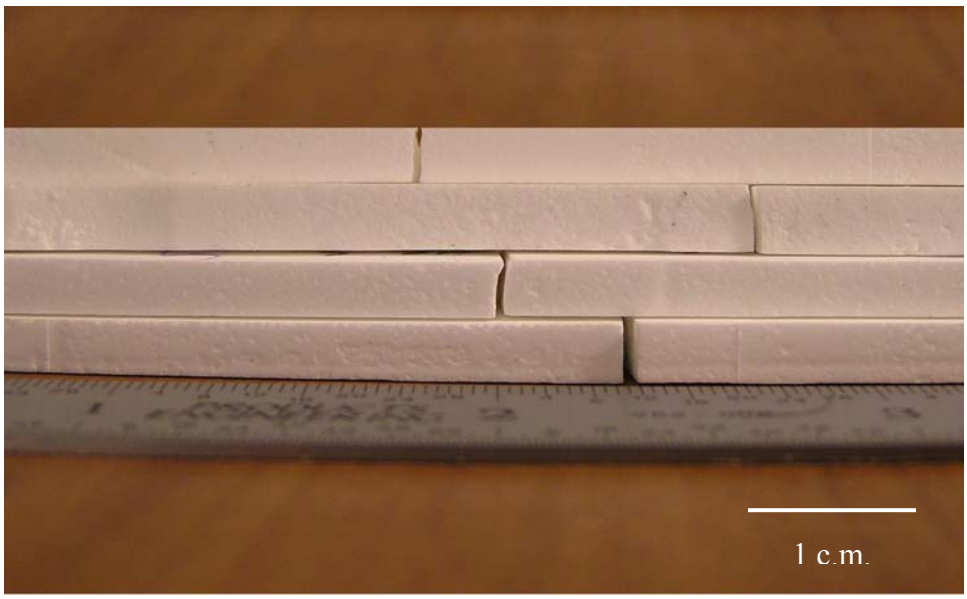

Figure 34. Crack pattern seen in various types of plain syntactic foams

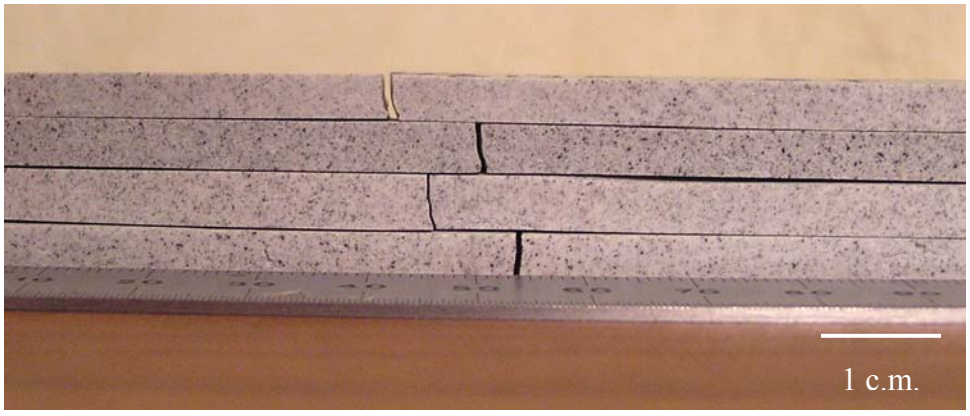

Figure 35. Crack pattern seen in rubber hybrid syntactic foams containing various types of microballoons

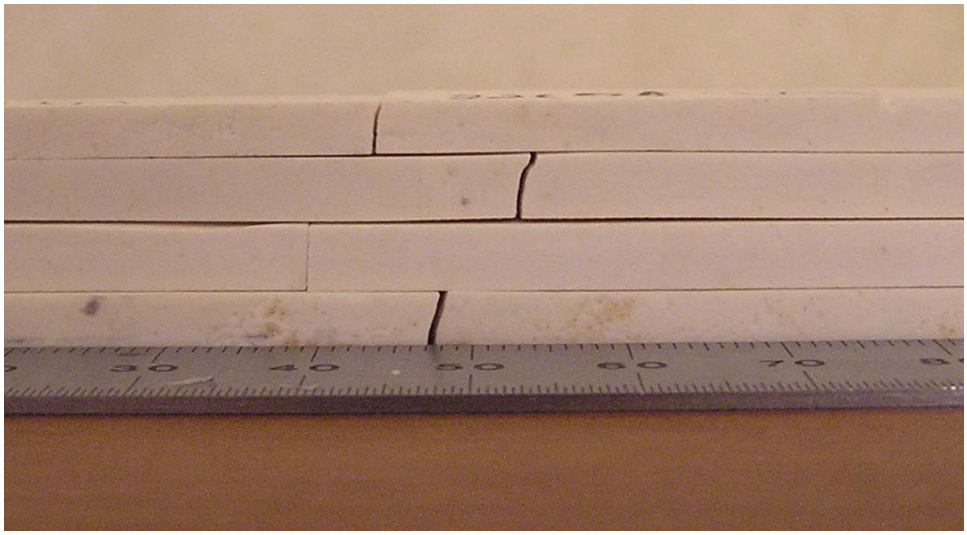

Figure 36. Crack pattern seen in nano hybrid syntactic foams containing various types of microballoons

All hybrid foams also show a similar pattern of crack propagation and failure. Crack originates on the tensile side (bottom) of the specimens shown and propagates to the top resulting in failure.

The fracture of microballoons may start even at small deflection in SF22 type microballoons because of their low strength. The strengths of microballoons can be compared by the values presented in Table 3. The maximum stress is generated at the surfaces of the specimen and can be calculated by Equation 18.

$$\sigma = \frac{3PL}{2bd^3} \tag{18}$$

Substituting the specimens dimensions used in the present testing it is calculated by Equation 18 that 5 MPa of stress will be generated in the top and bottom layers of the specimen only at a deflection of 0.3 mm. Considering that the final specimen failure takes place at a deflection of over 1 mm, the microballoon fracture is expected to take place much before the final failure of SF22 foams. Similarly, the fracture strength of S32 microballoons is also well below the fracture strain of corresponding syntactic foams in flexural testing. However, when similar calculations are carried out for SF38 and SF46 type foams then it is observed that the specimens fail at lower strength than the microballoon fracture strength. Hence, it is expected that in SF22 and SF32 type foams the failure under flexural loading is significantly affected by the microballoon fracture. However, in SF38 and SF46 type specimens the matrix failure is the primary failure phenomena because the microballoon fracture strength is greater than the flexural strength of the syntactic foams. Since the fracture of significant amount of microballoons is not expected in SF38 and SF46 type foams, their properties depend on the matrix properties and show nearly the same level of stiffness and modulus.

There is no significant difference observed in the modulus and stiffness of hybrid foams compared to the plain syntactic foams. The volume fraction of rubber particles is restricted to only 2% which may not be sufficient to cause a significant difference in the flexural elastic constants of hybrid foams.

Figure 37 shows a comparison of flexural strength of various types of syntactic foam samples. The effect of microballoon η appears to be similar to that on the flexural stiffness and modulus. Flexural strength of foams is seen to increase with a decrease in η, and remain nearly constant for SF38 and SF46 type foams.

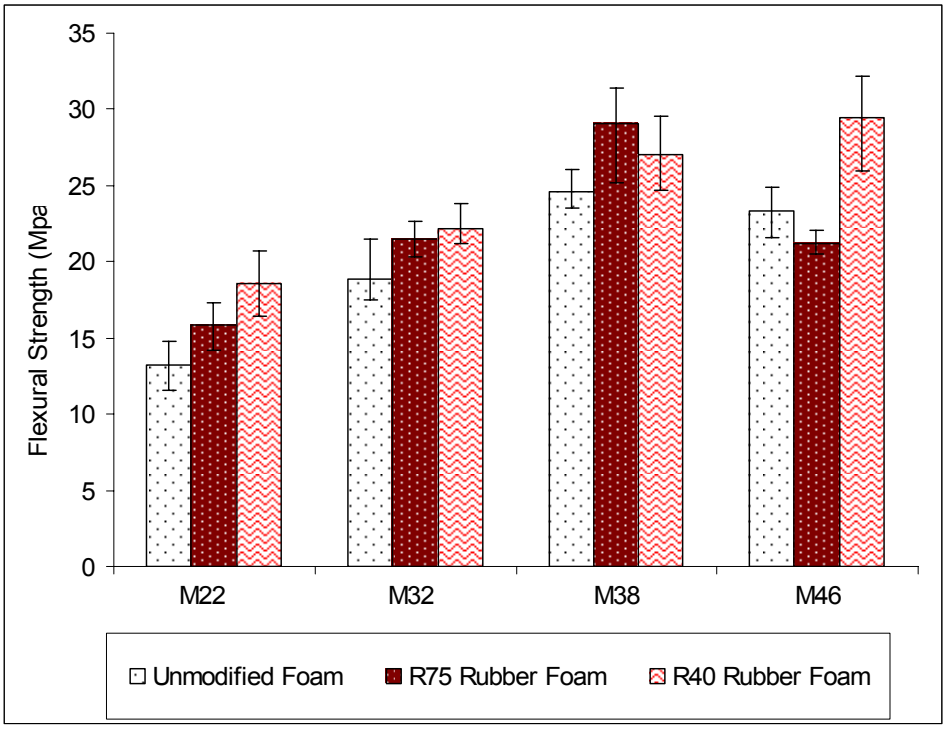

Figure 37. Flexural strength comparison of various types of foam samples.

Compared to flexural strength of plain syntactic foams it is observed, as a general trend, that an increase in flexural strength is achieved with the addition of rubber particles. R40 type particles seem to cause greater improvement in strength compared to the R75 type particles. The reason for such an observation is that the volume fraction of rubber particles is maintained at 2%, which leads to a higher number of smaller size rubber particles in the hybrid foam structure. Higher number of particles increases the number of rubber particles present on any fracture plane and increase the possibilities of crack bridging by these particles. Crack bridging is one of the main phenomena increasing the fracture strength and strain in rubber filled materials. Figure 38 shows a rubber particle coming out of the fracture surface of a rubber hybrid foam sample containing R40 type particles. Such particles are observed all over the fracture surface among microballoons.

The micrograph shown in Figure 38 is taken in the tensile side of the specimen. Most microballoons around the rubber particles have not fractured. The fracture seems to be governed by the fracture of matrix materials. Previous studies have established that the tensile failure of syntactic foams typically shows this kind of microstructure where large number of microballoons are unbroken, failure is dominated by the matrix failure and there is absence of any significant amount of microballoon debris. Figure 39 shows the compressive side of a rubber hybrid foam specimen. Extensive damage to microballoons is observed which is typical of compressive loading and failure in syntactic foams.

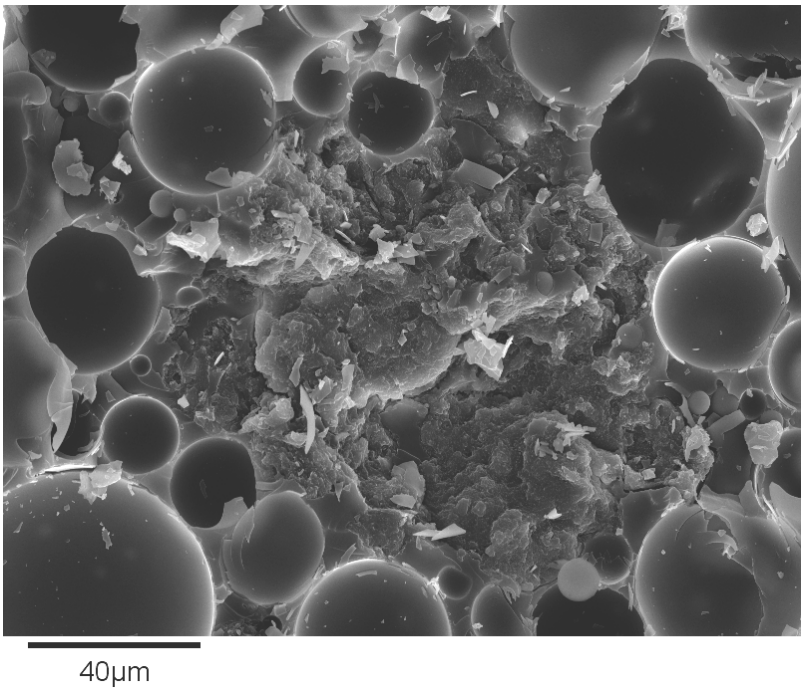

Figure 38. Fracture surface of a syntactic foam containing R150 type rubber particles.

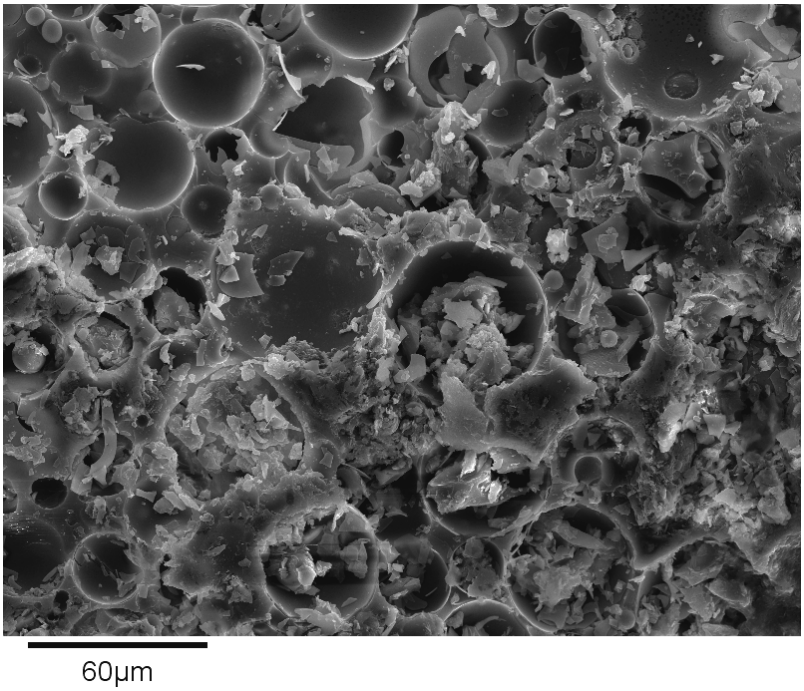

Figure 39. Extensive damage to microballoon on compressive side of a rubber hybrid foam specimen

The fracture in SF38 and SF46 type hybrid foams is governed by the matrix failure so their strength should also be comparable. This is true for most types of hybrid foams but significant difference is observed in the R75M38 and R46M46 type of foams. A close look at

Table 7 reveals that there is significantly higher void content in R46M46 specimen. Voids are known to cause deterioration in the strength of particulate composites.

Rubber and microballoon interaction in the foam matrix results in a phenomenon known as the plastic zone branching. If a crack is formed, the elastic stress field on its tip interacts with the stress field around microballoons. This interaction results in a distortion in the process zone stress field and promotes regions of higher stress gradient. Rubber particles engulfed in this region undergo cavitation, shear banding and void growth due to stresses, which results in the enhancement of material toughness [27]. Difference in flexural properties has been observed due to a difference in size of the rubber particles. Smaller sized rubber particles produce higher toughening of the foam matrix. This may be attributed to the fact that smaller size rubber particles have a greater probability of being engulfed in the process zone around the tip of cracks generated in the tensile side of a specimen [27]. This leads to greater crack bridging, rubber particle cavitation and shear banding in the foam matrix and higher toughness in foams with smaller rubber particles. Microballoons contribute towards crack bridging and crack pinning as seen in Figure 40.

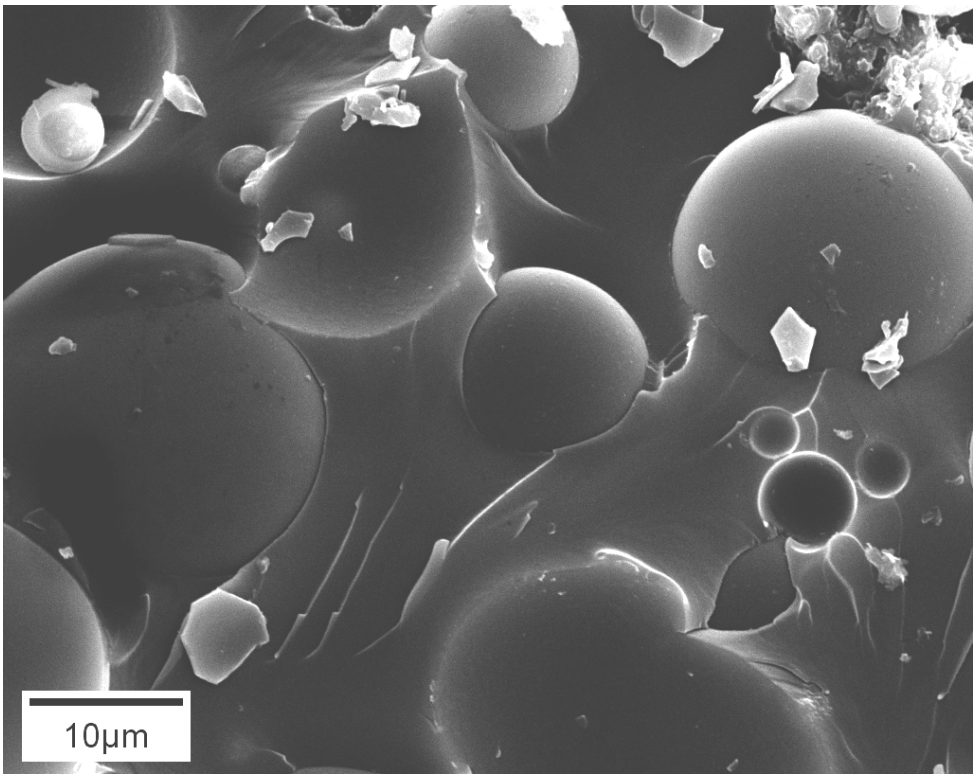

Figure 40. Crack propagation, bridging and pinning is seen in this micrograph.

4.2.1.4.2.3 Conclusion

Experimental investigation of plain and rubber hybrid syntactic foams is carried out in the present study. Addition of rubber particles has a significant effect on the flexural properties of syntactic foams. The fracture mode of plain syntactic foams shows a transition from microballoon fracture to matrix failure as the microballoon strength increases. Similar results are observed for all types of hybrid foams. Stiffness is observed to have increased by around 10% upon the addition of rubber particles. Flexural modulus in syntactic foams has been found to

increase by as high as 10%. Flexural strength has also been found to increase. R75 type rubber particles has resulted in an increase in strength of syntactic foams by 15%, whereas, R40 type rubber particles has resulted in an increase in strength of syntactic foams by 18%. This difference is seen due to the fact that smaller rubber particles have a higher probability of being engulfed in the process zone around a crack tip, which leads to crack bridging phenomenon. Such a phenomenon is also observed through SEM micrography. Flexural toughness has increased upon the addition rubber particles. It is observed that the amount of energy absorbed as area under load displacement curves is higher in foams containing the smaller R40 type particles. Plastic zone branching occurs in the foams matrix. Rubber particle cavitation, shear banding and void growth occurs, resulting in enhancement of material toughness.

4.2.1.4.3 Hygrothermal Testing

Standard ASTM D 5229-92 [48] was followed for hygrothermal testing. Dry samples were weighed before exposing them to moisture. The samples were then immersed in deionized fresh water and salt water media respectively at room temperature until complete saturation was attained. Saturation definition specified by the ASTM standard was followed. The samples were weighed at regular intervals according to the standard, to observe the change in weight due to moisture absorption. The samples were then subjected to compression testing. ASTM C365-94 standard is followed, which recommends a specimen size of $25 \times 25 \times 12.5$ mm^3 for length, width and height of the specimen respectively. A constant compression rate of 1.3 mm/min was used for testing. Stress stain values are calculated from the load-displacement data obtained from the tests. A computer controlled MTS 810 mechanical test system is used for compression tests.

4.2.1.4.3.1 Deionized Water Media

Figure 41 presents the water absorption profile of hybrid syntactic foams. It can be observed that saturation is reached in 64 days for all types of samples. Most specimens absorbed between 1 to 2.15% water before saturation. This value is found to be consistent with the water absorption values observed by researchers in previous studies [18, 20].

Figure 42 compares the strength of various hybrid composites obtained from compression tests of both dry and wet specimens. Strength of all the hybrid foam samples is observed to decrease after exposure to fresh water for a prolonged period of time. When comparing the strength of wet foams containing different types of rubber particles, it is observed as a general trend that foams containing larger particles (75 μm) have a lower strength as compared to foams containing smaller particles (40 μm). This result is consistent with the results obtained from the testing of dry samples. For most samples the decrease in strength is only about 15% or less.

The modulus of foam samples subjected to water immersion was observed to decrease drastically when compared with dry samples, as observed in Figure 43. It is observed that the reduction in modulus of all types of hybrid foams compared to corresponding dry specimens is about 65%. Such a high reduction in modulus is attributed to the plasticization of the foam matrix due to water absorption [20]. The effect of plasticization is expected to be higher in hybrid foams due to the presence of a ductile phase in the form of rubber particles. As a result of matrix plasticization the foam samples could be compressed to very high strain values of nearly 60-70%. Representative stress strain curves of foam samples containing rubber particles of 75 and 40 μm are shown in Figure 44 and Figure 45, respectively. It can be observed in these

figures that the hybrid foams are compressed to high strain values without any sign of instability in their stress response.

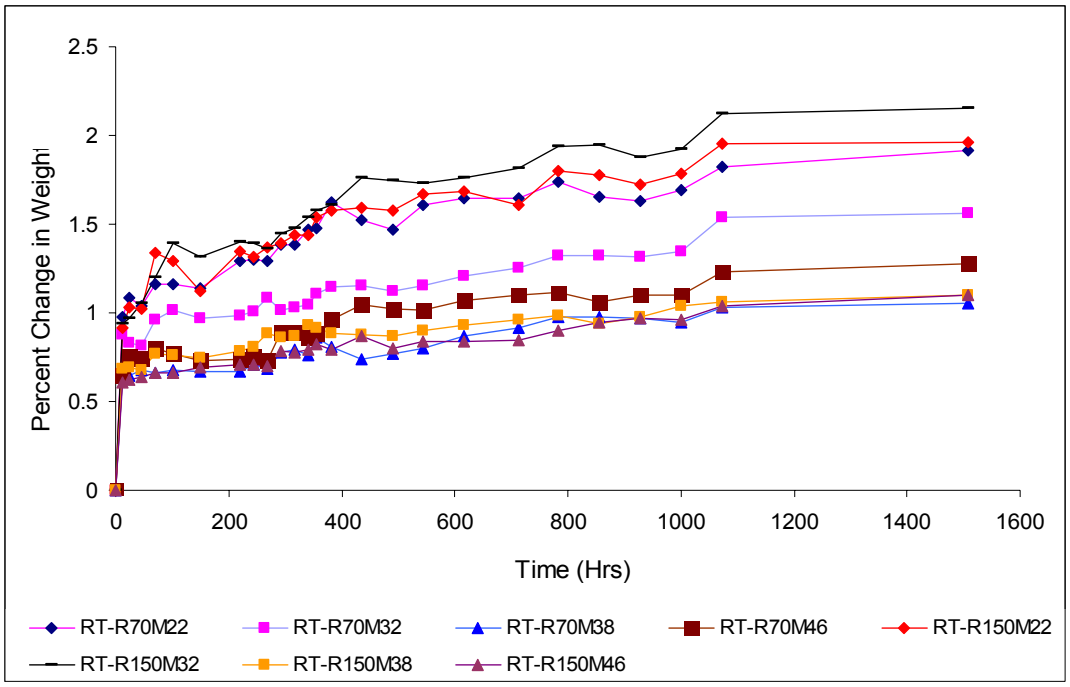

Figure 41. Moisture absorption profile of various foam composites containing R40 and R75 type rubber particles.

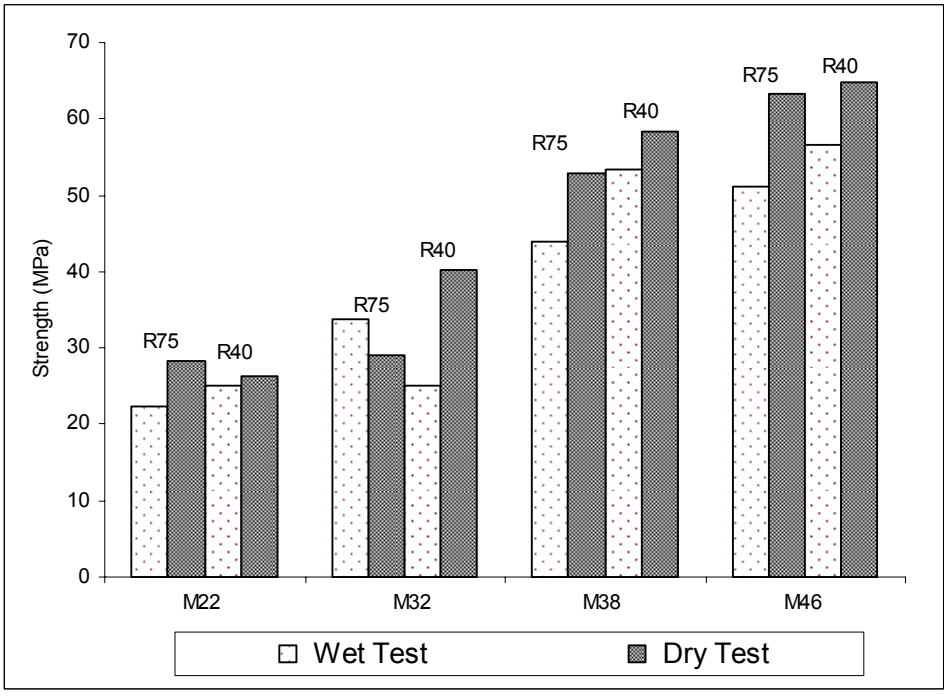

Figure 42. Comparison of compressive strength obtained from testing of dry and wet specimens of various hybrid composites containing R75 and R40 type rubber particles.

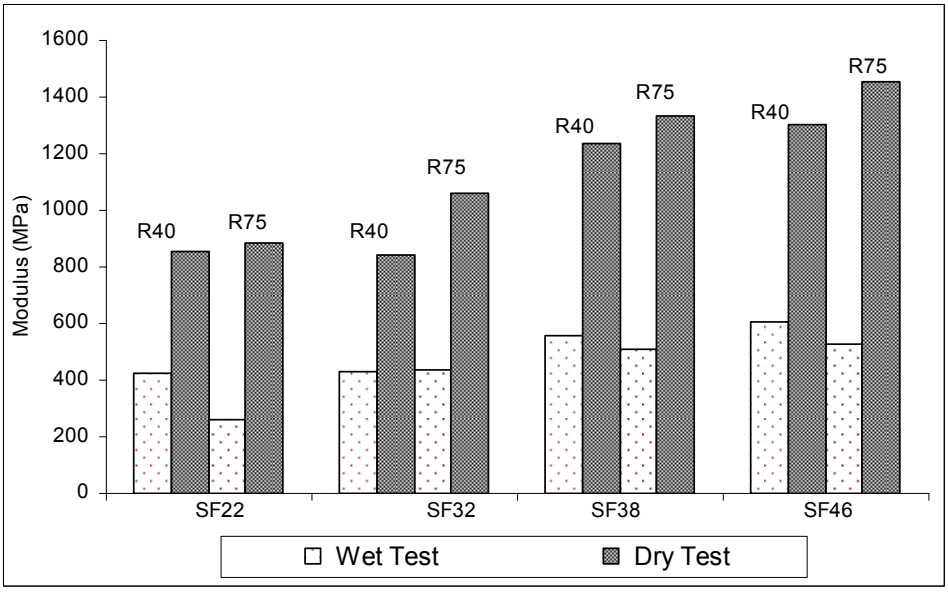

Figure 43. Comparison of modulus obtained from testing of dry and wet specimens of various hybrid composites containing R75 and R40 type rubber particles.

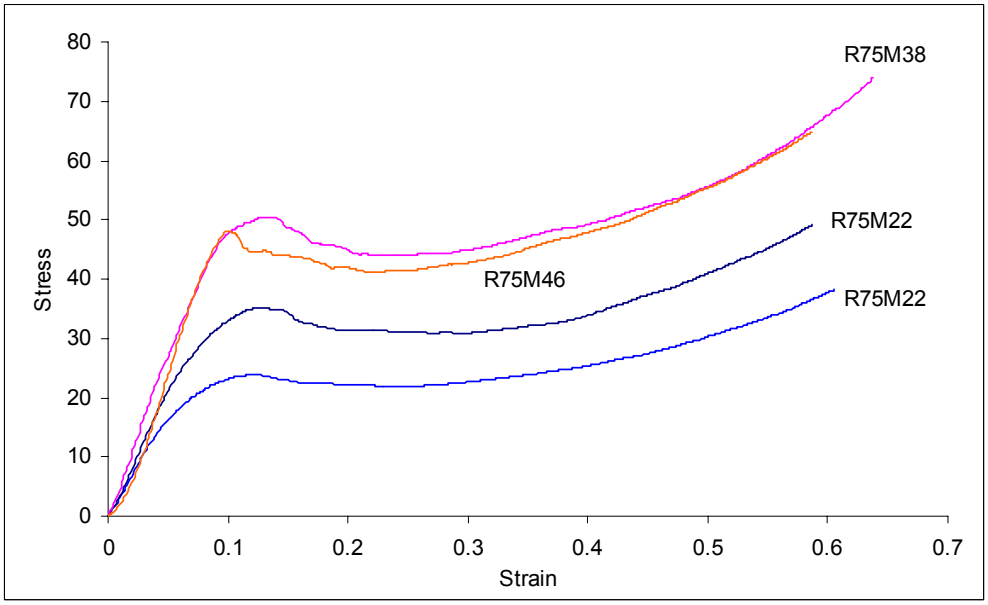

Figure 44. Representative stress strain curves for samples containing R75 rubber particles.

It can be observed in Figure 44 and Figure 45 that the stress plateau stage has ended around 30% strain and the stress started to increase, which is a sign that densification is complete in these samples around 30% strain. However, contrary to dry specimens of corresponding type, which were compressed to about 40% strain, these specimens are compressed to much higher strain without any noticeable failure in the specimen.

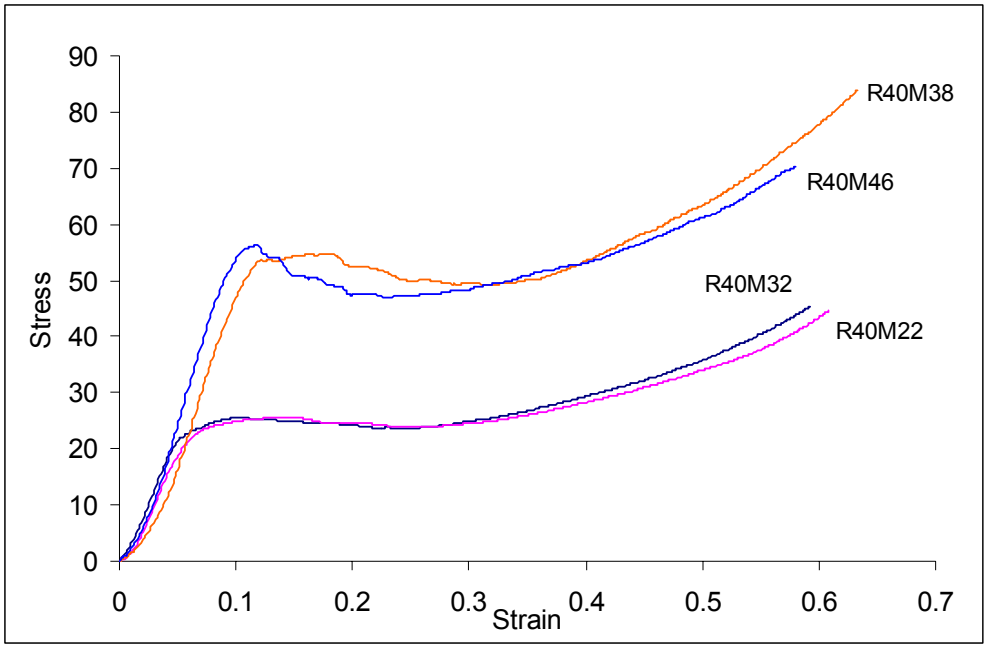

Figure 45. Representative stress strain curves for specimen with R40 rubber particles.

Compression test results of hybrid foam samples exposed to water can be compared with results obtained from previous hygrothermal testing of syntactic foam samples without rubber particles [18]. In that study only two types of syntactic foams, having microballoons of densities 200 kg/m^3 and 460 kg/m^3 (M22 and M46 type foams), were subjected to hygrothermal tests. Hence, results of only the corresponding types of hybrid composites are compared with those obtained in the published study. Figure 46 compares the strength of M22 and M46 type syntactic foams with and without rubber particles. It is observed that the strength of wet foam samples without rubber particles is higher when compared to foams with rubber particles. There is no appreciable change in strength of dry and wet syntactic foams when rubber particles are not present in the structure (Figure 47). However, as observed in Figure 46 rubber containing foams show change in strength due to moisture infusion.

The modulus of hybrid syntactic foams has reduced drastically as compared to syntactic foams that did not have rubber particles (Figure 48). In syntactic foams without rubber particles, nearly 48% reduction in modulus was observed, whereas in hybrid foams containing rubber particles nearly 50 to 70% reduction in modulus was observed. Reduction in compressive strength was higher for R75 type hybrid foams. Similar trend can be observed in case of modulus values also.

The significant reduction in strength and modulus of hybrid foams after prolonged exposure to water can be attributed to the higher amount of water absorption in hybrid composites as compared to foams without rubber particles. Figure 49 shows a comparison of the amount of water absorbed in terms of change in weight of pure and two types of hybrid syntactic foams (M22 and M46). It is clear that the hybrid composites have gained substantial amount of weight due to water absorption as compared to pure syntactic foams.

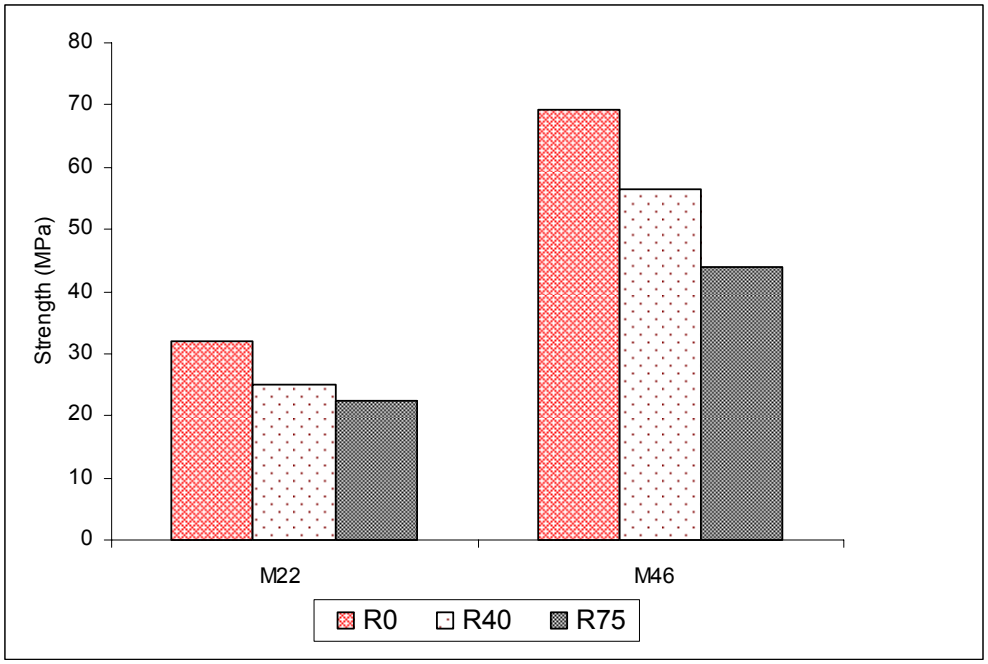

Figure 46. Comparison of Strength obtained from testing of wet specimens of foam composites containing 0% rubber particles and R75 and R40 type rubber particles.

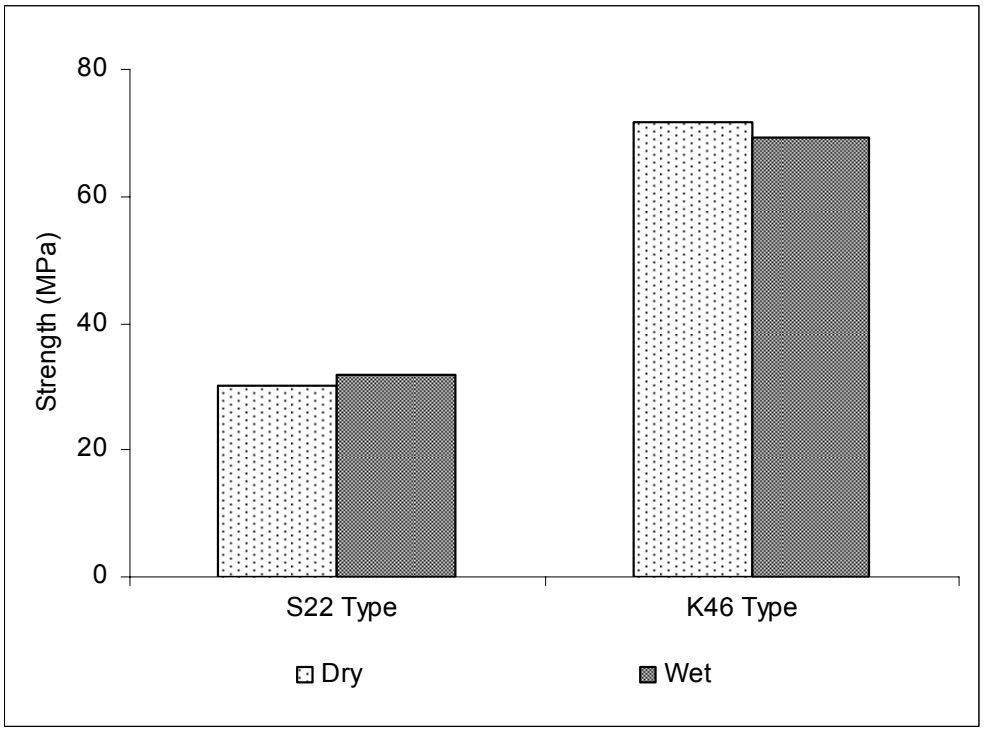

Figure 47. Comparison of strength obtained from previous testing of dry and wet specimens of various foam composites without rubber particles.

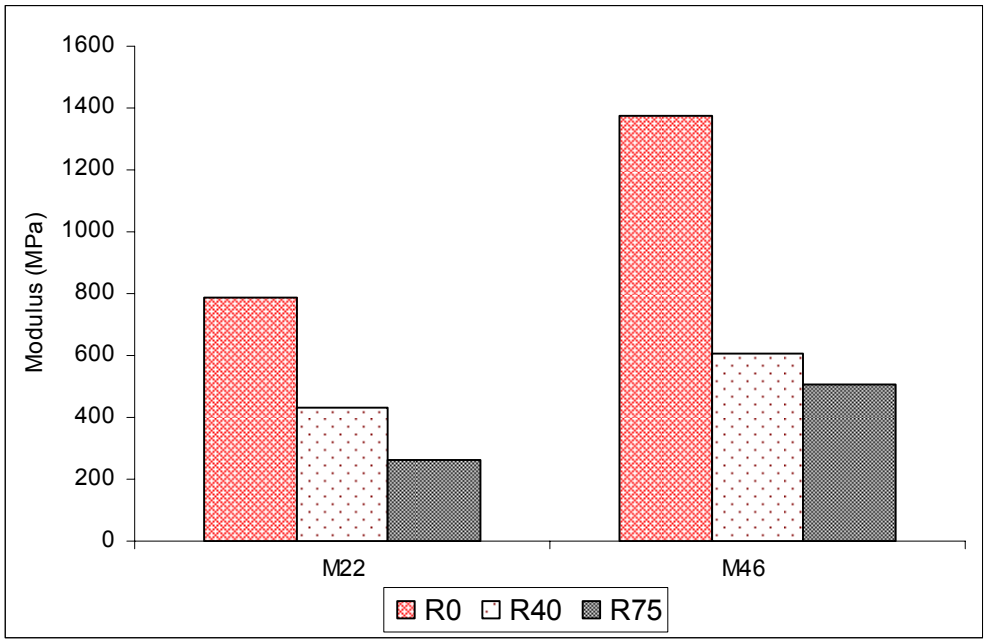

Figure 48. Comparison of modulus obtained from testing wet specimens of various hybrid composites containing 0% rubber particles and R75 and R40 type rubber particles.

Thus rubber particles have contributed to the absorption of water in hybrid composites. It is also observed that foams containing high density microballoons absorb lower amount of water as compared to foams containing low density microballoons.

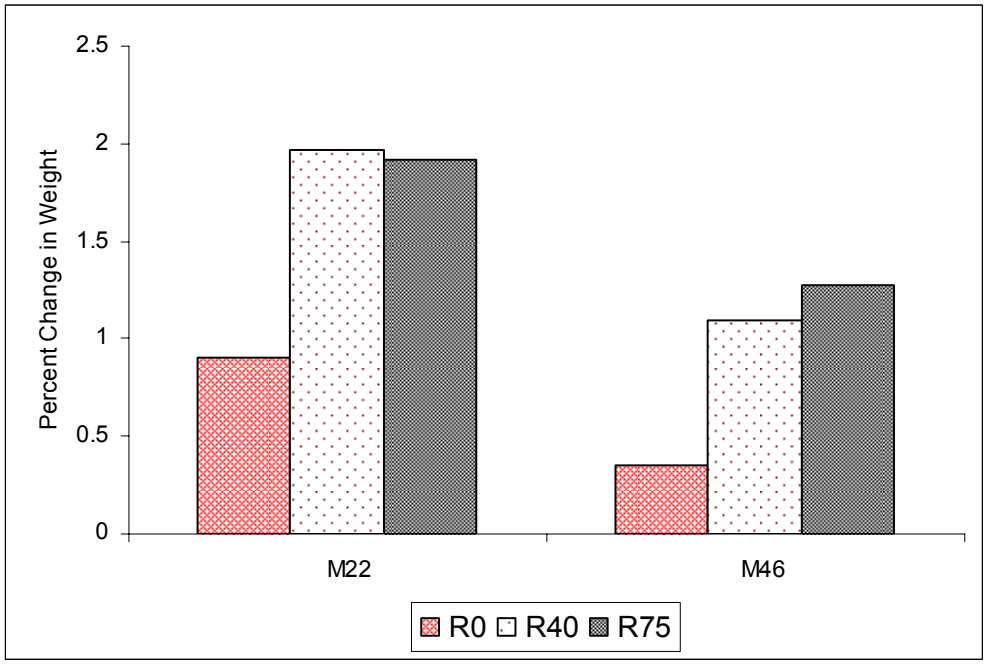

Figure 49. Comparison of percent change in weight due to moisture absorption of various foam composites containing 0% rubber particles and R40 and R75 type rubber Particles

Foams corresponding to both types of rubber particles absorbed nearly the same amount of moisture, as seen in Figure 49. The R40M38 type foam also showed a very small increase in moisture absorption, nearly 4.3%, as compared to corresponding R75M38 type particle foams. However, the R40M32 type foam showed a very large increase in moisture absorption, nearly 27.7%, as compared to corresponding R75M32 type foam.

Observations of increased water absorption, considerable reduction in modulus and reduction in strength indicate that substantial amount of absorbed water has gone into rubber particles. Rubber particles which are obtained from waste tires and are manufactured by heavy shearing contain microcracks in their structure. Additionally as observed in Figure 12, their structure is highly irregular. This irregular structure may make it difficult for epoxy resin matrix to penetrate into the folds of this particle and wet the entire surface. Existence of microcracks and presence of any area of inferior interfacial bonding between rubber and matrix contribute to increase in water absorption and reduction in strength. However, increase in compressive strain without failure is a desired result and compensated reduction in strength to maintain the level of energy absorbed before failure, and the damage tolerance of the material.

4.2.1.4.3.2 Conclusions

Significant change in mechanical properties is observed after hygrothermal testing of hybrid syntactic foams containing rubber particles and glass microballoons. It is observed that hybrid syntactic foams absorb a higher amount of moisture when exposed to water for a prolonged time period as compared to corresponding syntactic foams. Strength of different types of hybrid syntactic foams reduces by about 10 to 20% compared to dry specimens, whereas strength of syntactic foams without rubber particles reduces by less than 5% after hygrothermal testing. As a general trend, the moisture absorption in both types of hybrid foams is nearly the same. However, the strength of R40 type foams is higher than corresponding R75 type foams. This result is consistent with dry testing of samples. Reduction in compressive modulus and strength is observed compared to corresponding dry specimens. However, increase in fracture strain of hybrid foams due to moisture infusion may help in maintaining the same energy absorption before failure. The compressive failure strain is found to increase due to matrix plasticization.

4.2.1.4.3.3 Salt Water Media

Figure 50 and Figure 51 present the water absorption profile of hybrid syntactic foams with R70 and R40 type rubber particles respectively. It can be observed that saturation is reached within 68 days for all types of hybrid foam samples.

Most specimens absorbed between 0.8 to 1.64% water before saturation. Previous studies on hygrothermal testing of similar rubber hybrid foams in deionized water [47] shows moisture absorption between 1 to 2.15%. Therefore, presence of salt in water media has clearly reduced the amount of moisture absorbed by foam specimens. This may be attributed to the lower diffusivity of salt water ions, which retards moisture absorption by the foam specimen.

Figure 52 shows the percent change in weight of syntactic foams due to moisture absorption in salt water media, before and after the addition of rubber particles [20]. Plain syntactic foams absorb less than 0.68% water absorption, whereas all hybrid foams absorb much higher amounts of moisture.

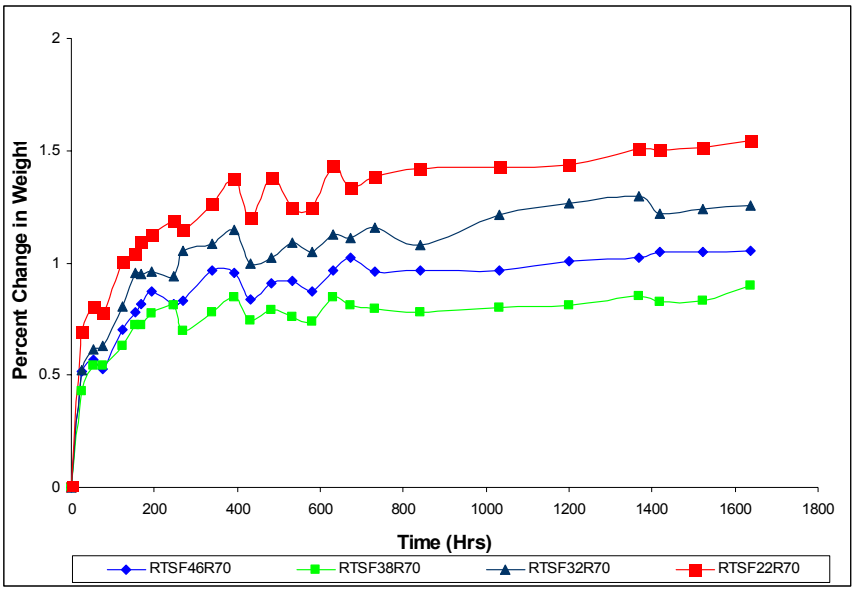

Figure 50. Moisture absorption profile of hybrid foam composites containing R70 type rubber particles.

Therefore it is seen that presence of rubber particles has increased the amount of water absorbed in foam specimens. These rubber particles have a highly irregular shape which may make it difficult to obtain a good interfacial bonding with the surrounding matrix throughout the particle surface. This may lead to water deposition in pockets developed between rubber particles and the surrounding matrix. Rubber particles contain microcracks which help in increasing the moisture absorption by the particles.

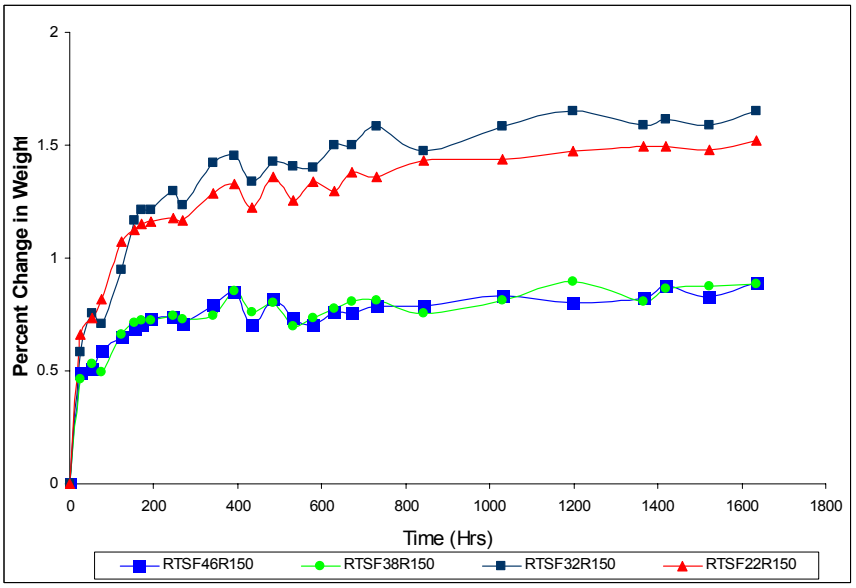

Figure 51. Moisture absorption profile of hybrid foam composites containing R40 type rubber particles.

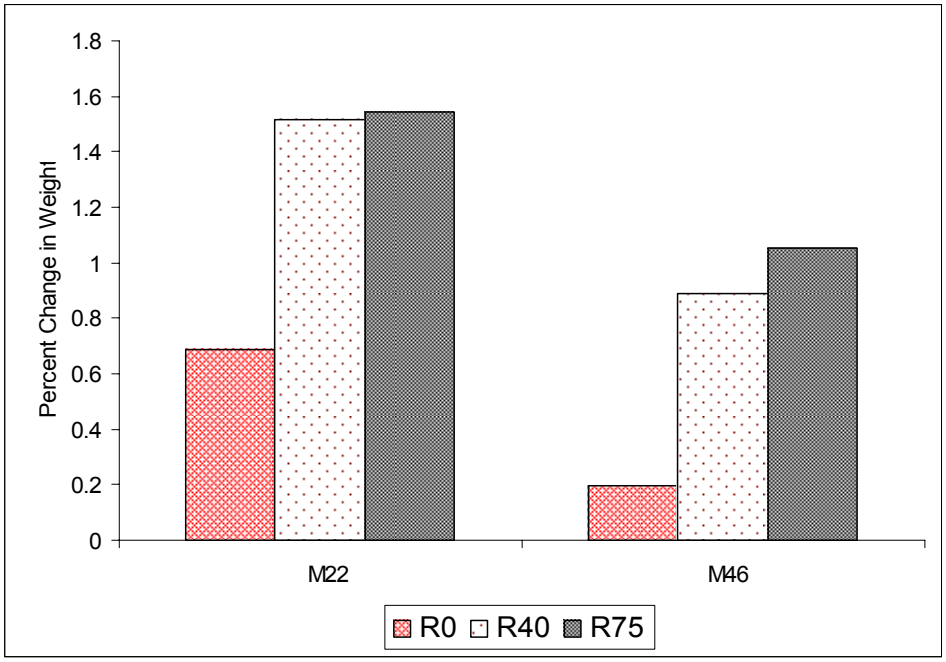

Figure 52. Comparison of percent change in weight due to moisture absorption of various foam composites containing 0% rubber particles and R40 and R75 type rubber Particles.

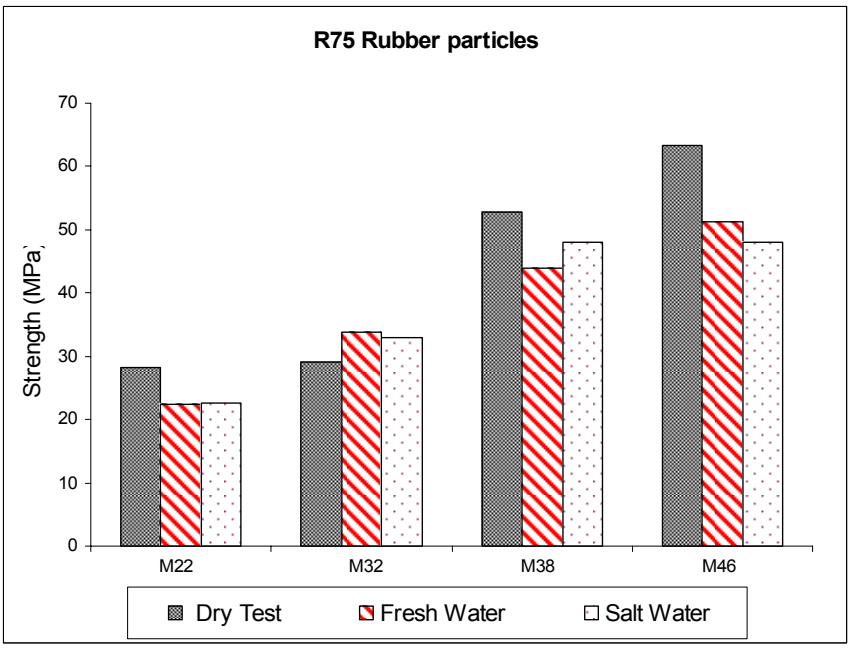

Figure 53. Comparison of compressive strength obtained from testing of dry and wet specimens of various hybrid composites containing R75 type rubber particles.

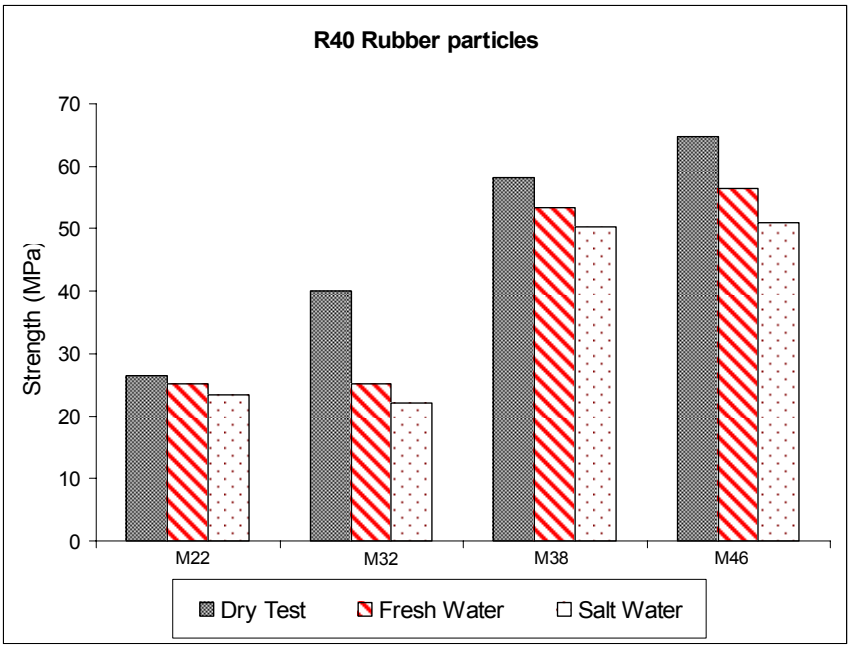

Figure 54. Comparison of compressive strength obtained from testing of dry and wet specimens of various hybrid composites containing R40 type rubber particles.

Figure 53 and Figure 54 show a comparison between the compressive strength of various types of dry and wet hybrid foam specimens. Wet specimens include those exposed to deionized water and salt water media. Due to moisture exposure for a prolonged period of time, compressive strength is generally observed to have decreased in all the hybrid foam samples. When comparing specimens subjected to deionized and salt water media, no significant difference is seen in strength of hybrid foams with larger R75 type rubber particles (Figure 53). However, foams with R0 type rubber particles show a higher reduction in strength when subjected to salt water media (Figure 54).

Figure 55 shows a decrease in modulus for all foam samples due to moisture absorption in salt water conditions. Nearly 50% reduction is observed in modulus of all foams. As a general trend, foams with smaller R40 type rubber particles show a higher modulus as compared to foams with R75 type rubber particles.

Rubber particles tend to harden up because of interaction with salt in the immersion media. This effect is more prominent in foams with smaller R40 type particles which show a greater reduction in strength and an increase in modulus as compared to foams with larger R75 type particles.

Moisture absorption under salt water is known to have very little effect on the strength of plain syntactic foams. However, as seen above, this is not true in the case of rubber hybrid foams. Figure 56 shows the difference in compressive strength of syntactic foams after the incorporation of rubber particles in them and exposure to moisture under salt water [47].

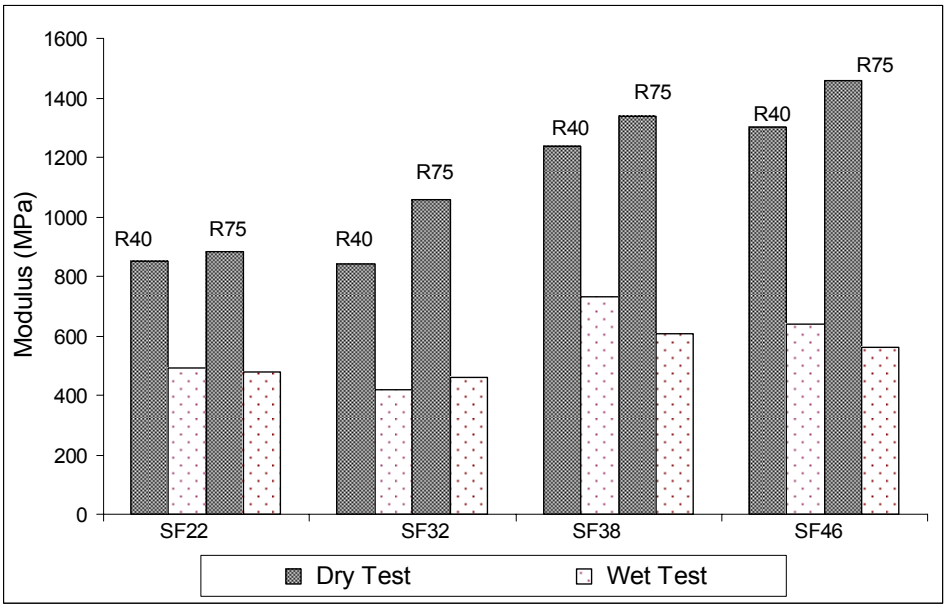

Figure 55. Comparison of modulus for various foam samples subjected to salt water media.

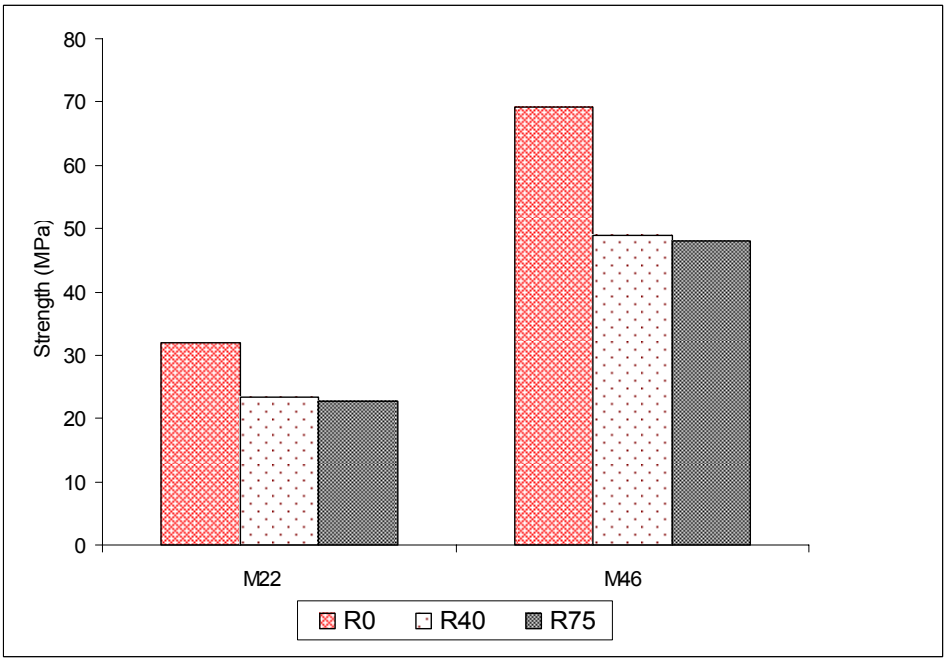

Figure 56. Comparison of Strength obtained from testing of wet specimens of foam composites containing 0% rubber particles and R75 and R40 type rubber particles.

A large reduction in strength is observed due to incorporation of R40 and R75 type rubber particles. Figure 57 compares the modulus of hybrid and plain syntactic foams exposed to moisture under salt water. Modulus in hybrid foams has reduced drastically as compared to plain syntactic foams.

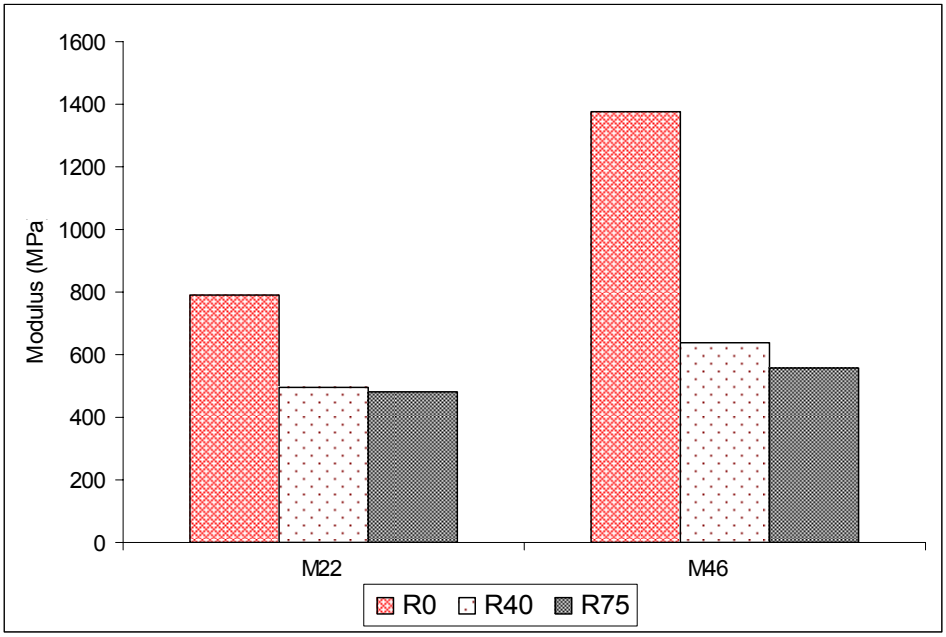

Figure 57. Comparison of modulus obtained from testing wet specimens of various hybrid composites containing 0% rubber particles and R75 and R40 type rubber particles.

Change in strength and modulus of hybrid foams is directly attributed to the presence of rubber particles which increases the amount of moisture absorbed by foams as seen by the percent change in weight of specimens in Figure 52.

A large reduction in modulus may be attributed to the presence of rubber particles as well as the plasticization of the foam matrix upon moisture absorption. This indicates that the foams may be able to absorb higher load energy which is desirable in applications involving high hydrostatic pressures. Compressive toughness viewed as area under curve of foams has increased as seen in Figure 58 and Figure 59 which show representative stress strain curves for various hybrid foams exposed to moisture under salt water.

Specimens are compressed to very high strain values even after the peak stress is reached at around 10% as compared to peak stress achieved at around 3% in plain syntactic foams [26]. Figure 60 shows cracking on the edges of a rubber hybrid foam specimen. Material chips off on the edges due to secondary tensile stresses due to poisons ratio effect. The stress plateau region in the curve (Figure 58 and Figure 59) ends at around 30%, at which point the densification of foams due to crushing of microballoons in completed, beyond which the stress started to increase again. Figure 61 shows the rubber hybrid specimen after the stress plateau region has ended and nearly all microballoons are crushed. It is observed that the specimen has undergone very little deformation and it shows similar cracking and fracture behavior as seen in dry testing of similar rubber hybrid specimens.

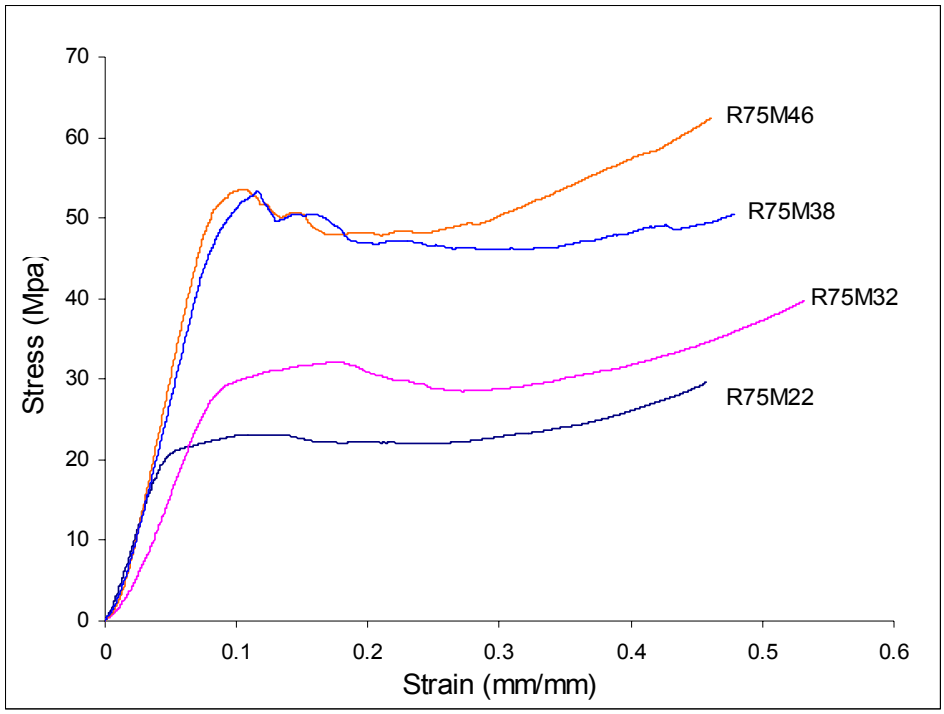

Figure 58. Representative stress strain curves for samples containing R75 type rubber particles.

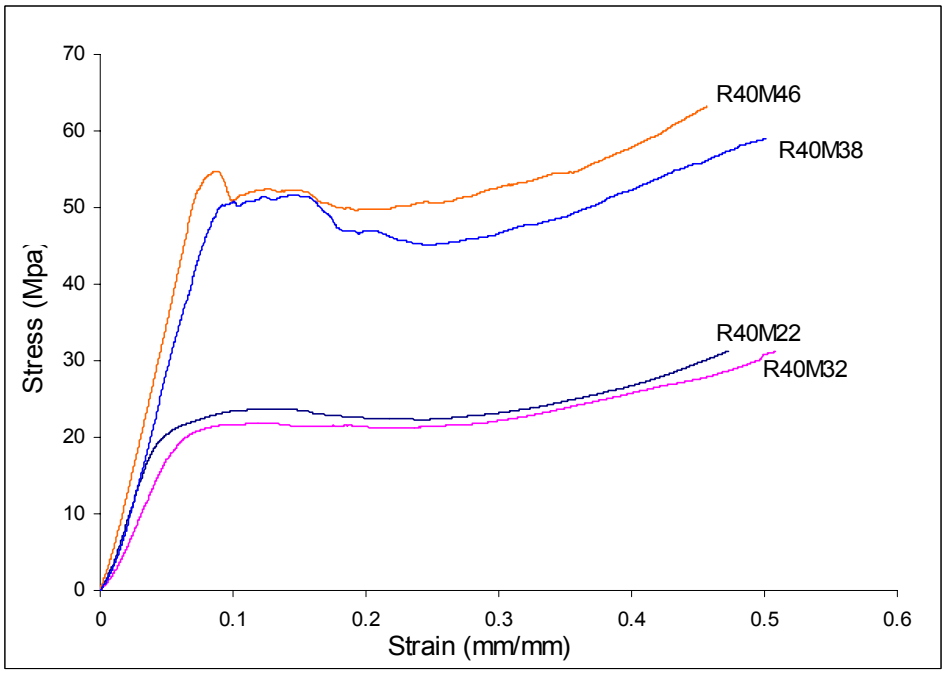

Figure 59. Representative stress strain curves for specimen with R40 rubber particles.

Figure 60. Cracking of a rubber hybrid foam specimen beyond peak stress after hygrothermal testing

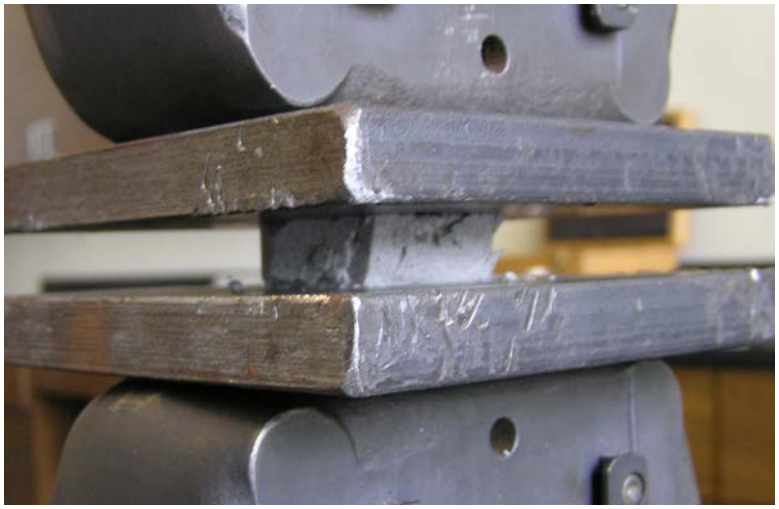

Figure 61. Rubber hybrid foam specimen under compression and almost intact even after the stress plateau region ends

4.2.1.4.3.4 Conclusions

Hybrid foams containing smaller R40 type and larger R75 type rubber particles are characterized for change in strength after hygrothermal testing under salt water conditions. Presence of rubber particles has a significant effect on the properties of syntactic foams after hygrothermal testing. Moisture absorption has increased and reduction in strength is observed in all hybrid foams. A drastic reduction in modulus is observed which indicates an increase in fracture strain and load energy absorption after hygrothermal testing. This is attributed to the large amount of matrix plasticization due to moisture absorption and presence of rubber particles. A comparison is also made with corresponding hybrid foam specimens tested under deionized water. It is seen that moisture absorption has reduced under salt water conditions. Strength and modulus have also reduced in all rubber hybrid foams upon exposure to moisture under salt water conditions. This can be attributed to the hardening of rubber particles due to interaction

with salt in the water media. Size of rubber particles has no significant effect on the moisture absorption in hybrid foams. However, the strength and modulus of R40 type foams is higher than corresponding R75 type foams. Material failure and deformation is similar to that of the dry specimens tested under compression.

4.2.2 Nanoclay Hybrid Syntactic Foam

4.2.2.1 Raw Materials

4.2.2.1.1 Glass Microballoons

Methods of selection of glass microballoons is the same as mentioned before for the rubber hybrid foams. Microballoon properties are listed in Table 3

4.2.2.1.2 Nanoclay Particles

Nanoclay has been procured from Nanocor Inc., and has commercial name of Nanomer I.30E. It is a surface modified montmorillonite mineral which will disperse to nanoscale in epoxy resin systems which creates a near-molecular blend or nanocomposite. It has a specific gravity of 1.71. Strength, thermal and barrier properties of the epoxy resin are enhanced due to the nanocomposite. Figure 62 shows the platey structure created upon exfoliation of nanoclay particles. During exfoliation the nanoclay platelets separate from one another.

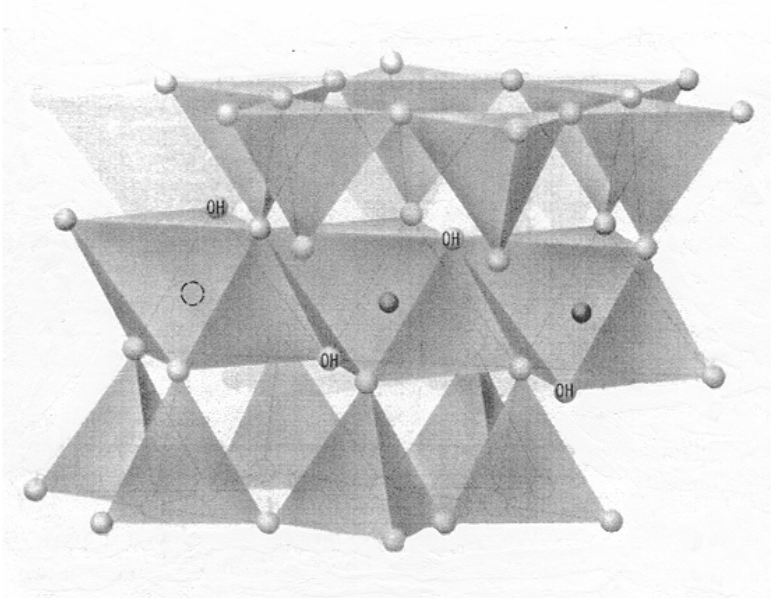

Figure 62. Montmorillonite's unique structure creates a platey particle

4.2.2.1.3 Resin System

Epoxy resin D.E.R. 332, manufactured by DOW Chemical Company is used as matrix material. Amine based hardener D.E.H. 24 is used with the selected epoxy resin. A diluent C_{12}-C_{14} aliphaticglycidylether is mixed with the epoxy resin in 5% by weight quantity to reduce its viscosity. Reduction in viscosity makes it easier to mix higher volume fraction of particles in the matrix resin.

4.2.2.1.4 Fabrication

Nanoclay syntactic foam samples with eight different compositions have been fabricated and tested for mechanical properties. Four types of glass microballoons have been used as

hollow particles. Each type of microballoon is mixed with two nanoclay volume fractions, 0.02 and 0.05, to fabricate eight types of nanoclay foams. The total volume fraction of microballoons and nanoclay is maintained at 0.65 in all types of specimen. Details of nanoclay syntactic foam compositions and measured density are given in Table 8 below. Nomenclature of all types of fabricated syntactic foams is also listed in Table 8.

In the first step nanoclay particles are mixed in the resin-diluent mixture at a mixing rate of 2540 rpm for 2 hrs followed by the addition of hardener and microballoons. Hand mixing is carried out at slow speed after microballoon addition to keep the microballoon damage minimum. The resin and particle paste obtained after mixing is poured into stainless steel molds and allowed to cure for 24 hours at room temperature. The mixture cures into a composite slab, which is then removed from the molds and post cured in an oven at a temperature of 100°C for three hours.

Table 8 Composition and density of nanoclay syntactic foams.

Nanoclay Volume %	Microballoon Type	Microballoon Density kg/m^3	Nanoclay Foam Nomenclature	Nanoclay Foam Density kg/m^3
2	S22	220	SF22C2	517
	S32	330	SF32C2	562
	S38	380	SF38C2	
	K46	460	SF46C2	643
5	S22	220	SF22C5	567
	S32	330	SF32C5	605
	S38	380	SF38C5	
	K46	460	SF46C5	674

4.2.2.2 Specimen Nomenclature

The first two letters in the nomenclature stand for “Syntactic Foam”, next two numbers are related to the density of microballoons used to fabricate that foam. The next letter C refers to “clay nanoparticles” and the last number represents nanoclay volume fraction. For syntactic foams that do not contain nanoclay particles, only four digit alpha-numeric code is used, which is similar to the first four digits of nanoclay reinforced foams. For the ease of presentation, the nanoclay reinforced foams are referred as “nanoclay foams” to differentiate them from syntactic foams that do not contain nanoclay.

4.2.2.3 Mechanical Testing

4.2.2.3.1 Compression Testing

Compression tests are carried out in accordance with ASTM C365-94 standard. Specimens of 25×25×12.5 mm in length, width and thickness, respectively, are compressed at a rate of 1.3 mm/mm. The compression tests were carried out using a computer controlled MTS 810 mechanical test system. Five specimens of each type of material are tested. Load-displacement data obtained from the tests are used to plot stress-strain curves and calculate compressive strength.

4.2.2.3.2 Results and Discussion

All types of microballoons selected in the present study have mean particle diameter

around 40 μm. The difference in their wall thickness causes a difference in their density and strength. This scheme allows changing the density of syntactic foams while keeping the particle volume fraction constant in the structure. This scheme also leads to the same interfacial area between microballoons and matrix resin. Hence, only one parameter, the microballoon strength, changes among various types of foams fabricated in the present work.

Published studies have indicated that upon exfoliation of nanoclay particles in epoxy-clay nanocomposites, an increase in the compressive strength and modulus of the epoxy polymer is obtained [27]. It was reported that the compressive strength increased from 76 MPa to 84-88 MPa and compressive modulus increased from 1.4 GPa to 1.7-1.8 GPa for various kinds of clays. However, there are some identified problems in syntactic foams with increase in modulus and strength. In the compression testing of syntactic foams, it is observed that increase in strength and modulus increase the stiffness of the sample and lead to cracking under secondary tensile stresses [33]. These secondary tensile stresses are generated due to the Poisson's Ratio effect. One such high density syntactic foam specimen tested under compressive loading is shown in Figure 63.

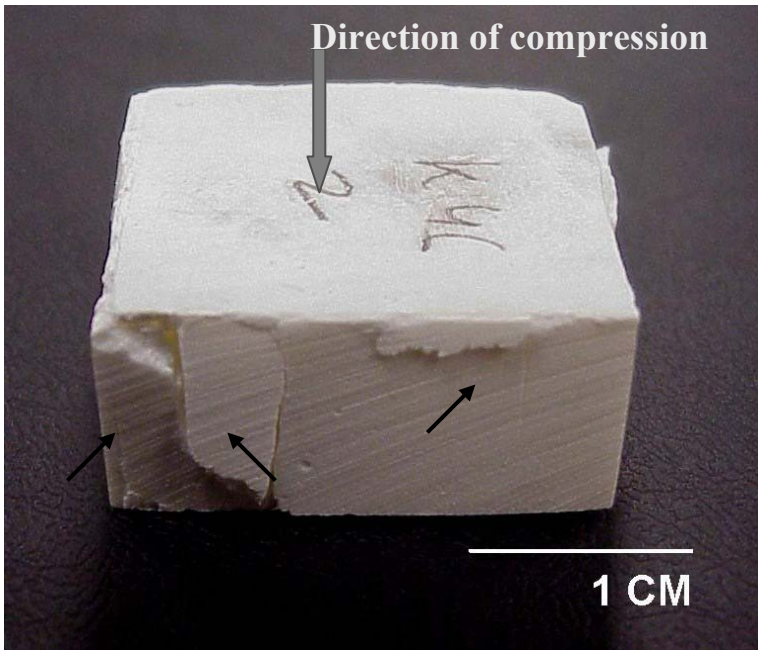

Figure 63 Low aspect ratio syntactic foam samples showing three vertical cracks in the side wall.

Prominent cracks can be observed in the direction of compression in this specimen, which led to its failure at a strain of only about 10%. This effect is so strong that high density (650 kg/m^3) foams fracture at strains of only 8-10% compared to a fracture strain of over 20% for lower density (450 kg/m^3) foams. The aspect ratio of the specimen shown in Figure 16 is 0.5. If the aspect ratio of specimens is increased to 2, then the effect of secondary tensile stresses is observed clearly as seen in Figure 64 [15].

The specimen shown in Figure 64 is also of high density (650 kg/m^3) and has fractured predominantly under secondary tensile stresses at a strain of about 8%.

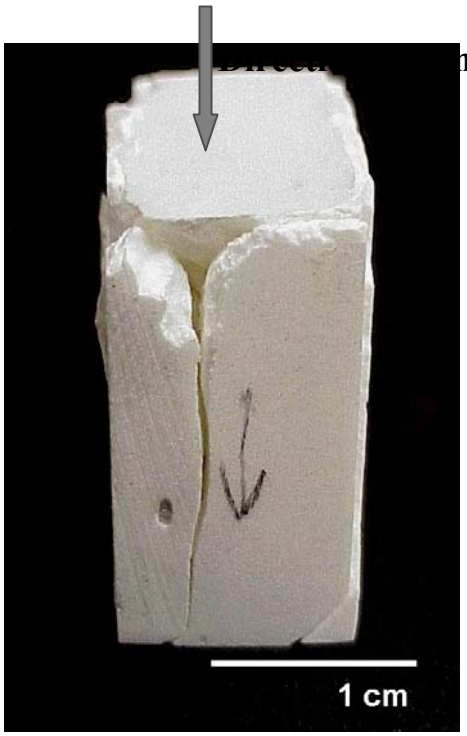

Figure 64 High aspect ratio syntactic foam specimen failed under secondary tensile stresses.

The lower fracture strain leads to poor energy absorption characteristics in high density foams. Therefore, it was decided to incorporate high volume fractions of nanoclay in matrix resin to achieve the aim of increasing the toughness by means of increasing the fracture strain with little change in strength. In the fabricated nanocomposites, 2 and 5% by volume nanoclay content actually gives nanoclay to resin ratio of about 5.7 and 10% by volume. The corresponding weight fractions of nanoclay in matrix material were about 9.5 and 20%, respectively. It is known that intercalation or exfoliation of such large amounts of nanoclay in matrix resin is not possible. Generally it is observed that for better exfoliation of clay particles in the epoxy matrix, the nanoclay loading should be restricted to around 5 weight percent and below [45]. Beyond this limit poor exfoliation results are obtained. Hence, partial intercalation/exfoliation will lead to increase in strength of epoxy resin, whereas remaining nanoclay in the form of micron size clusters may act as plasticizer/lubricant for deforming matrix material. The overall strength of the composite will depend on these two competing parameters. The expected microstructure of the material is presented in Figure 65.

Representative stress-strain curves for compression tests of 2% and 5% nanoclay foams are presented in Figure 66 and Figure 67, respectively. Features of these curves are compared with the stress-strain curves of syntactic foams without any nanoclay content shown in Figure 68.

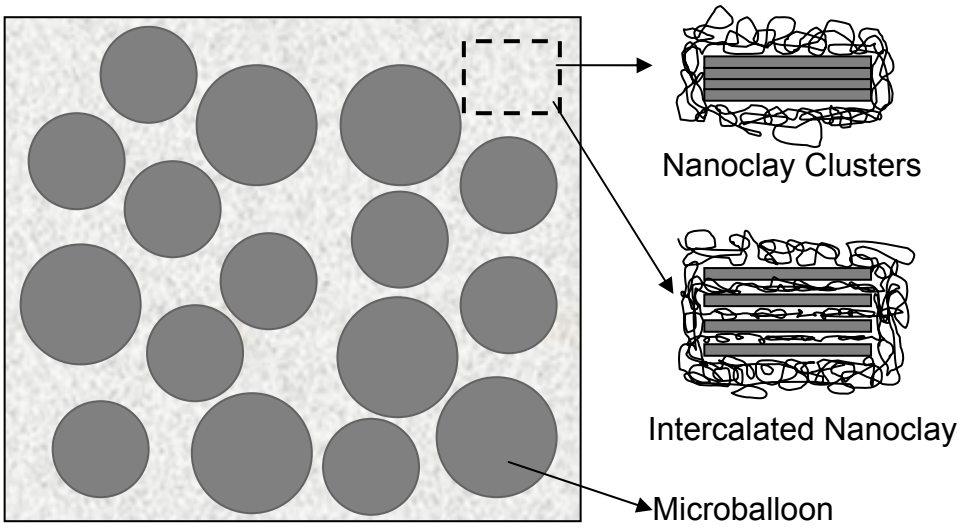

Figure 65 Schematic representation of the microstructure of nanoclay filled syntactic foam.

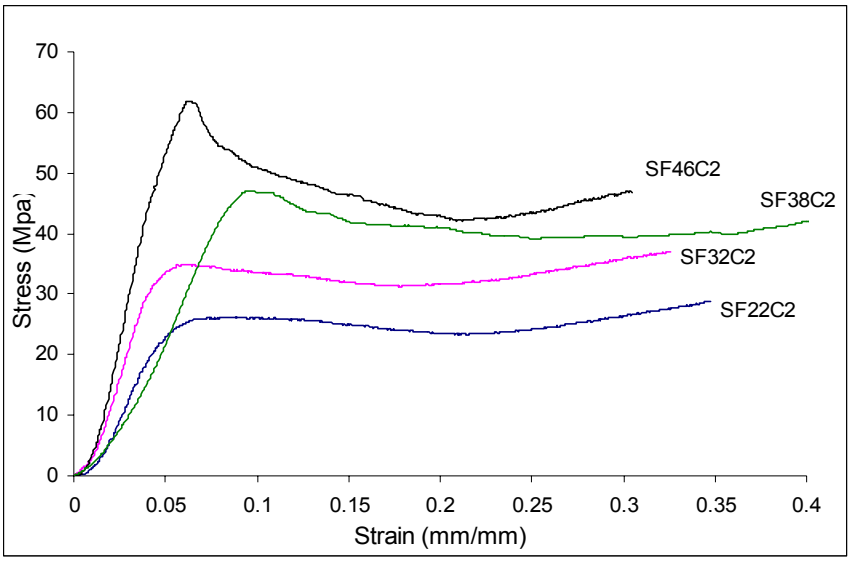

Figure 66 Representative stress-strain curves for Nanoclay Syntactic Foams with different microballoon types having 2% Nanoclay by volume.

It can be observed from these graphs that the fracture strain has improved considerably for high density foams due to the nanoclay incorporation. Extended stress plateau can be observed for all kinds of nanoclay foams, which is a typical feature in compressive stress-strain curves of syntactic foams [14]. Higher strength of higher density foams coupled with large fracture strain, over 30%, makes them more damage tolerant for applications requiring high strength.

Compressive strength values corresponding to foams with 0%, 2%, and 5% nanoclay particles have been calculated from stress-strain data and are presented in Figure 69 for comparison. The compressive strength values of nanoclay foams depend on the fraction of intercalated nanoclay particles.

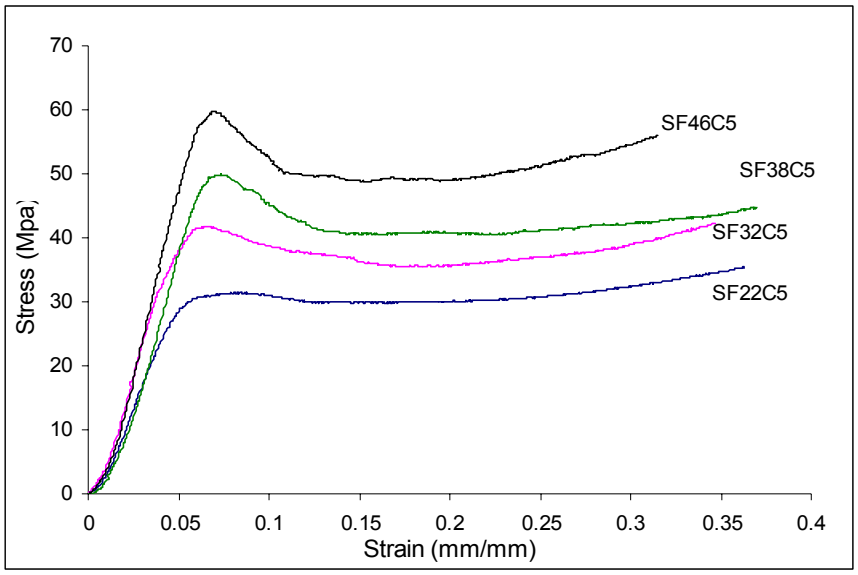

Figure 67 Representative stress-strain curves for Nanoclay Syntactic Foams with different microballoon types and 5% Nanoclay by volume.

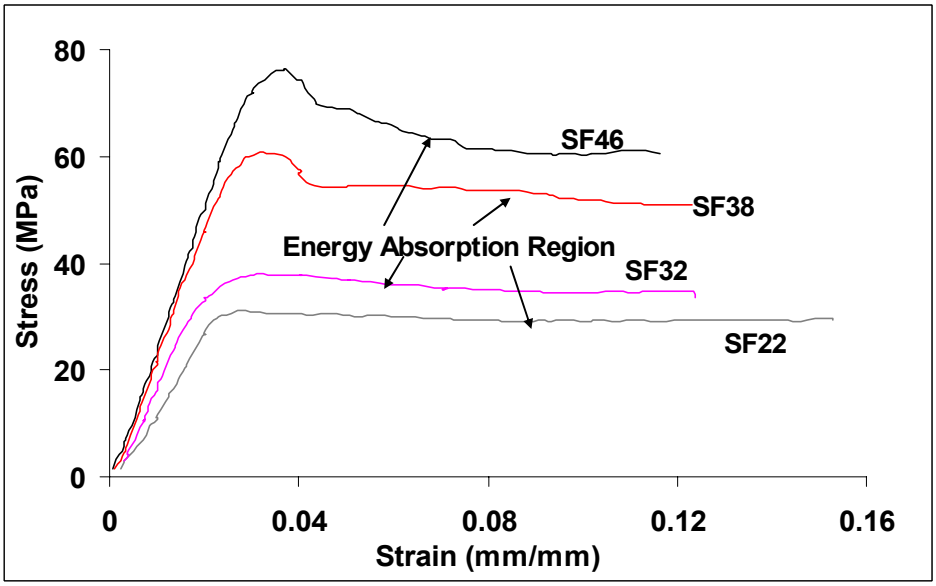

Figure 68 Stress-strain curves for various syntactic foams for comparison with those of Nanoclay Syntactic Foams.

Comparison of the compressive strengths of nanoclay foams reveal that the increase in the nanoclay content from 2-5% has resulted in an increase in the strength. This increase is found to be 18, 16, and 3% for foams containing 220, 320, 380 and 460 kg/m^3 density microballoons. Comparison of compressive strength of nanoclay foams with corresponding 0% nanoclay syntactic foams reveal that foams containing 2% nanoclay particles have 10-20% lower strength compared to the corresponding syntactic foams.

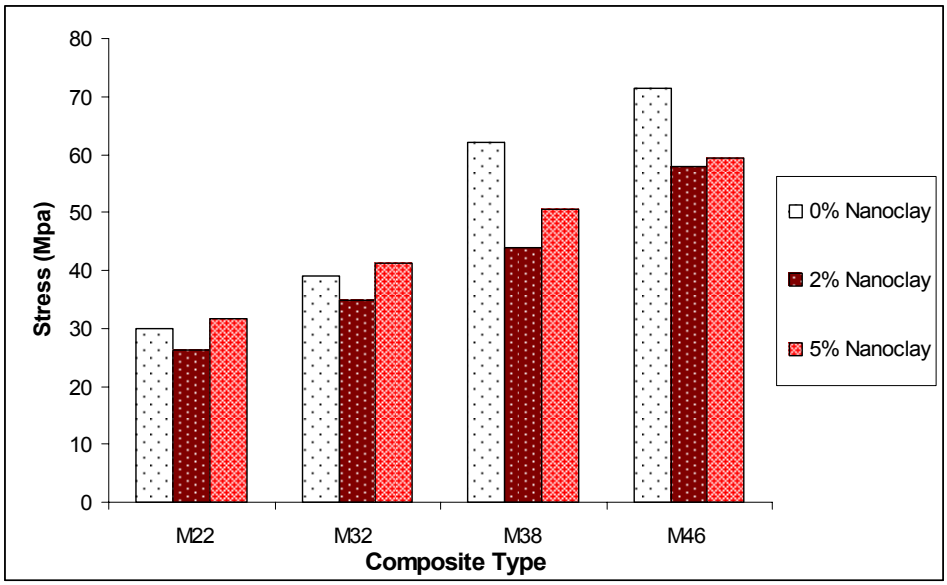

Figure 69 Comparison of compressive strength of foams with different types of microballoons and nanoclay volume fractions.

However, as a general trend it is seen that the strength of 5% nanoclay containing foams is higher than corresponding 0% nanoclay syntactic foams. The only exception appears to be the high density (460 kg/m^3 microballoons) nanoclay foams that show a decrease in strength of about 20% as compared to the corresponding 0% nanoclay syntactic foams. Such difference may occur due to the lower extent of intercalation in these composites. A high resolution Transmission Electron Micrograph (TEM) of the matrix resin is shown in Figure 70.

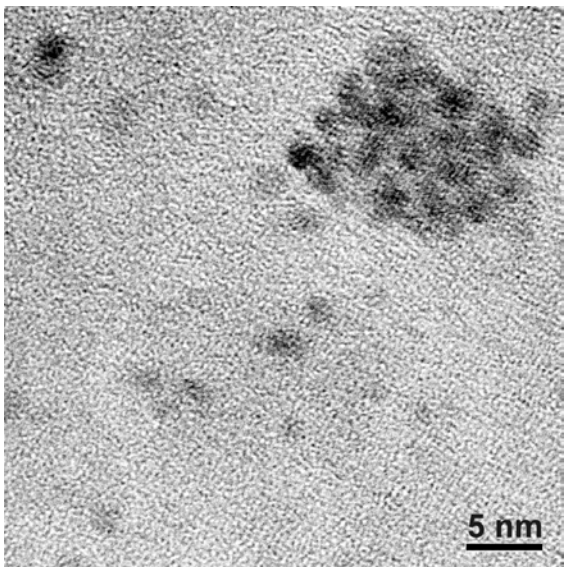

Figure 70 High-resolution TEM image of the synthesized nanoclay/epoxy composite with a 2% volume fraction of nanoclay.

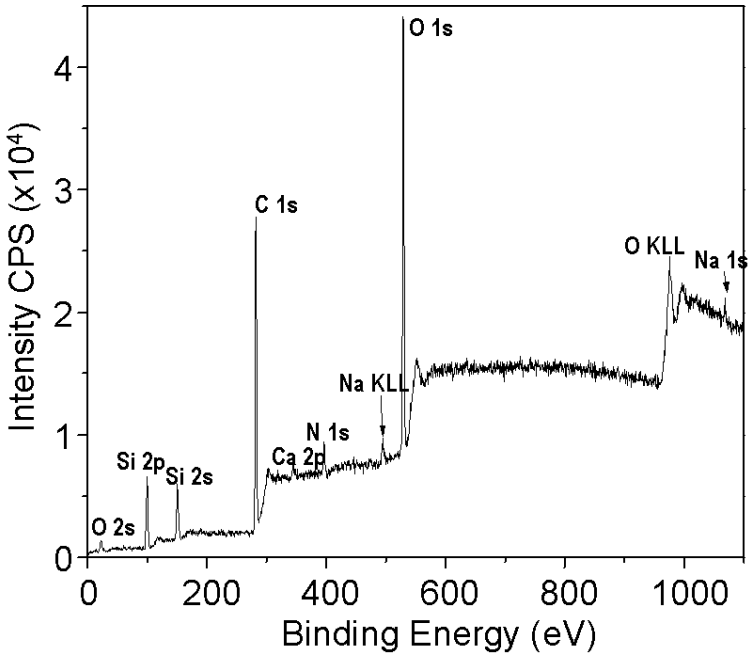

Figure 71 XPS spectrum of nanoclay reinforced foam.

An intercalated clay region in matrix material can be observed on the upper right side of this micrograph. This structure is similar to the platey structure seen above in Figure 62. Several such regions were observed in the matrix material in the detailed TEM study. X-ray photoelectron spectroscopy (XPS) confirmed the presence of nanoclay particles in these regions (Figure 71).

Scanning electron micrographs shown in Figure 72 present the microscopic structure of the material. Micron size clusters of nanoclay are observed in SEM observations.

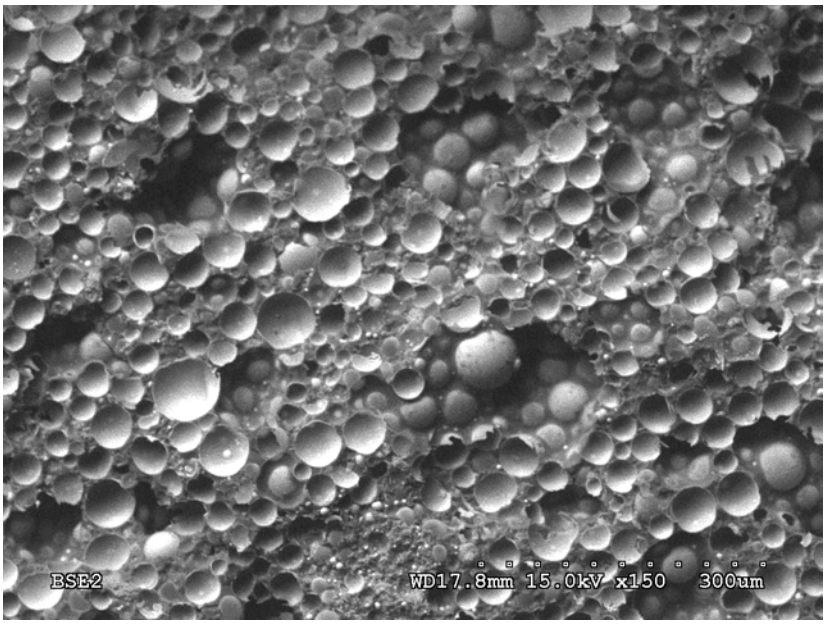

(a)

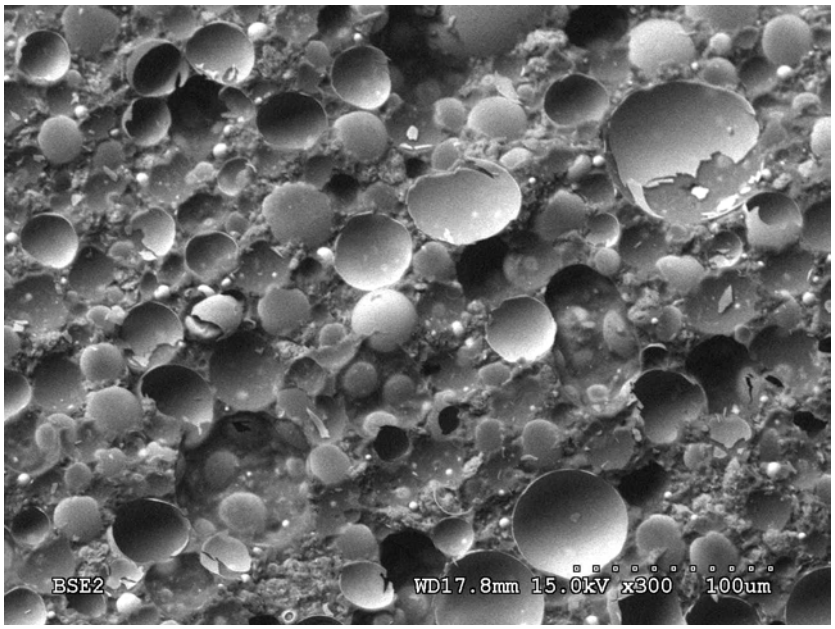

(b)

Figure 72 Scanning electron micrograph of nanoclay foam containing 5% nanoclay by volume (a) lower magnification micrograph and (b) higher magnification micrograph showing some small clusters of nanoclay among large number of glass microballoons.

The TEM and SEM observations confirm that the expected microstructure presented in Figure 65 is obtained in the material. Presence of large number of small clusters is attributed to a decrease in strength. In such clusters only the outer layer is bonded with the matrix resin. Large number of nano-sized particles within the cluster, which are not bonded with matrix directly can slide and move when the localized stress becomes sufficiently high. Such a structure causes decrease in strength of 2% nanoclay containing foams, although the intercalated nanoclay particles are present in the matrix structure. An increase in intercalated and exfoliated nanoclay particles in the matrix material will lead to increase in strength, which is observed for 5% nanoclay foams.

The most attractive characteristic of syntactic foams is the prolonged energy absorption region of constant stress in the stress strain curves. Such region is observed in stress-strain curves of nanoclay filled syntactic foams also. It is highly desirable to extend this region to increase the toughness and the damage tolerance of syntactic foams. Matrix plasticization may be one method to achieve such properties, where brittleness of epoxy resins is reduced and plastic strain is increased. As observed in Figure 66 and Figure 67, the plateau region is much longer in foams with nanoclay as compared to that of foams without nanoclay (Figure 68). A longer plateau region shows a higher amount of energy absorption in nanoclay foam specimens. In nanoclay foam specimens the stress starts increasing without occurrence of failure at the end of the stress plateau region. This corresponds to the complete crushing of microballoons and densification of the specimen. SF46 syntactic foams showed failure at a strain of 8-12% compared to 12-15% for SF32 and over 20% for SF22 foams. As a result of nanoclay incorporation, a considerable increase in failure strain is observed for all kinds of foams. Strain values as high as 35% were achieved, even for high density foams, without failure before the compression was stopped. These specimens did not show a definite compressive failure point

and appear to be much more damage tolerant than the corresponding syntactic foams that do not contain nanoclay. Toughness of the specimens is measured in the form of area under the stress-strain curves. Nanoclay foams do not show a specific fracture point, hence, for these foams area under the stress-strain curve is measured for 30% strain. Syntactic foams have specific fracture points, hence, for these materials area under the curve till fracture is measured. It can be observed in Figure 73 that the toughness of materials has increased considerably due to the incorporation of nanoclay particles.

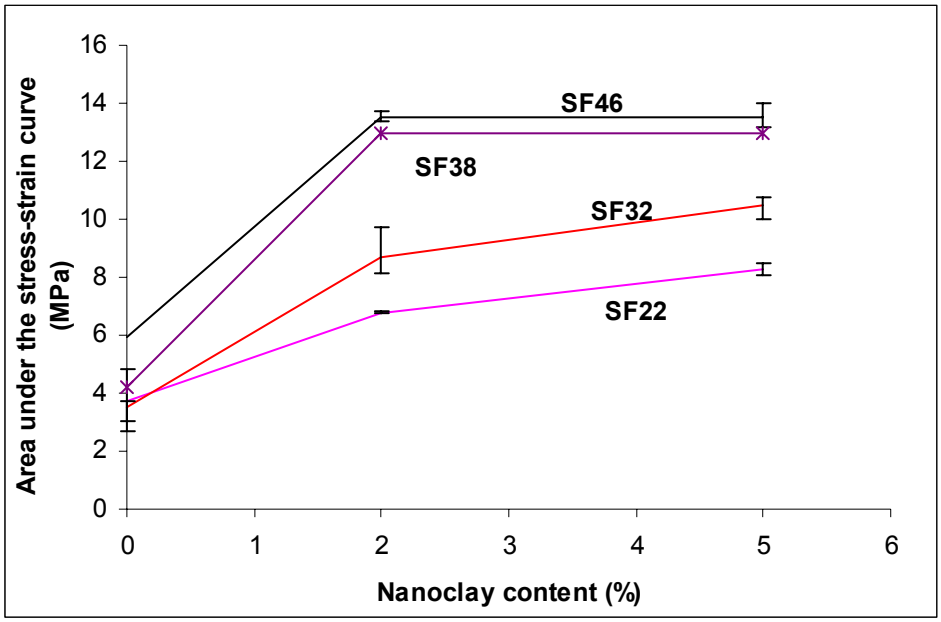

Figure 73 Effect of nanoclay content on the toughness of syntactic foams.

It can be observed that for low density foams, having 220 kg/m^3 microballoons, the area under the curve has increased by about 125% for 5% nanoclay content. In medium density foams containing 320 kg/m^3 microballoons the increase is found to be about 150 and 200% for 2 and 5% nanoclay contents, respectively. The increase in toughness is found to be about 125% for both, 2 and 5% nanoclay containing syntactic foams of high density. As the strength values are close for nanoclay foams and syntactic foams, the increase in toughness is observed due to the increase in fracture strain of the material.

Nanoclay foam specimens having 2 and 5% nanoclay content, compressed to about 30% strain are shown in Figure 74a and Figure 74b, respectively. Several cracks are observed in the sidewalls of these specimens. However, these cracks are not deep and do not have significant effect to cause fragmentation of the specimen. Material from the sidewall of SF46C2 specimen in Figure 74a has been removed to show that the crack has not penetrated deep into the specimen. Several cracks can be observed in the sidewalls of 5% nanoclay specimens also. However, compared to syntactic foam specimen shown in Figure 63, which was compressed to only about 10% strain, these specimens show cracks at three times higher strain level. Increase in the plasticity of the specimens has occurred due to the modification of matrix resin system with nanoclay particles. Hence, the modified microstructure provides advantage of enhancement of toughness of the material.

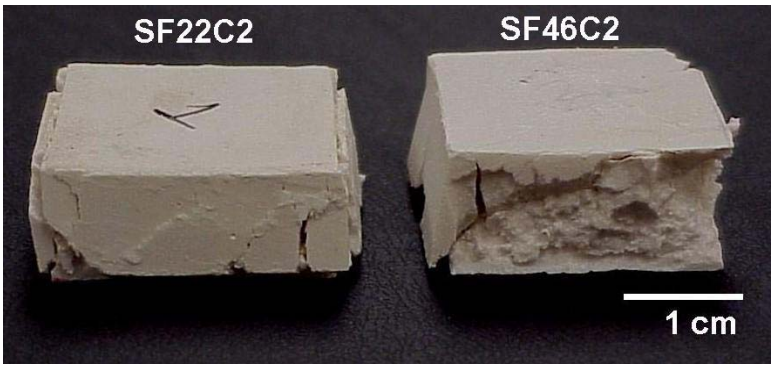

(a)

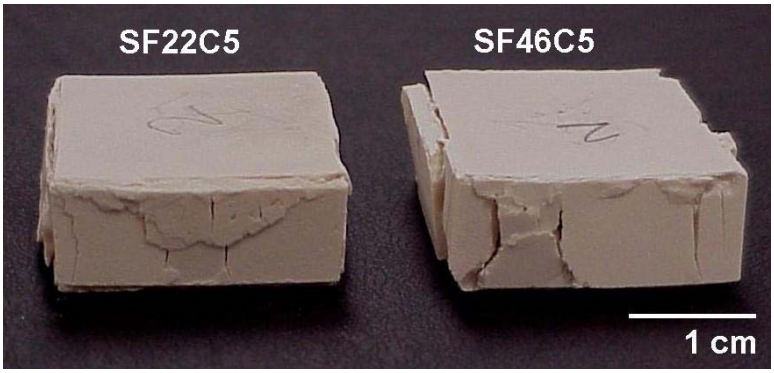

(b)

Figure 74 Specimen of nanoclay syntactic foam tested under compressive loading conditions (a) 2% nanoclay content (b) 5% nanoclay content.

4.2.2.3.3 Conclusions

Desired result of increase in fracture strain of high density and high strength syntactic foams was achieved in the study through microstructural modification. Nanoclay particles are incorporated in the matrix resin system of syntactic foams for this purpose. Partial intercalation of nanoclay particles is obtained in the matrix material, which is observed through TEM. The compressive strength has shown a decrease in the range of 10-20% due to the incorporation of 2% nanoclay by volume, whereas 5% nanoclay has given nearly the same level of strength. Increase in fracture strain with little change in strength caused considerable increase in toughness of the material. Toughness, measured as area under the stress strain curves, shows about 80 and 125% increase due to incorporation of 2 and 5% nanoclay in syntactic foams containing 220 kg/m^3 microballoons. In medium density foams containing 320 kg/m^3 microballoons the increase is found to be about 150 and 200% for the same nanoclay contents. In high density foams having 460 kg/m^3 microballoons the toughness has increased by about 125% due to the incorporation of nanoclay. Specimens do not show a definite fracture point even at strains as high as 35%.

4.2.2.4 Flexural Strength: Three Point Bending Test

ASTM D790 standard [44] is adopted for the flexural testing of the all foams. This standard recommends a span length to thickness ratio of 16:1 for the 3-point bend tests. All foam

specimens have a specimen length (l) and width (w) of 110 and 15 mm respectively. The average span length (L) is 64 mm and average sample thickness (t) is 4 mm. At least five specimens of each type of foam are tested in the three point bend configuration as shown in Figure 25.

A computer controlled MTS QTEST/150 mechanical test system is used to carry out the flexural tests. Load-displacement data obtained in the tests is used to calculate bending stress and deflection. Tangent modulus and flexural strength are calculated for all specimens using Equations 15 and 18 given before.

4.2.2.4.1 Density Measurement

The density of foams is measured by measuring weight and volume of at least five specimens of $64 \times 12 \times 4$ mm^3 size. Measured densities and calculated void volume fraction of pure syntactic foams and rubber hybrid foams are given in Table 6 and Table 9 respectively. The void volume fractions are calculated by using measured and theoretical densities in the Equation 12.

Table 9 Composition and density of nanoclay hybrid syntactic foams.

Nanoclay Volume %	Microballoon Type	Microballoon Density kg/m^3	Nanoclay Foam Nomenclature	Nanoclay Foam Density kg/m^3	Void Volume %
2	S22	220	SF22C2	497.55	10.35
	S32	330	SF32C2	552	11.96
	S38	380	SF38C2	601.72	9.47
	K46	460	SF46C2	632.68	11.64
5	S22	220	SF22C5	543.49	9.42
	S32	330	SF32C5	594.69	11.24
	S38	380	SF38C5	603.73	13.75
	K46	460	SF46C5	658.58	12.19

4.2.2.4.2 Results and Discussion

Figure 75 shows a comparison of stiffness values for various types of foam samples. Stiffness is observed to have increased by around 10% upon the addition of nanoclay particles. Figure 76 shows a comparison of flexural modulus for various syntactic foam samples. As a general trend it is observed that flexural modulus in syntactic foams has increased by as high as 10%, upon the addition of nanoclay particles.

Figure 77 shows a comparison of flexural strength of various types of syntactic foam samples. All types of foams show a similar trend on the effect of microballoon η. Flexural strength of foam samples is seen to increase with a decrease in η, i.e. with an increase in foam density.

Figure 78 shows a comparison of fracture strain values for various syntactic foams. Fracture strain is observed to decrease by 15% due to the addition of 2% nanoclay particles. However, only a small change(less than 3%) is observed upon the addition of 5% nanoclay particles.

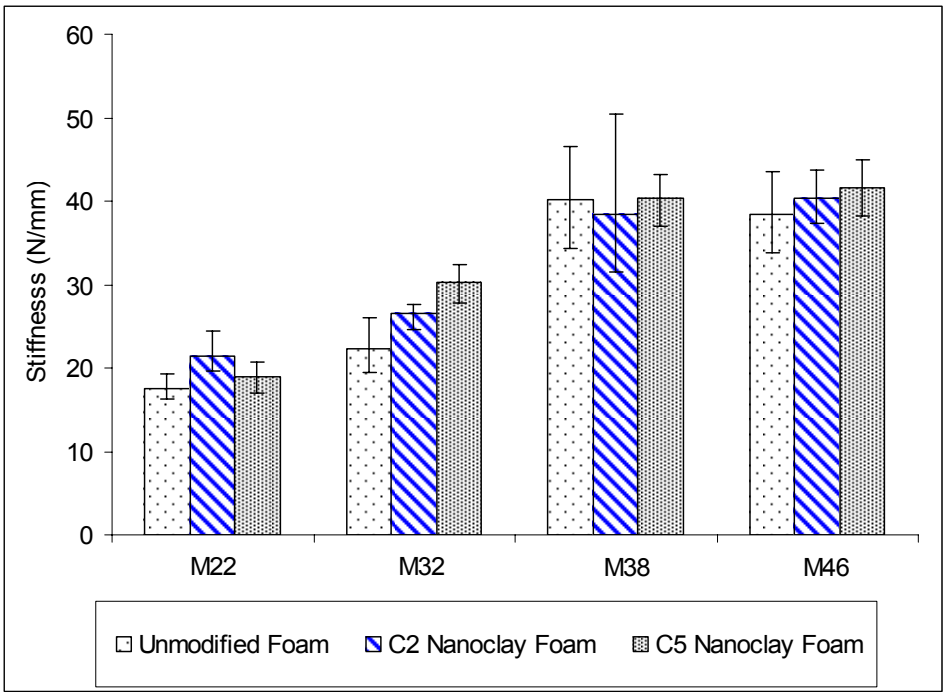

Figure 75. Comparison of flexural stiffness for various syntactic foam samples

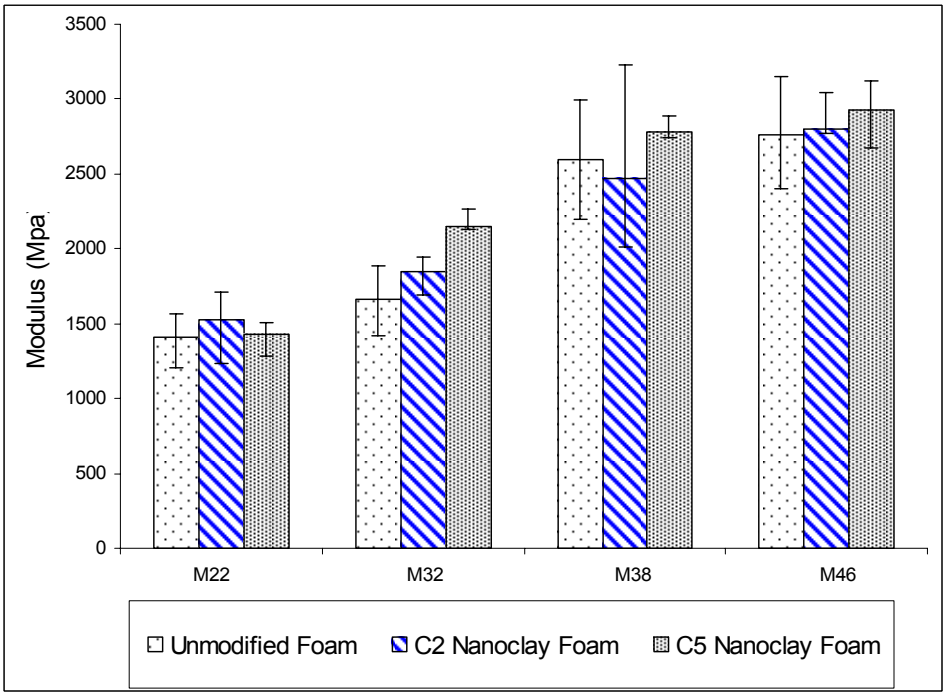

Figure 76. Comparison of flexural modulus for various syntactic foam samples

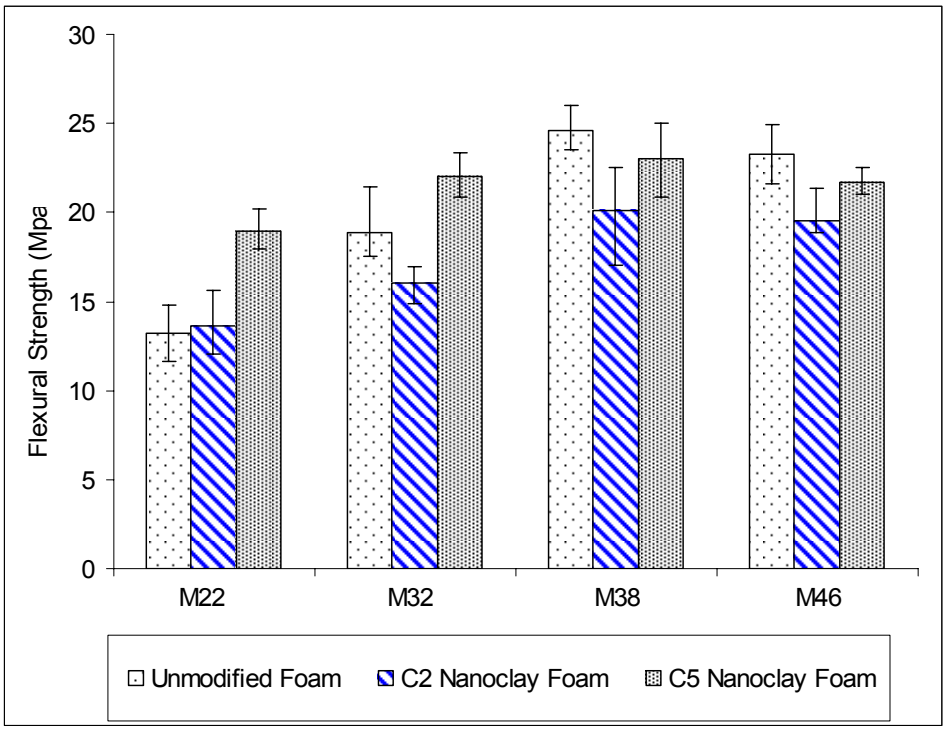

Figure 77. Comparison of flexural strength for various syntactic foam samples

Figure 79 to Figure 81 show representative load displacement curves obtained from flexural testing of foams with various types of syntactic foams. Area under curve has been measured from corresponding graphs for various types of foams.

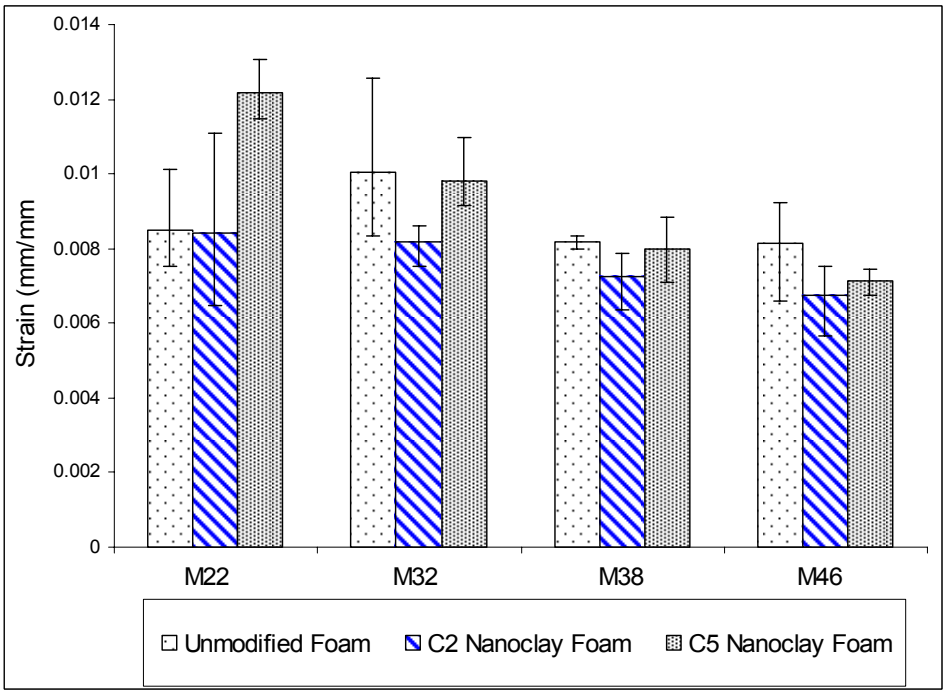

Figure 78. Comparison of fracture strain values for various syntactic foam samples

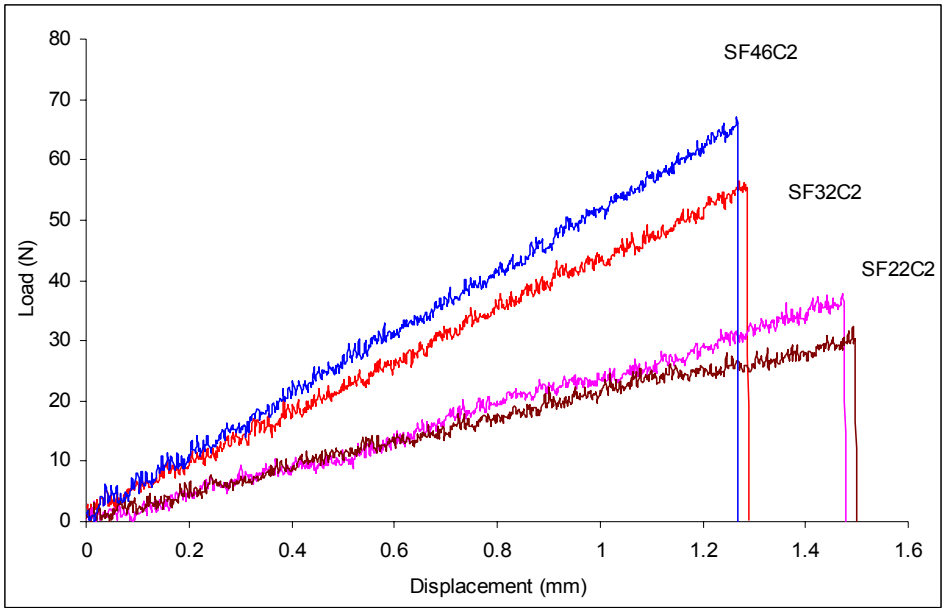

Figure 79. Representative load displacement curve for hybrid foams containing nanoclay particles in 2% volume fraction.

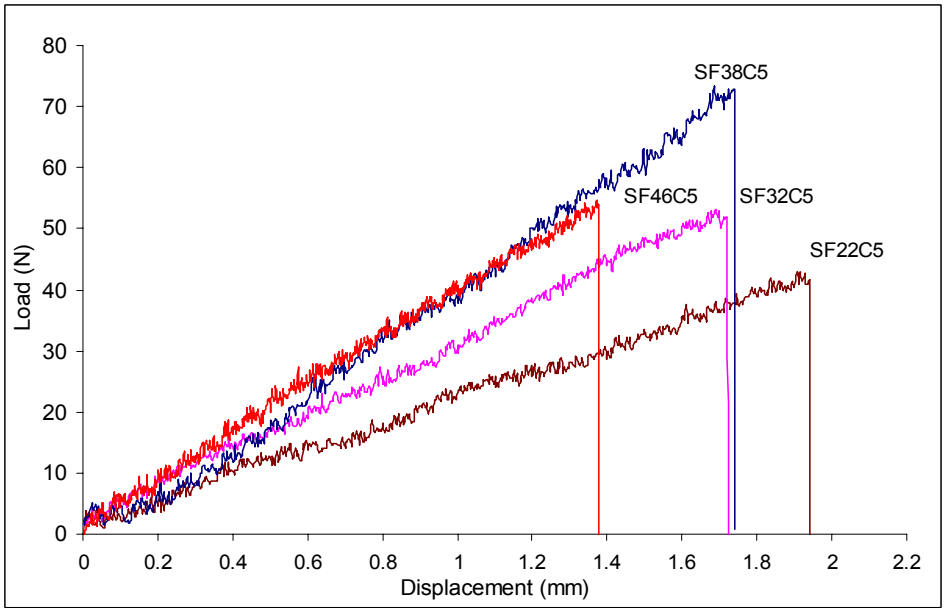

Figure 80. Representative load displacement curve for hybrid foams containing nanoclay particles in 5% volume fraction.

Figure 82 shows the comparison of flexural toughness as area under curve for various syntactic foams. Effect of nanoclay particles on syntactic foams is seen to vary with their volume fraction in the foam matrix.

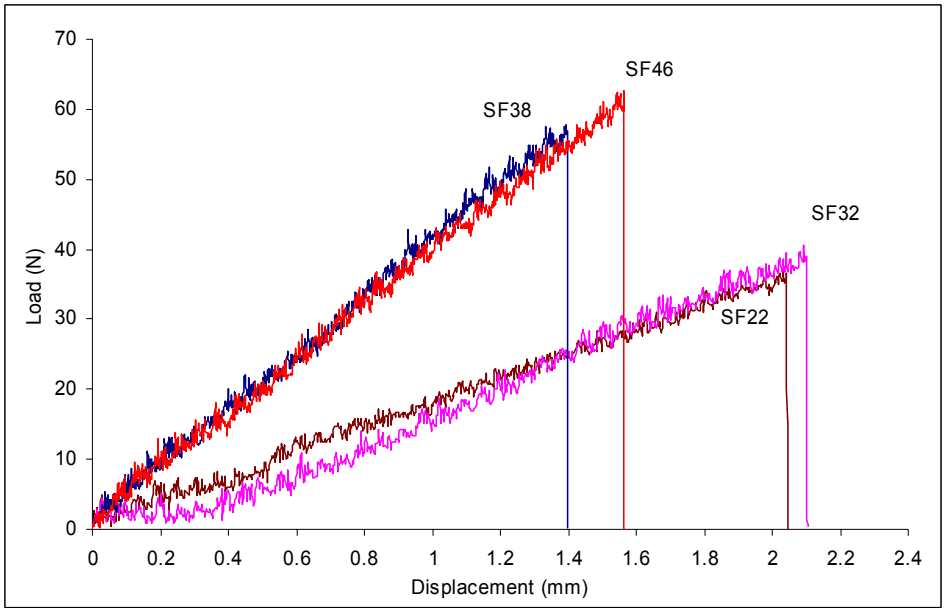

Figure 81. Representative load displacement curve for pure syntactic foam without any filler particles.

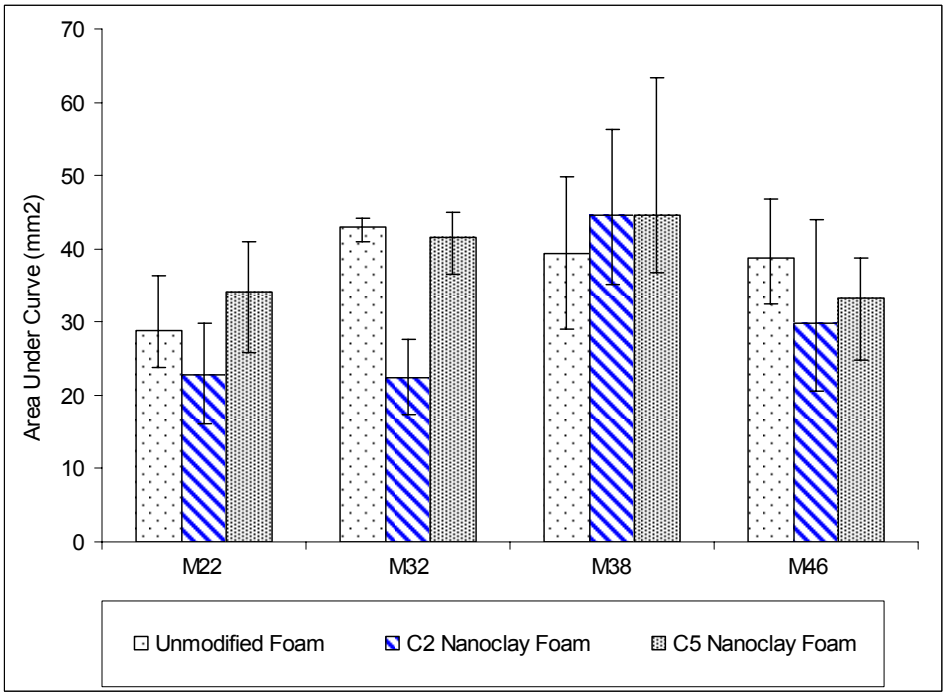

Figure 82. Comparison of flexural toughness for various syntactic foam samples

Addition of 2% nanoclay particles has resulted in an overall reduction in flexural strength of the syntactic foams by around 11%. Addition of 5% nanoclay particles has resulted in an increase in strength of low density (SF22C5 and SF32C5) syntactic foams by around 22%, with no significant difference in the strength of nanoclay syntactic foams containing higher η microballoons. Previous studies have shown that 2 vol.% of nanoclay is sufficient to increase the

strength and modulus of polymers if the nanoclay is completely exfoliated. However, in the present study only a small fraction of nanoclay was exfoliated and most of the nanoclay was present as clusters. These clusters were observed to increase the fracture strain and modulus of syntactic foams under compressive loading conditions. Thus, the decrease in strength due to the presence of 2% nanoclay filled foams is observed. At higher volume fraction (5%) the intercalated and exfoliated content of nanoclay increases and provides strengthening effect. The fracture in SF38 and SF46 type hybrid foams is governed by the matrix failure so their strength should also be comparable.

The fracture strain is seen to reduce by 15% due to the addition of 2% nanoclay particles. However, only a small change(less than 3%) is observed upon the addition of 5% nanoclay particles. Flexural toughness is seen to have increased upon the addition of 5% nanoclay particles. However the toughness has decreased upon the addition of 2% nanoclay particles.

There is no significant difference is observed in the modulus and stiffness of hybrid foams compared to the plain syntactic foams. The volume fraction of nanoclay particles is 2 and 5% in the hybrid foam structure, which may not be sufficient to cause a significant difference in the elastic constants of hybrid foams.

4.2.2.4.3 Conclusion

Experimental investigation of plain and nanoclay hybrid syntactic foams is carried out in the present study. The fracture mode of plain syntactic foams shows a transition from microballoon fracture to matrix failure as the microballoon strength increases. Nanoclay particles have a significant effect on the flexural properties of syntactic foams. Effect of nanoclay particles on hybrid foams vary with their volume fraction in the foam matrix. Addition of 2% nanoclay particles has led to a reduction in strength of syntactic foams whereas addition of 5% nanoclay particles has increased the strength of syntactic foams. No significant difference is observed in the modulus and stiffness of nanoclay hybrid foams.

5 SUMMARY

Hybrid syntactic foams have been developed in order to improve damage tolerance properties of syntactic foams. Analytical study is done in order to study the micromechanical effects of stresses around microballoons in syntactic foams. Stress Intensity Factor approach is used to study the distribution of stresses around microballoons and interaction between adjacent microballoons. Significantly high stresses are observed on the microballoon surface due to stress concentration, which makes syntactic foams brittle and less damage tolerant. Rubber and nanoclay particle fillers are used in varying sizes and concentrations respectively, to modify the syntactic foam microstructure, resulting in high damage tolerant hybrid syntactic foams. Extensive experimentation is carried out under varying loading and environmental conditions to determine the mechanical properties of hybrid foams. A detailed study has been carried out using SEM, TEM and XPS techniques in order to characterize the microstructure of all foams before and after loading. Rubber hybrid foams are characterized for compressive and flexural properties. An increase in damage tolerance properties has been observed for all rubber hybrid foams. Foams with smaller sized rubber particles show better mechanical properties as compared to foams with larger rubber particles as explained in the respective sections above. Hygrothermal properties of rubber hybrid foams are characterized under deionized water and salt water conditions at room temperature. Increase in water absorption is observed due to the presence of rubber particles in rubber syntactic foams. Higher reduction in strength is observed in hybrid foams as compared to foams without rubber particles. However, increase in fracture strain of hybrid foams due to moisture infusion may help in maintaining the same energy absorption before failure. The compressive failure strain is found to increase due to matrix plasticization. Nanoclay hybrid foams are characterized for compressive and flexural properties. Partial intercalation of nanoclay is used to obtain a unique microstructure containing exfoliated nanoparticles and nanoclay clusters. Such a structure increases strength along with increasing the damage tolerance properties and reducing brittleness in syntactic foams. Foams with higher (5%) nanoclay concentration show better mechanical properties as compared to foams with lower (2%) nanoclay concentration. This dependence is due to the larger number of exfoliated nanoclay particles 5% nanoclay foams.

REFERENCES

1. Bhagwan D. Agarwal and Lawrence J. Broutman, Analysis and Performance of Fiber Composites, Wiley, US, 2nd Edition, 24th September, 1990.

2. Katz, H. and Milewski, J.V., Handbook of reinforcements for plastics, Van Nostrand Reinhold Co., New York, 1987.

3. N. Gupta, C. S. Karthikeyan, S. Sankaran, Kishore, Mater. Charact., 43(4) (1999) 271-277.

4. Ashida, K. in Handbook of Plastic Foams: Types, properties, Manufacture and Applications, A. H. Landrock (ed.), Noyes Publications, 1995, 147-163.

5. Shutov FA. 1991. "Syntactic polymeric foams. In: Klempner D, Frisch KC, editors. Handbook of polymeric Foams and Foam Technology". New York: Hanser Publishers, p.355-374.

6. Hiel, C., Dittman, D. and Ishai, O., 'Composite sandwich construction with syntactic foam core: A practical assessment of post-impact damage and residual strength', Composites **24**, 5, 1993, 447-450.

7. Ishai, O., Hiel, C. and Luft, M., 'Long-term hygrothermal effects on damage tolerance of hybrid composite sandwich panels', Composites **26**, 1, 1995, 47-55.

8. Bardella, L and Genna, F., 'Elastic design of syntactic foamed sandwiches obtained by filling of three-dimensional sandwich-fabric panel', International Journal of Solids and Structures **38**, 2001, 307-333.

9. Gupta, N., Woldesenbet, E., Kishore and Sankaran, S., 'Response of syntactic foam core sandwich structured composites to three-point bending', Journal of Sandwich Structures and Materials **4**, 2002, 249-272.

10. Z. H. Liu, J. Li, N. G. Liang, H. Q. Liu, J Reinf Plast Comp, 16(16) (1997) 1523-1534.

11. Leidner, J. and Woodhams, T., 'The strength of polymeric composites containing spherical fillers', J Appl. Polym. Sci. **18**, 1974, 1639-1654.

12. D'Almeida, J.R.M., 'An analysis of the effect of the diameter of glass microspheres on the mechanical behavior of glass microsphere/epoxy-resin composites', Compos Sci Technol 59, 1999, 2087-2091.M. Palumbo, E. Tempesti, Acta Polym., 49 (1998) 482-486.

13. Gupta, N., Karthikeyan, C.S., Sankaran, S. and Kishore, 'Correlation of Processing Methodology to the Physical and Mechanical Properties of Syntactic Foams With and Without Fibers', Materials Characterization **43,** 4, 1999, 271-277.

14. Bunn, P. and Mottram, J.T., 'Manufacture and Compression Properties of Syntactic Foams', Composites **24,** 7, 1993, 565-571.

15. Gupta, N., Kishore, Woldesenbet, E., and Sankaran S., 'Studies on compressive failure features in syntactic foam material', Journal of Materials Science **36**, 18, 2001, 4485-4491.

16. H. S. Kim, H. H. Oh, J. Appl. Polym. Sci., 76 (2000) 1324-1328.

17. H. S. Kim, M. A. Khamis, Compos. Part A-Appl S., 32 (2001) 1311-1317.

18. Todo M, Takahashi K and Higuchi K. Impact fracture behavior of glass bubbles filled epoxy resins. In Proceedings of ASC 16th Annual Conference, Paper # 059, Blacksburg, VA, Sept. 9-12, 2001.

19. Karthikeyan C. S., Kishore, and S. Sankaran. 2001. "Effect of absorption in aqueous and hygrothermal media on the compressive properties of glass fiber reinforced syntactic foam". J Reinf Plast Comp, 20(11):982-993.

20. Gupta N, and E. Woldesenbet. 2003. "Hygrothermal studies on syntactic foams and compressive strength determination". Compos Struct, 61(4):311-320.

21. Tessier NJ. Fire performance and mechanical property characterization of a phenolic matrix syntactic foam core material for composite sandwich structures. Proceedings of 46th International SAMPE Symposium, May 6-10, 2001; 2593-2599.

22. N. Gupta, E. Woldesenbet, Kishore, J. Mater. Sci., 37(15) (2002) 3199-3209.

23. E. Lawrence, D. Wulfshon, R. Pyrz, Polym. Polym. Compos., 9(7) (2001) 449-457.

24. N. Gupta, E. Woldesenbet, In: Proceedings of ETCE-2002 Conference. Houston, (2002) Paper # CMDA-29069.

25. C. S. Karthikeyan, S. Sankaran, M. N. Jagdish Kumar, Kishore., J. Appl. Polym. Sci., 81 (2001) 405-411.

26. H.R. Azimi, R.A. Pearson and R. W. Hertzberg. 1996. "Fatigue of hybrid composites: Epoxies containing rubber and hollow glass spheres". Polymer Engineering and Science, 36, 18, 2352-2365.

27. Pinnavia, T.J. and Beall, G.W., Polymer-Clay Nanocomposites, Wiley Series in Polymer Science, 2000.

28. Messersmith, P.B. and Stupp, S.I., 'Synthesis of Nanocomposites – Organoceramics', Journal of Materials Research 7, 1992, 2599-2611.

29. Giannelis, E.P., 'Polymer layered silicate nanocomposites', Adv. Mater. **8,** 1, 1996, 29-35.

30. Novak, B.M., 'Hybrid Nanocomposite Materials – Between Inorganic Glasses and Organic Polymers', Adv. Mater. **5**, 1993, 422-433.

31. Yasmin, A., Luo, J.J., Abot, J.L. and Daniel, I.M., 'Mechanical and Thermal Behavior of Clay/Epoxy Nanocomposites at Room and Elevated Temperatures', Proceedings of ASC, 18th Annual Technical Conference, Oct 2003.

32. ASTM C365-94 Standard Test Method for Flatwise Compressive Properties of Sandwich Cores, ASTM International, PA, USA.

33. Rizzi E, Papa E and Corigliano A. Mechanical behavior of a syntactic foam: experiments and modeling. Intl J Solids Struct 2000; 37:5773-5794.

34. Xiao, Z.M., M.K. Lim and K.M Liew. 1995. Stress Intensity Factor of two Internal Elliptical Cracks in Three-Dimensional Solids., Engg Fract Mech, 50(4):431-441.

35. Timishenko, S. and J.N. Goodier. 1951. Theory of Elasticity, McGraw Hill, New York.

36. Papanicolaou G. C. and D. Bakos. Feb. 1992. .The influence of the adhesion bond between matrix and filler on the tensile strength of particulate-filled polymer, J. Reinforced Plastics and Composites, 11:104-126.

37. Kassir MK and Sih GC. 1975. Three Dimensional Crack Problems, Noordhoff Intl.

38. Callister W. D., Materials Science and Engineering: An Introduction, John Wiley & Sons, Inc. New York, NY. 1994.

39. Torquato S, Turskett, TM and Debenedetti PG. Is random close packing of spheres well defined?. Phy Rev Lett 2000; 84(10):2064-2067.

40. Gupta N. and Nagorny R., 'Tensile Strength of Glass Microballoon-Epoxy Resin Syntactic Foams,' for Proceedings of the American Society for Composites—Twentieth Technical Conference, Philadelphia, PA, Sep 2005.

41. Gupta, N. and Woldesenbet, E., 'Microballoon wall thickness effects on properties of syntactic foams', Journal of Cellular Plastics, 2004, in press.

42. N. Gupta, E. Woldesenbet, In: Proceedings of ASC 16th Annual Conference. Blacksburg, (2001) Paper # 055.

43. Gupta N, E. Woldesenbet, and P. Mensah. 2004. "Compression properties of syntactic foams: effect of cenosphere radius ratio and specimen aspect ratio". Composites A: Appl Sci and Manuf, 35(1): 103-111.

44. ASTM D790-03 Standard Test Methods for Flexural Properties of Unreinforced and Reinforced Plastics and Electrical Insulating Materials, ASTM International, PA, USA.

45. Subramaniyan, A.K., Bing, O. Nakaima, D. and Sun C.T., 'Effect of Nanoclay on Compressive Strength of Glass Fiber Composites', Proceedings of ASC, 18th Annual Technical Conference, Oct 2003.

46. Gupta N. and Nagorny R., Tensile Strength of Glass Microballoon-Epoxy Resin Syntactic Foams for Proceedings of the American Society for Composites—Twentieth Technical Conference, Philadelphia, PA, Sep 2005.

47. Maharsia R., Gupta N., and Jerro H.D., Hygrothermal Testing and Evaluation of Mechanical Properties of Rubber-Glass Particulate Hybrid Composites, Proceeding of the American Society for Composites, Annual 19th conference, Atlanta, Oct 2004.

48. ASTM D 5229/D 5229M . 92 Standard test method for moisture absorption properties and equilibrium conditioning of polymer matrix composite materials. ASTM-International, PA, USA.

49. Zhou J and Lucas JP. Hygrothermal effects of epoxy resin. Part I: the nature of water in epoxy. Polymer 1999; 40:5505-5512.

50. Springer GS (editor). Environmental effects on composite materials, Westport, CT: Technomic Publishing Company, 1981.

51. Gupta N., Maharsia R., and Jerro H.D., Compressive Properties of Rubber and Glass Particulate Hybrid Composites," Materials Science and Engineering A, Vol. 395, Issues 1-2, pp. 233-240 (2005).

52. Gupta, N., and Maharsia, R., Enhancement of Energy Absorption in Syntactic Foams by Nanoclay Incorporation for Sandwich Core Applications. Applied Composite Materials, Vol. 12, No. 3-4. (May 2005), pp. 247-261.

53. Maharsia, R., Gupta, N. and Li, G., Compressive properties of nanoclay syntactic foams for sandwich core applications. Society for Experimental Mechanics X International Congress & Exposition, Costa Mesa, CA. June 7- 10, 2004, Paper #25.

VITA

Rahul R. Maharsia was born on September 22nd 1977, in Nawalgarh, (Rajasthan), India. Rahul joined the bachelor's program in The Department of Mechanical Engineering at Mumbai University (Vidyavardhini's College of Engineering and Technology, Vasai Road) in 1994. He secured First class in his final year and graduated in 1999. His interest in learning optimization techniques for manufacturing and production in the field of mechanical engineering led him to join the master's program in Industrial Engineering at Louisiana Tech University, Ruston. His master's project work was on the life cycle cost analysis of Smart Fiber Reinforced Composite Piping systems for use in civilian applications. He graduated with a master's in industrial engineering in 2001.

His interest in the field of composite materials and an interest in building a career in teaching and research led him to pursue a doctoral degree in the field of engineering science at Louisiana State University, Baton Rouge. He joined Dr. H. Dwayne Jerro, Assistant Professor in the Department of Mechanical Engineering at LSU for his doctoral study. His primary area of interest for research was hybrid syntactic foams for use as sandwich material in weight sensitive aerospace and marine structural applications. Rahul's research for his doctorate has resulted in over 11 publications including journal papers, conference proceedings and presentations.

He received the 'Johnston Science Foundation Award' Grant for the year 2004-05. Rahul has been instrumental in writing several research proposals, and has succeeded in receiving funding for three of these proposals including a grant from NASA's LaSpace consortium.